

https://dspace.org/

A re-evaluation of the cranial morphology and taxonomy of the Triassic dicynodont genus Kannemeyeria

Renaut, Alain, Joseph

2000-12-22
University of the Witwatersrand
http://hdl.handle.net/10539/19499

Downloaded from a DSpace repository. https://dspace.org/

A RE-EVALUATION OF THE CRANIAL MORPHOLOGY AND TAXONOMY OF THE TRIASSIC DICYNODONT GENUS *KANNEMEYERIA*

VOLUME TWO

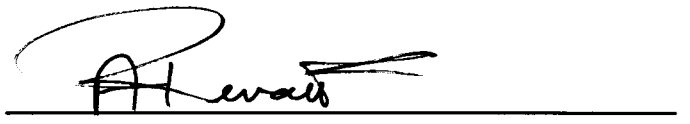
Alain Joseph Renaut

A thesis submitted to the Faculty of Science, University of the Witwatersrand, Johannesburg, in fulfilment of the requirements for the degree of Doctor of Philosophy.

Johannesburg, 2000

DECLARATION

I declare that this thesis is my own, unaided work. It is being submitted for the Degree of Doctor of Philosophy at the University of the Witwatersrand, Johannesburg. It has not been submitted before for any degree or examination at any other University.



Alain Joseph Renaut

This 22nd **day of** December **2000**

ABSTRACT

The genus *Kannemeyeria* is one of the most important and distinctive taxa of the Triassic dicynodonts. It became the first Triassic dicynodont known to science, and thus forms the benchmark for the comparison of the evolution and morphology of other Triassic dicynodonts. An understanding of this genus forms an integral part of the biozonation of the Beaufort Group, and is pivotal in influencing the interpretation of the evolution, physiology and phylogenetic relationships of the Triassic dicynodonts. This study focuses on the detailed cranial morphology and relationships of the *Kannemeyeria*, and uses a rigorous morphological investigation as the basis for a meaningful elucidation of the functional and thus physiological aspects of this dicynodont.

The descriptions demonstrate that variations related to the skull size, distortion or naturally occurring variation within the genus allow for the synonymy of the formerly recognised species *K. latifrons* Broom (1898; 1913), *K. erithrea* Haughton (1915) and *K. wilsoni* Broom (1937). This conclusion is further supported by the allometric analysis which cannot distinguish the variation observed in the holotypes with that occurring naturally within a growth series. Apart from the large specimen, the other smaller individuals are accommodated in the genus as different ontogenetic stages of the growth series represented by *K. simocephalus* Weithofer (1888). Several allometric variables show unusual patterns of development, indicating that *Kannemeyeria* can be subdivided into ontological classes, as juvenile and adult forms, separated from each other by a particular level of development. An age-related threshold level is suggested, and considered to represent an animal reaching sexual maturity. It is consequently proposed that the *Kannemeyeria* population was, at an age-related level, subdivided into sexually mature and immature groups but remained ecologically homogeneous.

Both the descriptions and the allometric analysis of the species *K. cristarhynchus* Keyser & Cruickshank (1979) clearly indicate that it does not conform to the growth series of *K. simocephalus* and thus the differences observed between these two taxa are not constrained to size increases. Consequently, the recognition of the species *K. cristarhynchus* is considered valid. From the observations of the cranial morphology, tested using an

allometric analysis, generic and specific diagnoses are constructed for *Kannemeyeria* and its two African species.

Several features of *Kannemeyeria* are discussed in a functional context. A corrugated horn-covered snout and large caniniform processes are considered to be associated with defence and posturing behaviour. Several features of the braincase also suggest herding behaviour. *Kannemeyeria* also has a slightly different occipital musculature arrangement than that proposed for many other dicynodonts. Most *Kannemeyeria* cranial features are related to its masticatory function. From the analysis of masticatory cycle it is clear that the jaw action is described via a single pivot-point, which in *Kannemeyeria* approached the original, primitive position of the jaw hinge. The vertical orientation of the articulation and this pivot-point ensured that the muscle action during second phase of mastication produced an upward crushing and grinding action instead of the typical fore-and-aft motion of many other dicynodonts. It also meant that the muscle force was at their maximum, and little or no energy was lost to translation of the moment arm at the jaw articulation. Consequently, the *Kannemeyeria* masticatory cycle was both highly effective and extremely efficient. The morphology, and resultant physiology, of *Kannemeyeria* skull is considered to represent the innovative foundation for much of the success of many of the later Triassic dicynodonts.

ACKNOWLEDGEMENTS

I am extremely grateful to my supervisors, Prof. B. S. Rubidge and Dr. P. J. Hancox, for their advice, understanding and patience. I trust they will find this thesis worth the time and effort invested to produce a body of work I know to be the best possible. The following people assisted in the preparation of the numerous specimens: Mr. R. Lewis, Mr. Dr. J. W. Kitching, C. Dube and Mr. G. Modise, as well as sundry work by several other technical staff of the Bernard Price Institute, for which I am deeply grateful. I am indebted to the invaluable discussions and criticisms from Drs. J. W. Kitching, M. Raath, W. De Klerk, S. P. Modesto, R. Damiani, and especially J. van den Heever. Their critique helped to crystallise many of the specific hypotheses critical to this thesis. Dr. R. Adendorff and Mr. P. Emmanual helped with the drawing and preparation of some of the figures, and their assistance is appreciated. This project was completed with the financial assistance of the Foundation for Research Development (National Research Foundation), with the provision of a postgraduate research grant. Finally, this thesis would not have been completed without the honest support and help from my wife, Ray.

LIST OF FIGURES

Figure 1 Cranial reconstructions of the genotype of *Kannemeyeria* modified from Pearson (1924a) 1

Figure 2 Drawing of the floor of the nasal cavity and ventral skull roof of BP/1/4648. 2

Figure 3 Dorsal view of specimen BP/1/5624. 2

Figure 4 Photographs of the nasal cavity floor and maxillary fovea of the right side of the nasal cavity of BP/1/4648 and the dorsal view of BP/1/5624 3

Figure 5 Dorsal and lateral views BP/1/1168 4

Figure 6 Photographs of the dorsal and lateral views of BP/1/1168 . . **5**

Figure 7 Dorsal and lateral views of SAM/PK/10555 6

Figure 8 Photographs of the dorsal and lateral views of SAM/PK/10555 . . **7**

Figure 9 Dorsal and lateral views of NMQR/1127 8

Figure 10 Photographs of the dorsal and lateral views of NMQR/1127 . . 9

Figure 11 Dorsal and lateral views of PE/1199P. Holotype of *K. latifrons* Broom 1913. 10

Figure 12 Photographs of the dorsal and lateral views of PE/1199P. Holotype of *K. latifrons* Broom 1913. 11

Figure 13 Dorsal and lateral views of BP/1/4648. 12

Figure 14 Photographs of the dorsal and lateral views of BP/1/4648 . . 13

Figure 15 Photographs of the dorsal and lateral view of BP/1/989 . . . 14

Figure 16 Dorsal and ventral views of BP/1/2092 15

Figure 17 Photographs of the dorsal and the lateral views of BP/1/2092 . . 16

Figure 18 Dorsal and lateral views of SAM/PK/3017 17

Figure 19 Dorsal and lateral views of BP/1/4523 18

Figure 20 Photographs of the dorsal and lateral views of BP/1/4523 . . 19

Figure 21 Dorsal and lateral views of EL/1. Holotype of *K. wilsoni* Broom 1937 20

Figure 22 Photographs of the dorsal and lateral views of EL/1 Holotype of *K. wilsoni* Broom 1937. 21

Figure 23 Dorsal and lateral views of BP/1/4524 22

Figure 24 Photographs of the dorsal and lateral views of BP/1/4524 . . 23

Figure 25 Ventral view of BP/1/5624 24

Figure 26 Ventral view of BP/1/1168 24

Figure 27 Photographs of the ventral views of BP/1/5624 and BP/1/1168 . . 25

Figure 28 Ventral view of SAM/PK/10555 26

Figure 29 Ventral view of NMQR/1127 26

Figure 30 Photographs of the ventral views of SAM/PK/10555 and NMQR/1127 27

Figure 31 Ventral view of PE/1199P. Holotype of *K. latifrons* Broom 1913. 28

Figure 32 Ventral view of BP/1/4648 28

Figure 33 Photographs of the ventral view of PE/1199P and BP/1/4648 . . 29

Figure 34 Ventral view of BP/1/989 30

Figure 35 Ventral view of SAM/PK/3017. Holotype of *K. erithrea* Haughton 1915. 30

Figure 36 Ventral view of BP/1/2092 31

Figure 37 Ventral view of BP/1/4523 31

Figure 38 Photographs of the ventral views of BP/1/2092 and BP/1/4523 . . 32

Figure 39 Ventral view of EL/1. Holotype of *K. wilsoni* Broom 1937. . . 33

Figure 40 Ventral view of BP/1/4524 33

Figure 41 Photographs of the ventral views of EL/1 and BP/1/4524 . . 34

Figure 42 Sphenethmoid region of SAM/PK/3017 35

Figure 43 Occipital view of BP/1/5624 35

Figure 44 Photographs of the dorsal surface of the basisphenoid of BP/1/5624 and the distal end of the quadrate complex of BP/1/5624 and the occiput of BP/1/5624 . . . 36

Figure 45 Occipital view of BP/1/1168 37

Figure 46 Occipital view of NMQR/1127 37

Figure 47 Photographs of the occipital views of BP/1/1168 and NMQR/1127 38

Figure 48 Occipital view of SAM/PK/3017. Holotype of *K. erithrea* Haughton 1915 39

Figure 49 Occipital view of BP/1/4523 39

Figure 50 Occipital view of EL/1. Holotype of *K. wilsoni* Broom 1937. . . 40

Figure 51 Photographs of the occipital views of BP/1/4523 and EL/1 . . 41

Figure 52 Dorsal, lateral and lingual views of the lower jaw of BP/1/5624. 42

Figure 53 Photographs of the dorsal, lateral and lingual views of the lower jaw of BP/1/5624 43

Figure 54 Dorsal, lateral and medial views of the lower jaws of BP/1/4524. 44

Figure 55 Photographs of the dorsal, lateral and medial views of the lower jaw of BP/1/4524 45

Figure 56 Dorsal and lateral view of the lower jaw SAM/PK/3017 Holotype of *K. erithrea* Haughton 1915 46

Figure 57 Dorsal, lateral and medial views of the lower jaw EL/1 Holotype of *K. wilsoni* Broom 1937 47

Figure 58 Photographs of the dorsal, lateral and medial views of the lower jaw of El/1 48

Figure 59 Dorsal and right lateral view of BP/1/3638. Holotype *K. cristarhynchus* Keyser and Cruickshank 1979. . . . 49

Figure 60 Photographs of the dorsal and right lateral views of BP/1/3638 Holotype of *K. cristarhynchus* Keyser and Cruickshank 1979. . . 50

Figure 61 Ventral and occipital views of BP/1/3638. Holotype of *K. cristarhynchus* Keyser and Cruickshank 1979 . . . 51

Figure 62 Photographs of the ventral and occipital views of BP/1/3638 . . 52

Figure 63 Dorsal, lateral and medial views of the lower jaw of BP/1/3638 Holotype of *K. cristarhynchus* Keyser and Cruickshank 1979 . . 53

Figure 64 Photographs of the dorsal, lateral and medial views of the lower jaw of BP/1/3638 54

Figure 65 *Kannemeyeria* skull measurements 55

Figure 66 Selected bivariate plots of taxonomic significance, or demonstrating the effects of specific ontological growth patterns 56

Figure 67 Further selected bivariate plots showing the allometric-growth trends of the genus *Kannemeyeria.* 57

Figure 68 Cranial reconstruction of the skull of ***Kannemeyeria simocephalus*:** 58

Figure 69 Cranial reconstructions of the skull *Kannemeyeria simocephalus*: ventral and occipital views 59

Figure 70 Cranial reconstruction of the dorsal and lateral views of the skull of *Kannemeyeria cristarhynchus* 60

Figure 71 Cranial reconstructions of the skull of *Kannemeyeria cristarhynchus*: ventral and occipital view 61

Figure 72 Dorsal and lateral views of PVL/3465. Holotype of *K. argentinensis* Boneparte 1966 62

Figure 73 Ventral and occipital views of PVL/3465. Holotype of *K. argentinensis* Boneparte 1966 63

Figure 74 Lateral views of the lower jaw of PVL/3465. Holotype of *K. argentinensis* Boneparte 1966 63

Figure 75 Occiput of *Kannemeyeria* demonstrating major muscle insertion sites, illustrated as functional units 64

Figure 76 Diagrammatic representation of the *Kannemeyeria* external adductor musculature 65

Figure 77 Diagrammatic representation of the posterior adductor and the internal adductor musculature 66

Figure 78 Phase One of the *Kannemeyeria* masticatory cycle 67

Figure 79 Force diagram depicting the movements of the lower jaw during Phase One of the *Kannemeyeria* masticatory cycle . . 68

Figure 80 Phase Two of the *Kannemeyeria* masticatory cycle . . . 69

Figure 81 Force diagrams depicting the movements of the lower jaw during Phase Two of the *Kannemeyeria* masticatory cycle . . 70

Figure 82 Masticatory cycle of *Kannemeyeria* 71

LIST OF ABBREVIATIONS

Cranial

a.bpt - anterior process of the basipterygoid
ao.s - antorbital sulcus
asr - anterior sphenethmoid ridge
bcr - braincase roof
bo - basioccipital
bot - basioccipital tubera
bpy - basipterygoid of the parasphenoid
bs - basisphenoid
cm - caniniform process of the maxilla
cp - cultriform process
cv - cervical vertebrae
d.ep - dorsal pterygoid process of the epipterygoid
dz - dorsal zygomatic process of the maxilla
e.ac - exoccipital articulation condyle for the proatlas
en - external naris
enr - external naris roof
eo - exoccipital
ep - epipterygoid
ep.af - anterior footplate of the epipterygoid
ep.h - epipterygoid head
ep.pf - posterior footplate of the epipterygoid
f - frontal
f.p - posterior process of the frontal
fm - foramen magnum
fo - fenestra ovalis
gjo - groove for the duct of Jacobson's organ
ic - internal choana
icc - foramen leading to internal carotid canal
ip - interparietal
ipv - interpterygoid vacuity
j - jugal
jf - jugular foramen
lac - lacrimal
lac.f - lacrimal foramen
lc.q - lateral condyle of the quadrate
lf - labial fossa
lo - opening to the labial fossa
lpf - lateral palatal foramen
m - maxilla
mc.q - medial condyle of the quadrate
m.np - nasal plate of the maxilla
mes - mesethmoid
mg - median groove
mj - maxillary-jugal cavity
mnr - median nasal ridge
mor - medial
mtr - medial tympanic ridge
mvf - maxillary fovea
mvr - median ventral ridge
n - nasal
oc - occipital condyle
op - opisthotic
or - orbit roof
os - orbitosphenoid
p - parietal
p.ant - pila antotica
p.pad - palatal pad
p.ptf - posterior post temporal fenestra
p.sq - parietal flange of the squamosal
pa - palatine
par - paroccipital process of the opisthotic
pb - parasphenoid-basisphenoid complex
pbs - para-basisphenoid sulcus
pf - pineal foramen
pgf - pterygoid fossa
plas - plaster of paris
pm - premaxilla
pm.b - broken surface of the premaxilla
po - postorbital
pp - preparietal
pre - presphenoid
prf - prefrontal
pro - prootic
psph - parasphenoid
psph.f - parasphenoid foramen
pt - pterygoid
pt.m - pterygoid process of the maxilla
pt.pf - pterygo-parasphenoid fenestra
ptf - post temporal fenestra
ptf.r - recess of the post temporal fenestra
q.sq - quadrate flange of the squamosal
qj - quadratojugal
qjf - quadratojugal foramen

qjr - quadratojugal recess
ql - quadrate lamina
qr - quadrate ramus of the pterygoid
qre - quadrate recess
rp.psph - rostral plate of the parasphenoid
sm - septomaxilla
so - supraoccipital
sor - supraoccipital ridge
sp - sphenethmoid
sq - squamosal
st - stapes
st.f - stapedial foramen
tb - tabular
tkr - tusk root
tp - temporal plate of the parietal
typ - tympanic process of the opisthotic
v - vomer
v.pa - vertical plate of the palatine
v.tr - ventral tympanic ridge
vf - vidian foramen
vr.f - ventral ridge of the frontal
vz - ventral zygomatic process of the maxilla
z.sq - zygomatic flange of the squamosal
za - zygomatic arch
zp.sq - zygomatic process of the squamosal

Mandible

ang - angular
ap.art - anterior process of the articular
art.r - articular recess
d - dentary
d.pad - dentary pad
d.sh - dentary shelf
dl.d - dorsal ledge of the dentary
dp.d - dorsal plate of the dentary
dr - dentary recess of the angular
dr.d - dorsal ridge of the dentary
ds - dentary symphysis
dt - dentary table
lc.art - lateral condyle of the articular
ldg - lateral dentary groove
ldr - lateral ridge of the dentary symphysis
lg.ds - lateral groove of the dentary symphysis
lhc - limit of horny covering
mc.art - medial condyle of the articular
mcn - medial condylar notch
mdg - median dentary groove
mf - mandibular fenestra
mfe - mandibular fosse
mr.d - medial ridge of the dentary
mr.lc - medial ridge of the lateral condyle of the articular
pra - prearticular
r.art - retroarticular process
rl.ang - reflected lamina of the angular
spl - splenial
sa - surangular
tsk - tusk
vp.d - ventral plate of the dentary
vp.sa - ventral plate of the surangular

Institutional

BP/BPI - Bernard Price Institute for Palaeontological Research, Johannesburg
EL - East London Museum
PE - Port Elizabeth Museum
MACN - Muséo Argentino de Ciencias Naturales, Beunos Aires, Argentina
NMQR - National Museum, Bloemfontein
PVL - Paleontologia de Vertebrados, Instituto Lillo, Tucuman, Argentina
RC - Rubidge Collection, Graaff-Reinet
SAM - South African Museum, Cape Town

Other abbreviations are explained in the text.

CONTENTS

Page

DECLARATION i

ABSTRACT ii

ACKNOWLEDGEMENTS iv

LIST OF FIGURES v

LIST OF ABBREVIATIONS ix

VOLUME ONE

Chapter 1

INTRODUCTION

1.1 The Dicynodont Genus *Kannemeyeria* 1

1.2 Historical Review 3

1.3 Re-evaluation of the Genus *Kannemeyeria* 7

1.4 *Kannemeyeria* as Index Fossil of the Triassic 10

Chapter 2

MATERIALS, METHODS AND PRESERVATION

2.1 *Kannemeyeria simocephalus* and Synonomised Species . . 12

2.1.1 Holotype Specimen 12

2.1.2 Study Sample and Referred Specimens 12

2.2 *Kannemeyeria wilsoni* 18

2.3 *Kannemeyeria cristarhynchus* 19

2.4 *Kannemeyeria argentinensis* 20

2.4.1 Holotype Specimen 20

2.4.2 Referred Specimens 21

Chapter 3

CRANIAL MORPHOLOGY OF THE GENUS *KANNEMEYERIA*

3.1 Introduction: Definitive Aspects of *Kannemeyeria* Cranial Morphology . 22

3.2 General Description 24

3.3 Dermocranium 26

3.3.1 Snout Region 27

3.3.2 Anterior Palate and Nasal Cavity 31

Anterior Palate 31
Nasal Cavity 32
3.3.3 Skull Roof 34
3.3.4 Palatal Region 43
3.4 Neurocranium
3.4.1 Occiput and Braincase 48
Occiput 48
Braincase 54
3.4.2 Sphenethmoid Region 57
Sphenethmoid Complex 58
3.5 Visceral Arch Skeleton 60
3.5.1 Palatoquadrate 60
3.6 Lower Jaw 62
3.7 Discussion 69
3.7.1 Revised Generic Diagnosis 70
Systematic Palaeontology 70
3.7.2 *Kannemeyeria* and Permian Dicynodont Taxa . . . 72

Chapter 4
CRANIAL MORPHOLOGY OF *KANNEMEYERIA SIMOCEPHALUS*
4.1 General Description 75
4.2 Dermocranium 77
4.2.1 Anterior Palate and Nasal Cavity 79
Anterior Palate 79
4.2.2 Skull Roof 79
4.2.3 Palatal Region 81
4.3 Neurocranium 82
4.3.1 Occiput 82
4.4 Visceral Arch Skeleton 82
4.4.1 Palatoquadrate 82
4.5 Lower Jaw 83
4.6 Discussion 85

Chapter 5

CRANIAL MORPHOLOGY OF *KANNEMEYERIA CRISTARHYNCHUS*

5.1 Introduction 87

5.2 General Description 88

5.3 Dermocranium

5.3.1 Snout Region 89

5.3.2 Anterior Palate 91

5.3.3 Skull Roof 92

5.3.4 Palatal Region 93

5.4 Neurocranium

5.4.1 Occiput 95

5.4.2 Sphenethmoid Region 95

5.5 Visceral Arch Skeleton

5.5.1 Palatoquadrate 96

5.6 Lower Jaw 97

5.7 Discussion 98

Chapter 6

COMPARATIVE CRANIAL MORPHOLOGY OF *KANNEMEYERIA ARGENTINENSIS*

6.1 Introduction 103

6.2 General Description 104

6.3 Snout Region 107

6.4 Anterior Palate 108

6.5 Skull Roof 109

Occiput 111

6.6 Palatal Region and Quadrate Complex 112

6.7 Lower Jaw 113

6.8 Discussion 114

Chapter 7

ALLOMETRIC ANALYSIS: ASPECTS OF RELATIVE GROWTH IN *KANNEMEYERIA*

7.1 Introduction 116

7.2 Materials and Methodology

7.2.1 Methodology 117

7.2.2 Materials and Allometric Variables 119

7.3 Relative Growth and Variability 120

7.4 Discussion and Conclusions 124

Chapter 8

VARIATION AND TAXONOMY OF THE GENUS *KANNEMEYERIA*

8.1 Skull Variation Within the Genus *Kannemeyeria*. . . . 126

8.2 Age-Related Variation

8.2.1 Allometric Growth 127

8.2.2 Continuous Growth 128

8.2.3 Temporal Ossification 130

8.3 Distortion Effects 132

8.4 Intraspecific Variation 134

8.5 Revised Specific Diagnoses

8.5.1 *Kannemeyeria simocephalus* 135

8.5.2 *Kannemeyeria cristarhynchus* 137

8.5.3 Taxonomic Status of *Kannemeyeria argentinensis* . . 139

Chapter 9

FUNCTIONAL AND EVOLUTIONARY ASPECTS OF THE *KANNEMEYERIA* CRANIAL MORPHOLOGY

9.1 General 141

9.2 Nasal Capsule 144

9.3 Pterygoid Complex and Sphenethmoid Region . . . 145

9.4 Palatoquadrate 148

9.5 Occipital Musculature and Blood-vessels 150

Chapter 10

LOWER JAW FUNCTION AND THE *KANNEMEYERIA* MASTICATORY CYCLE

10.1 Introduction 154

The Dicynodont Masticatory Cycle 155

10.2 Masticatory Apparatus of *Kannemeyeria* 156

10.3 *Kannemeyeria* Jaw Musculature

10.3.1 External Adductor Musculature . . . 160

10.3.2 Internal Adductor Musculature 162

10.3.3 *Depressor Mandibulae* 163

10.4 Jaw Action and Muscle Forces

10.4.1 Phase One: Depression and Elevation 165

10.4.2 Phase Two: Orthal Movements with the Jaw Closed . . 169

10.5 The Masticatory Cycle of *Kannemeyeria* 171

Chapter 11

CONCLUSIONS

11.1 The *Kannemeyeria* Anatomical Pattern 174

11.1.1 The Genus and Species of *Kannemeyeria* . . . 174

11.1.2 The Anatomical Pattern and Taxonomic Status of *K. argentinensis* 176

11.1.3 Palaeobiogeographic Considerations 177

11.2 Masticatory Cycle of *Kannemeyeria* 182

11.3 Anatomical Patterns and the Consequent Taxonomy of the Triassic Dicynodonts: An Interpretative Diagnosis of *Kannemeyeria* Cranial Morphology 184

11.3.1 Physiological Significance of the *Kannemeyeria* Anatomical Pattern 185

11.3.2 Origins of Triassic Dicynodonts. 185

REFERENCES 187

VOLUME TWO

FIGURES 1

APPENDIX A

A.1 Materials and Methods 72

A.2 List of Reference Specimens 73

APPENDIX B

B.1 Table of Allometric Measurements 74

B.2 Table of Allometric Variables and Results 75
B.3 Cranial Measurements. 76

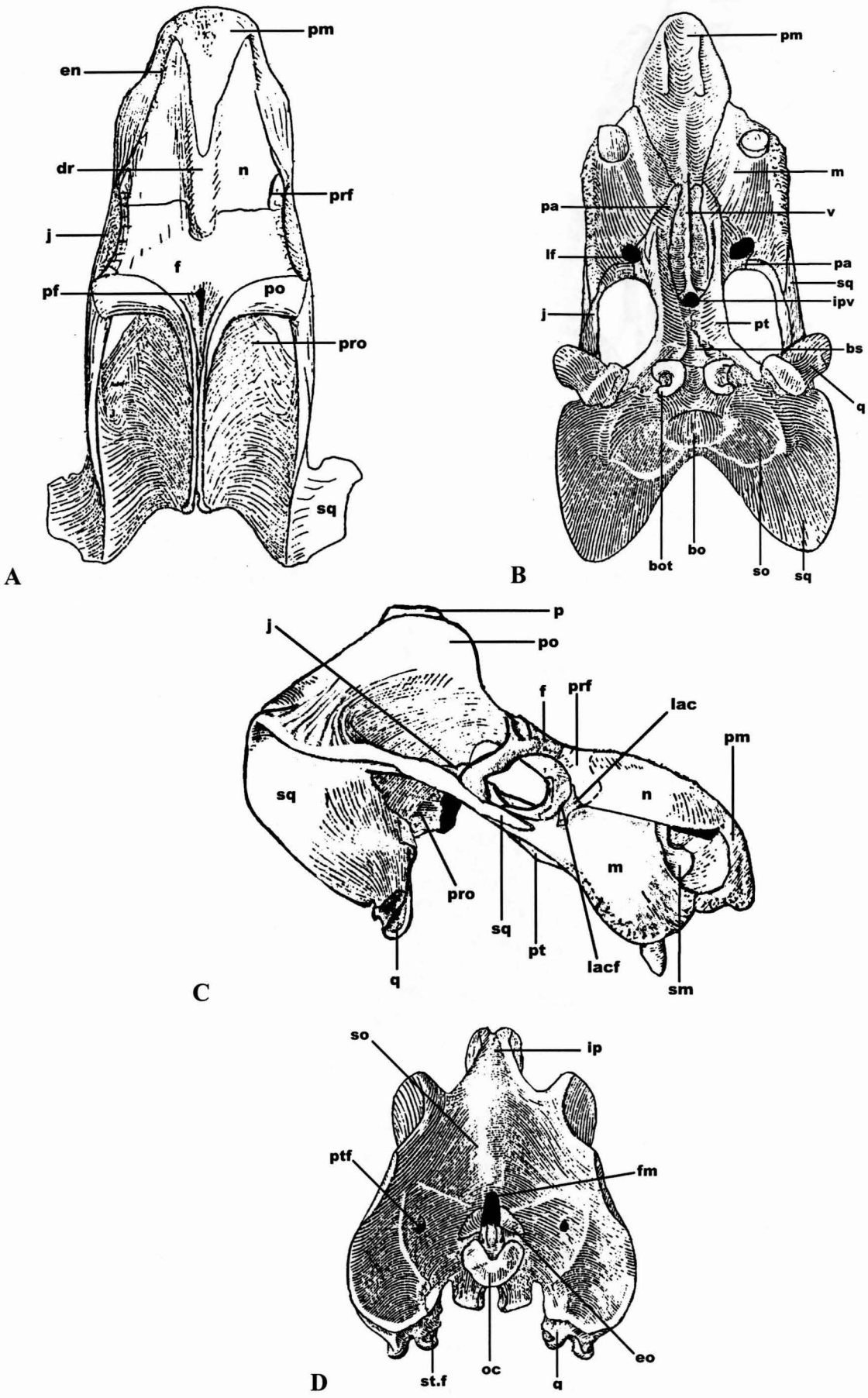


Figure 1. Cranial reconstructions of dorsal **A**, ventral **B**, lateral **C** and occipital **D** views of the genotype of *Kannemeyeria* modified from Pearson (1924a). Not drawn to same scale, abbreviations as on p. xii.

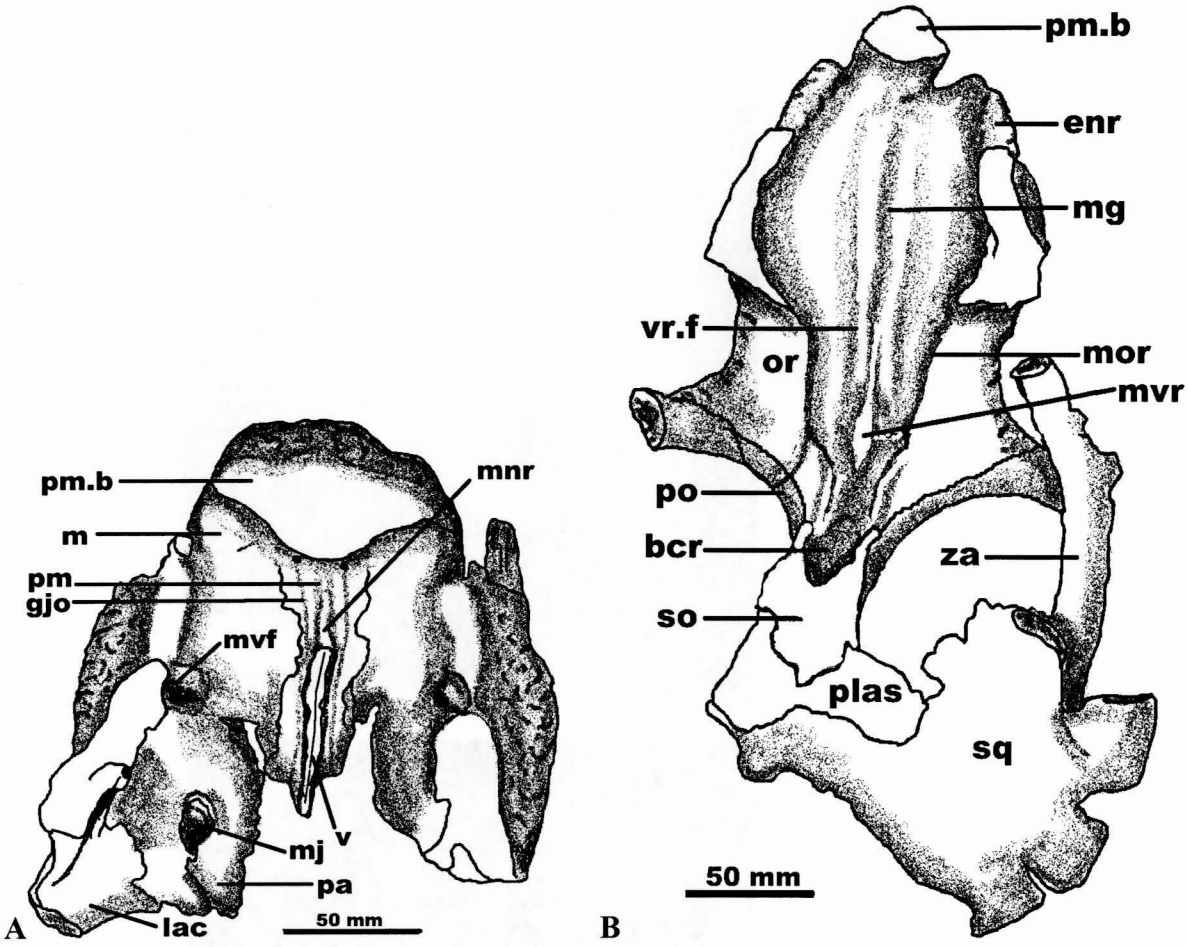


Figure 2. Drawing of the floor of the nasal cavity **A**, and ventral skull roof **B** of specimen BP/1/4648, abbreviations as on p. ix.

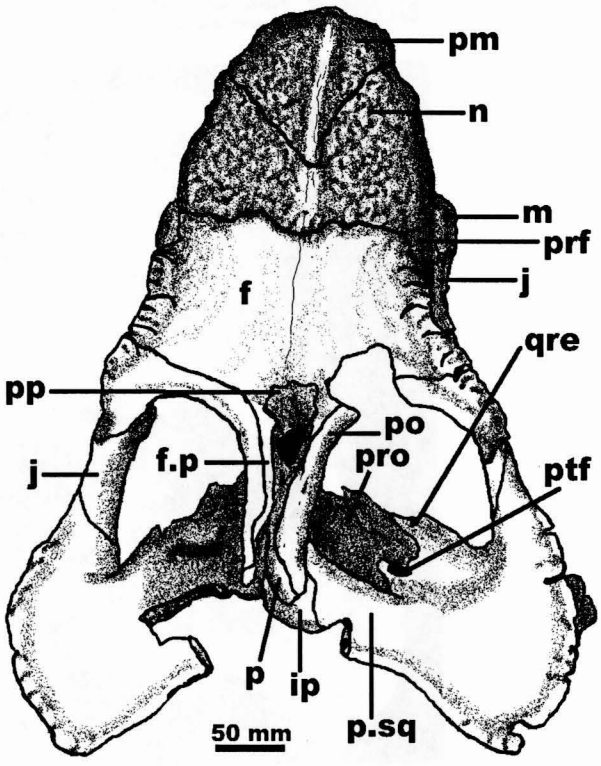
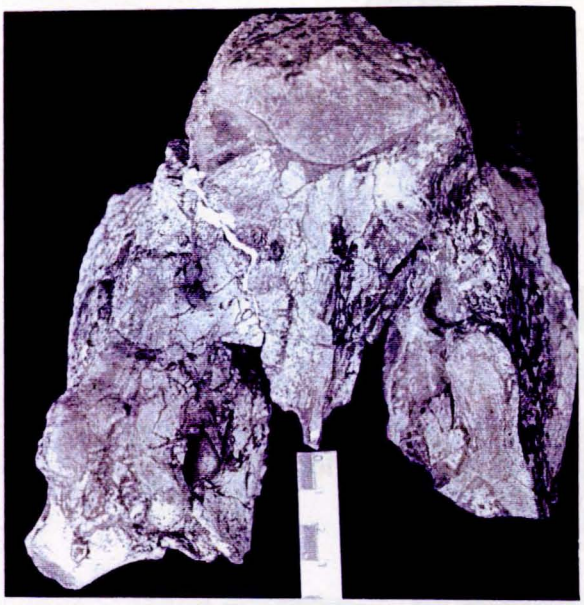
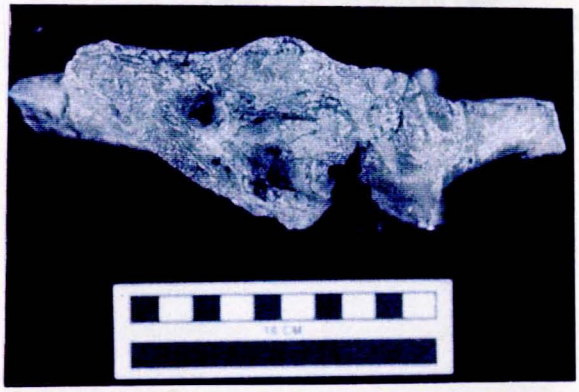


Figure 3. Dorsal view of specimen BP/1/5624, abbreviations as on p. ix.

A



B



C

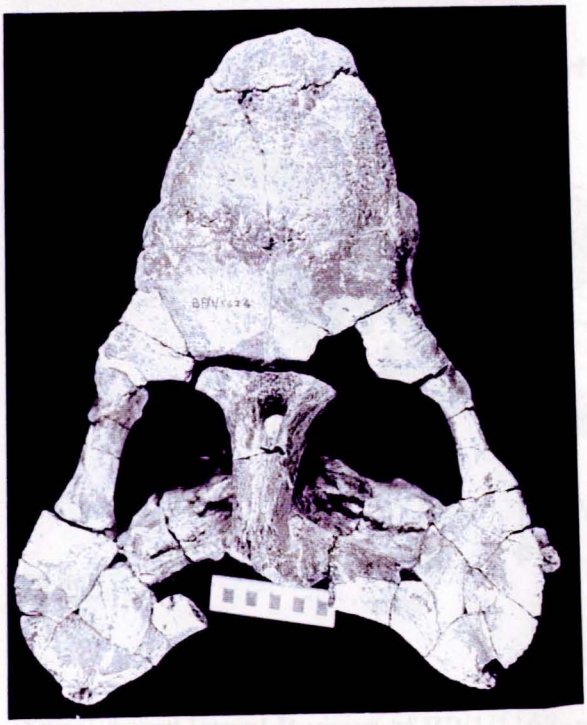


Figure 4. Photographs of the nasal cavity floor **A** and maxillary fovea of the right side of the nasal cavity **B** of BP/1/4648; and the dorsal view of BP/1/5624 **C**.

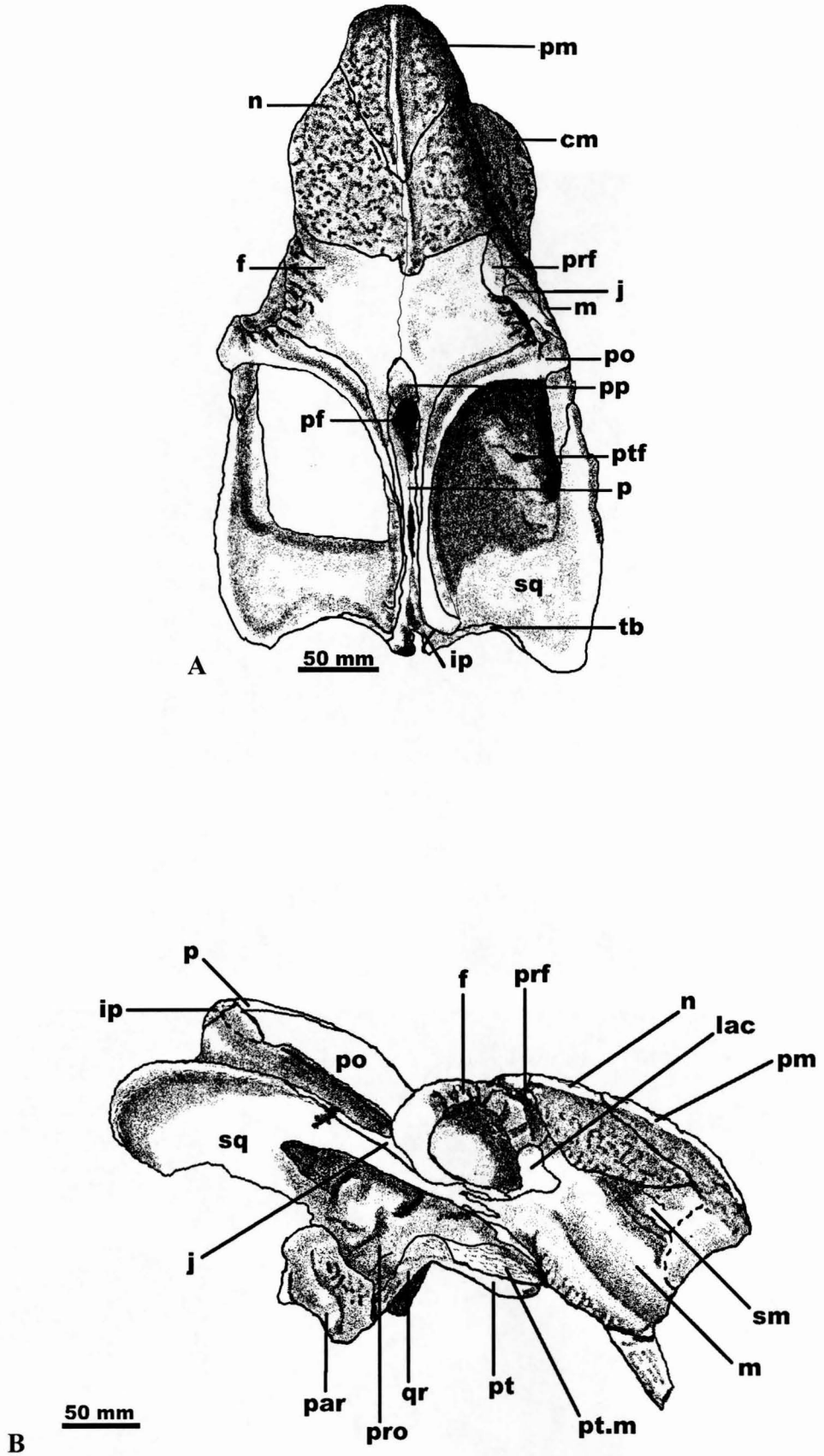


Figure 5. Dorsal **A** and lateral **B** views of BP/1/1168, abbreviations as on p. ix.

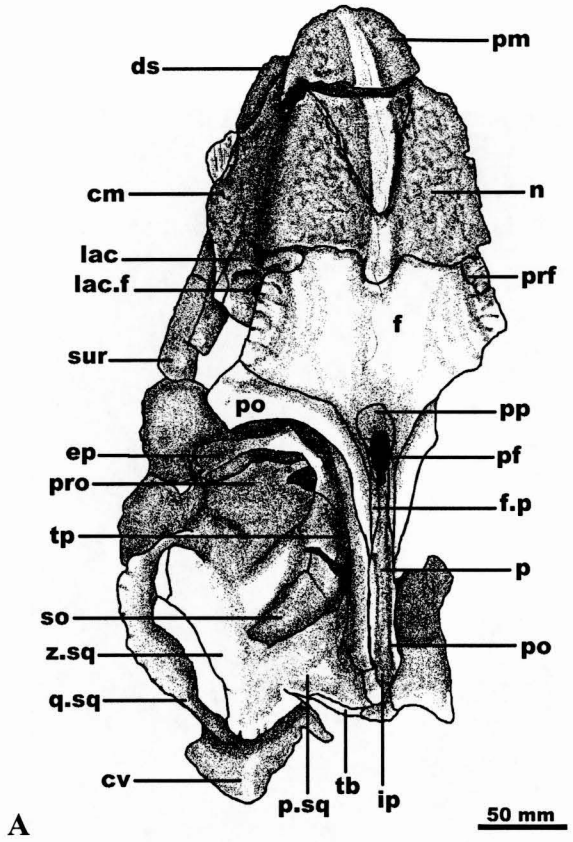
A



B



Figure 6. Photographs of the dorsal **A** and lateral **B** views of BP/1/1168.



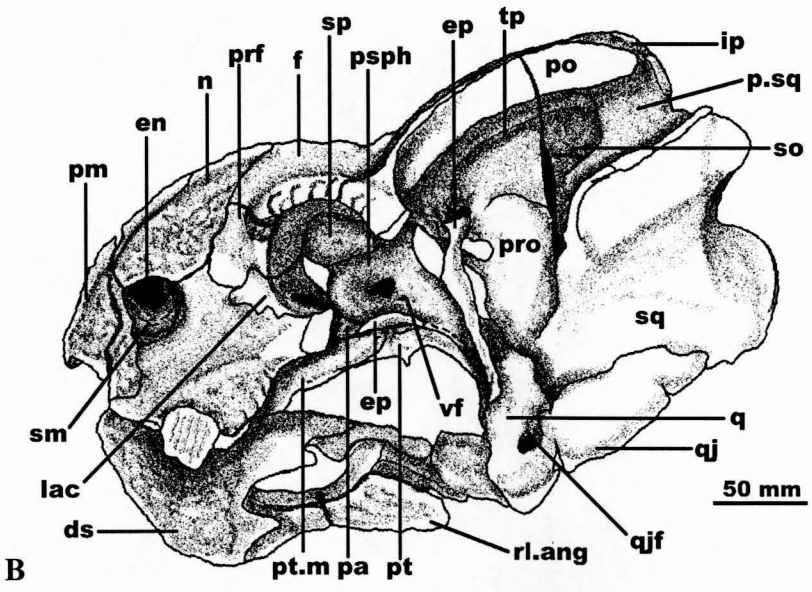


Figure 7. Dorsal **A** and lateral **B** views of SAM/PK/10555, abbreviations as on p. ix.

A



B

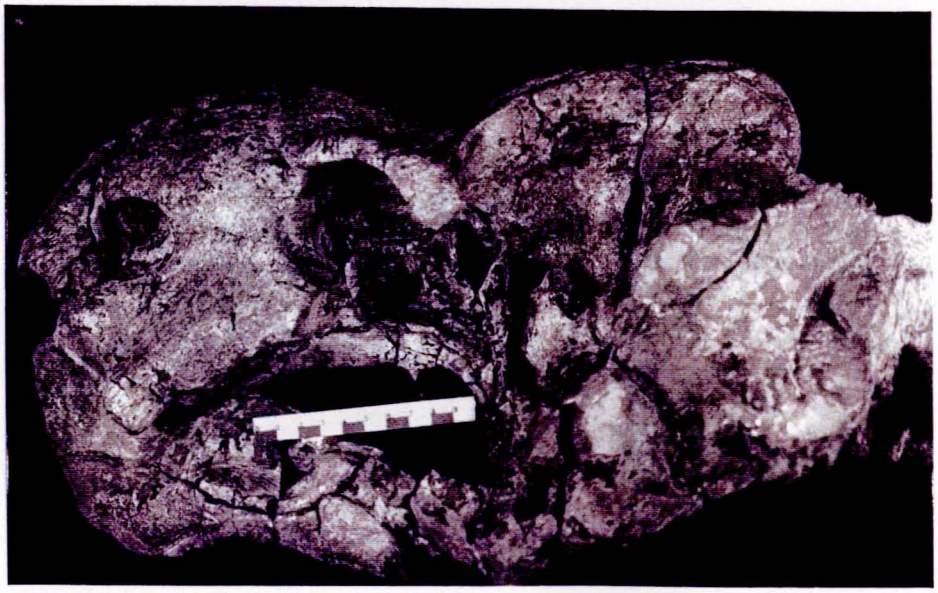


Figure 7. Photographs of the dorsal **A** and lateral **B** views of SAM/PK/10555.

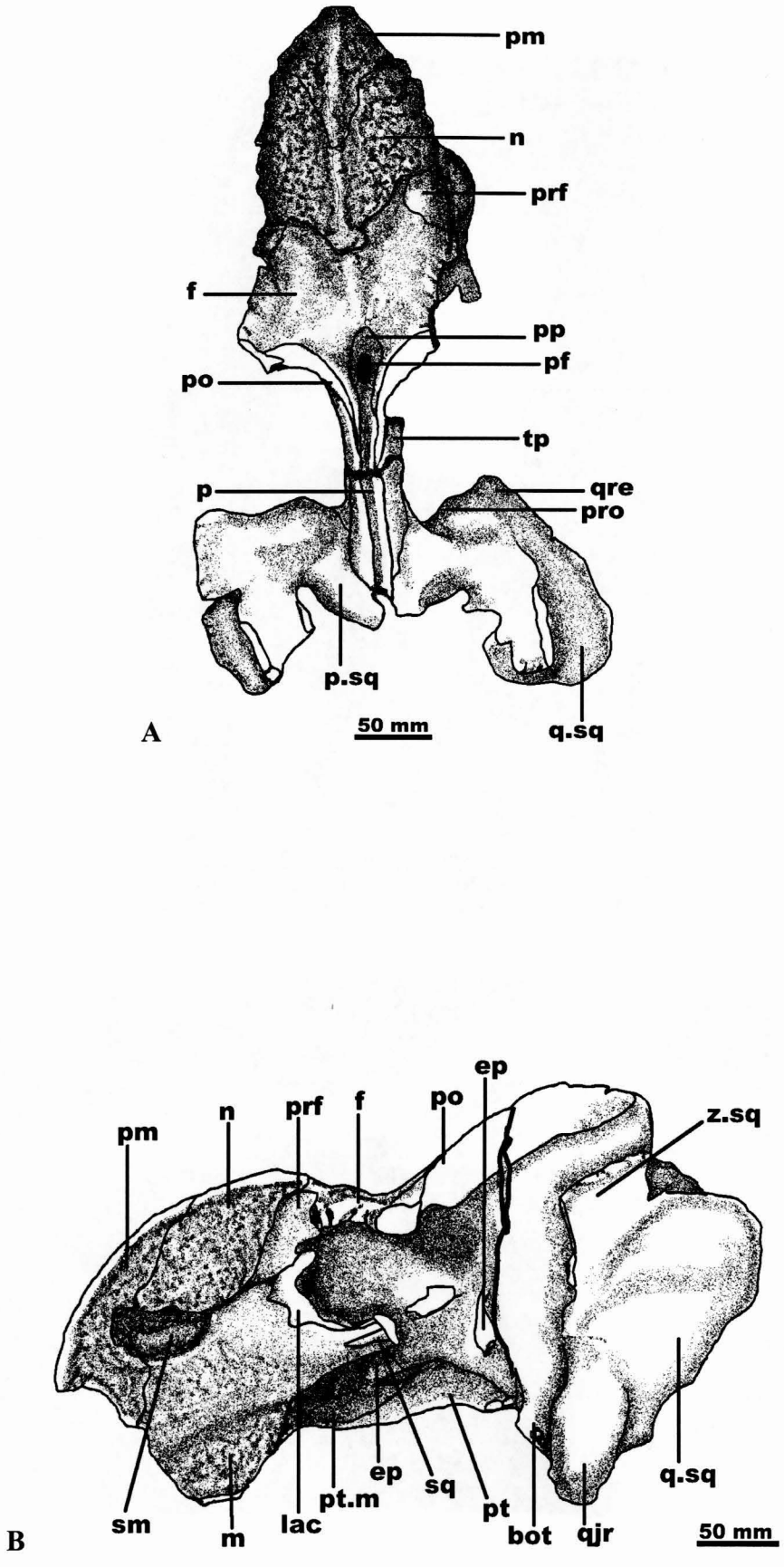
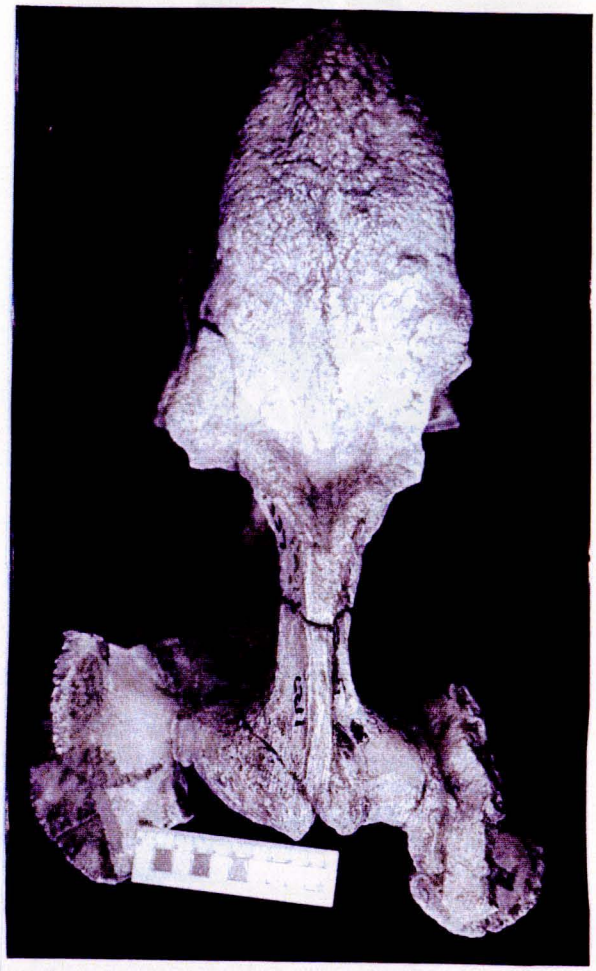


Figure 9. Dorsal **A** and lateral **B** views of NMQR/1127, abbreviations as on p. ix.

A



B

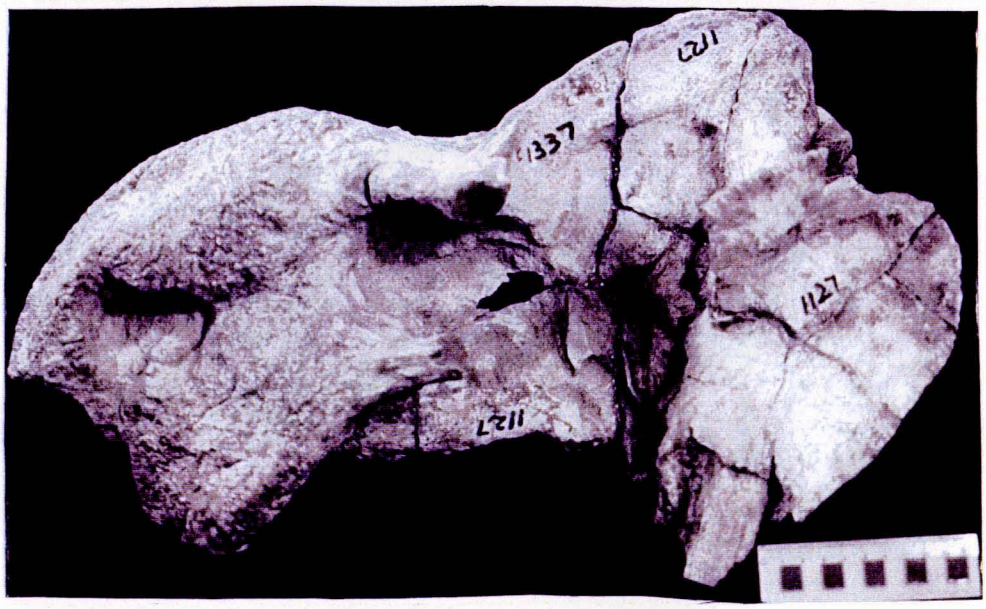
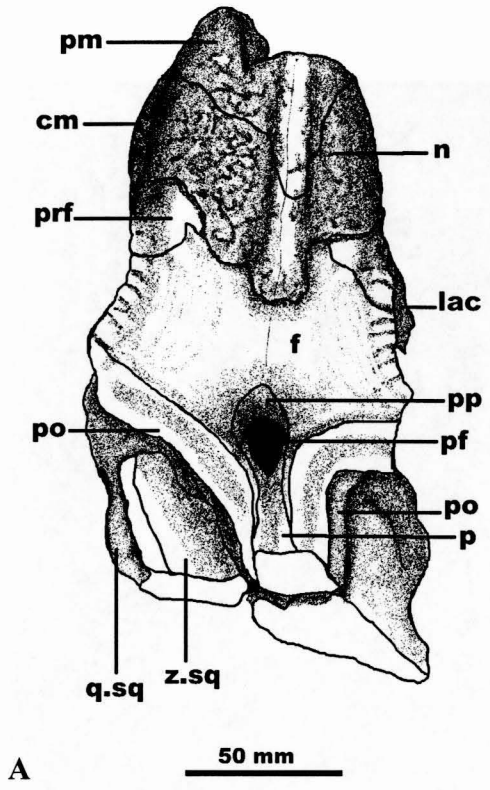


Figure 10. Photographs of the dorsal **A** and lateral **B** views of NMQR/1127

.



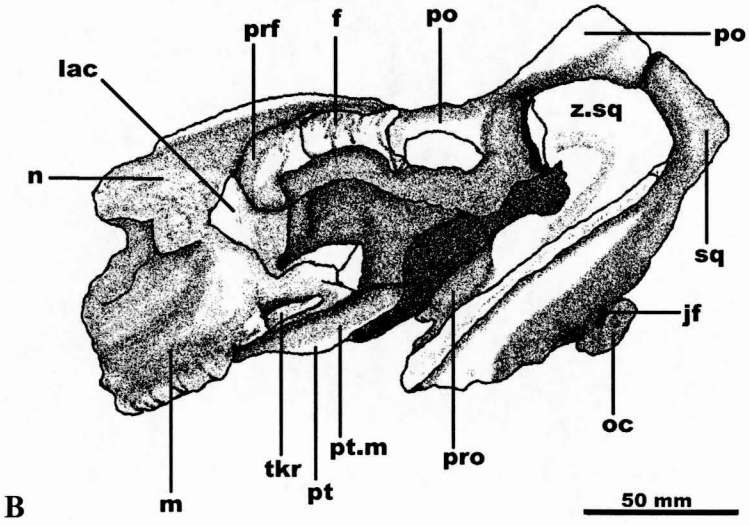
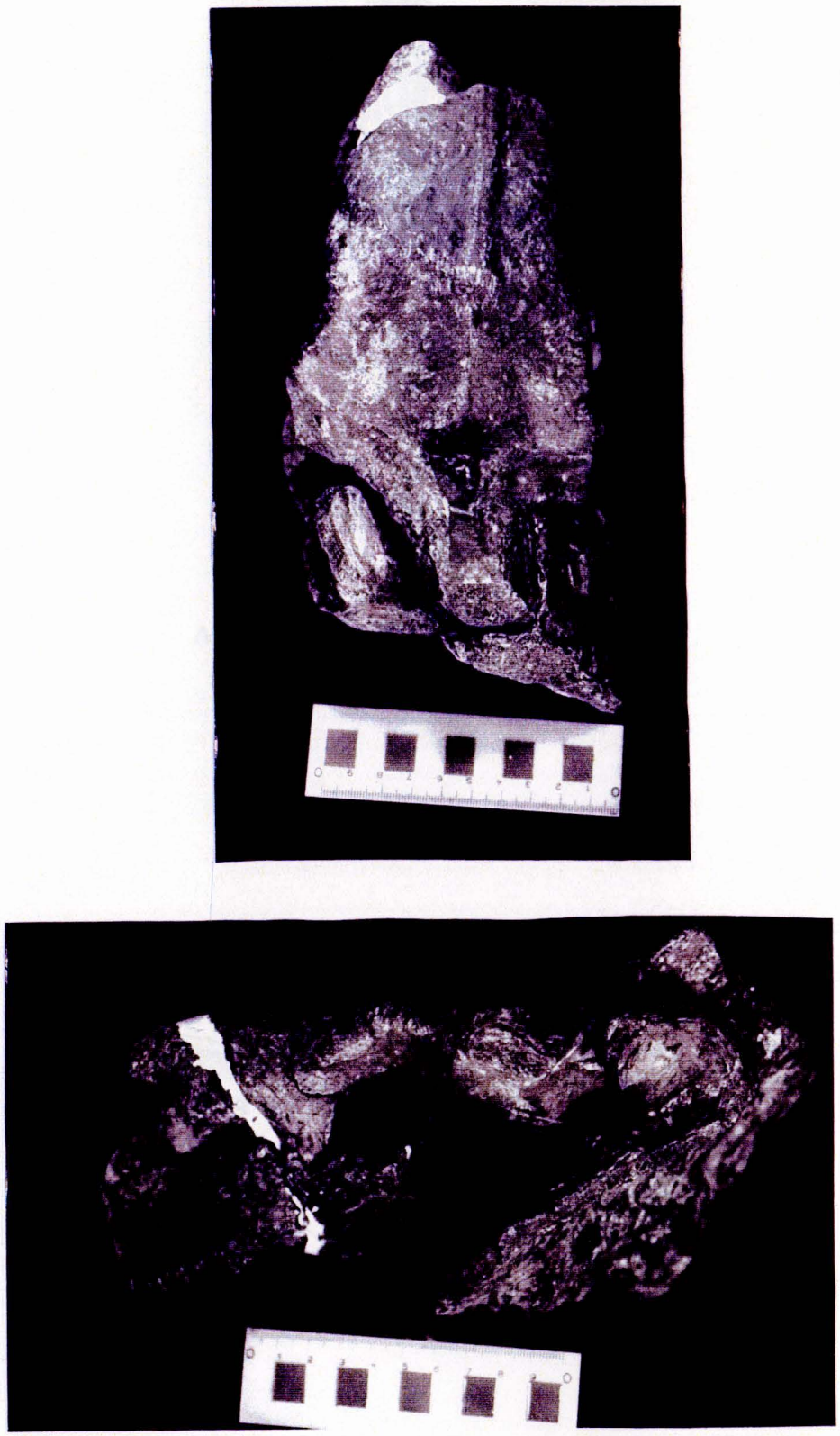


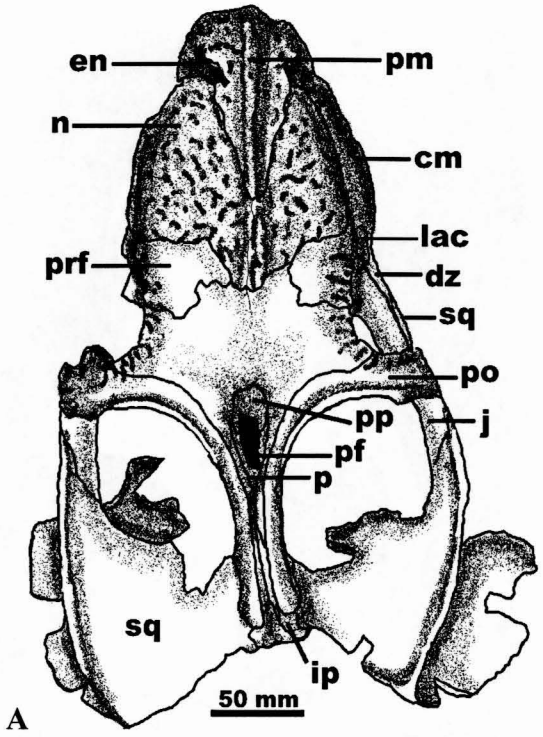
Figure 11. Dorsal **A** and lateral **B** views of PE/1199P (holotype of *K. latifrons* Broom 1913), abbreviations as on p. ix.



A

B

Figure 12. Photographs of the dorsal **A** and lateral **B** views of PE/1199P (holotype of *K. latifrons* Broom 1913)..



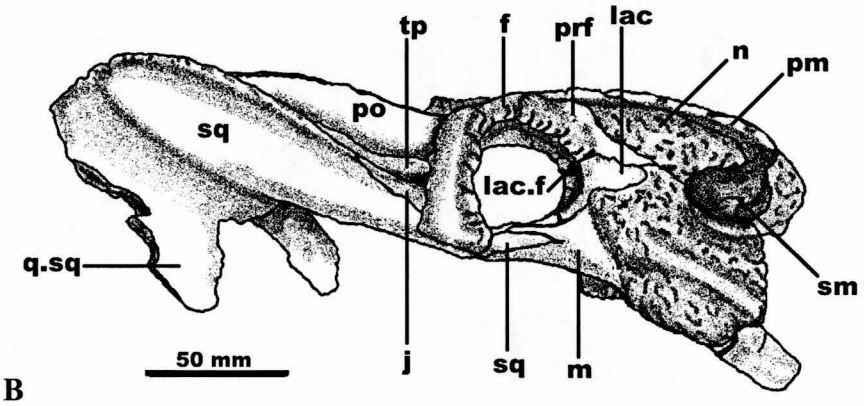
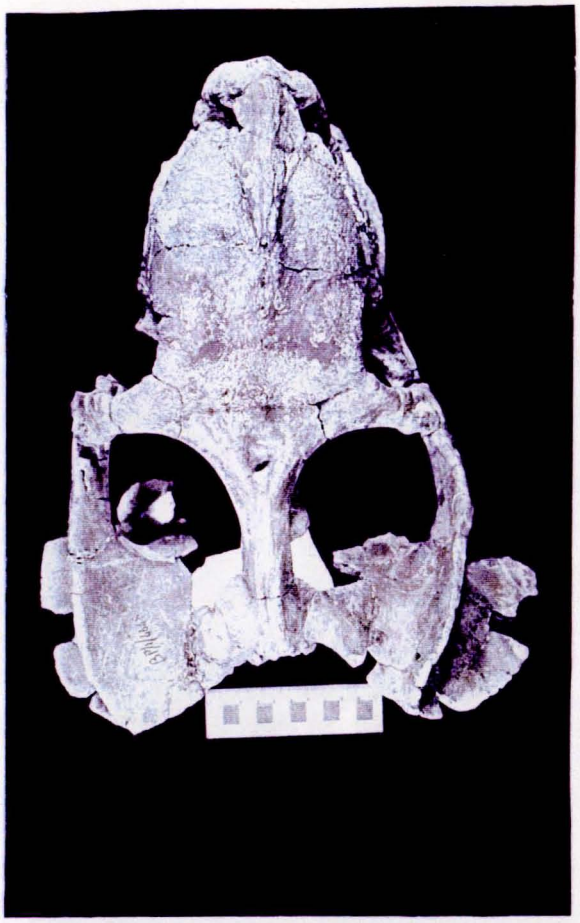


Figure 13. Dorsal **A** and lateral **B** views of BP/1/4648, abbreviations as on p. ix.

A

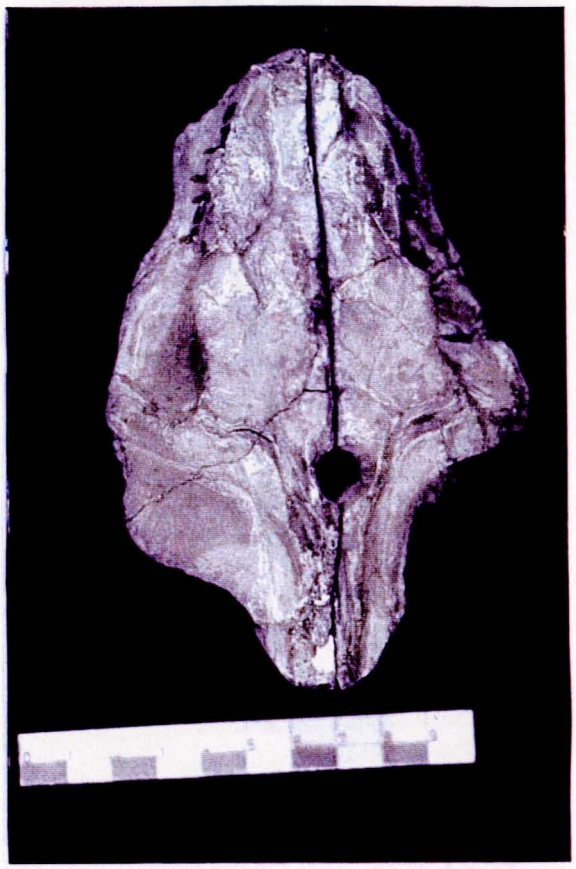


B



Figure 14. Photographs of the dorsal **A** and lateral **B** views of BP/1/4648.

A



B



Figure 15. Photographs of the dorsal **A** and lateral **B** views of BP/1/989.

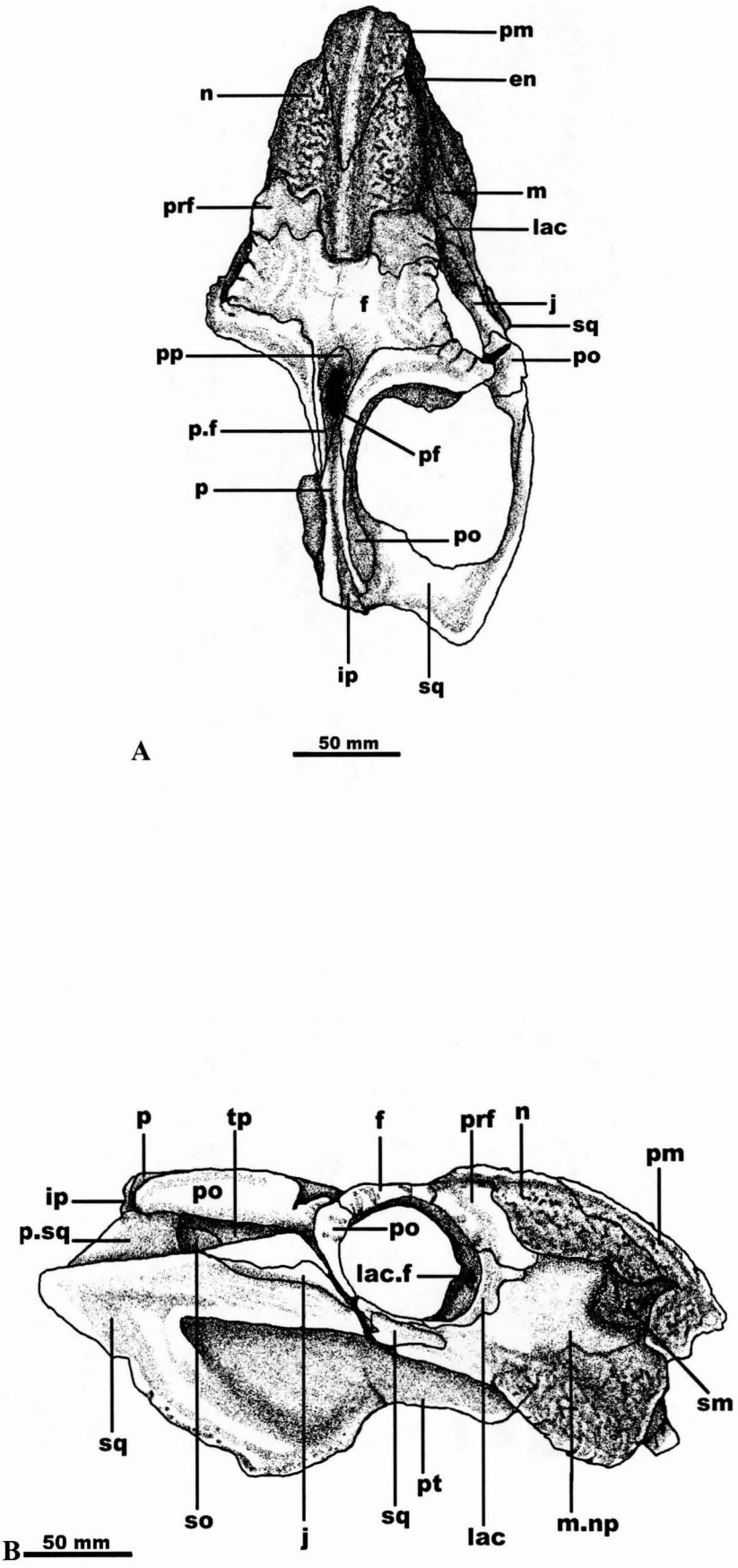


Figure 16. Dorsal **A** and lateral **B** views of BP/1/2092, abbreviations as on p. ix.

A



B

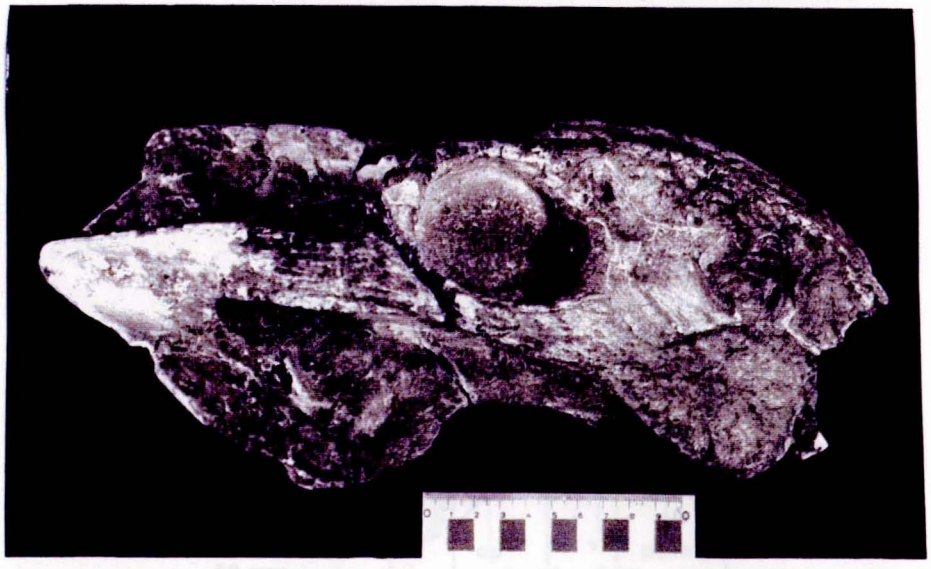
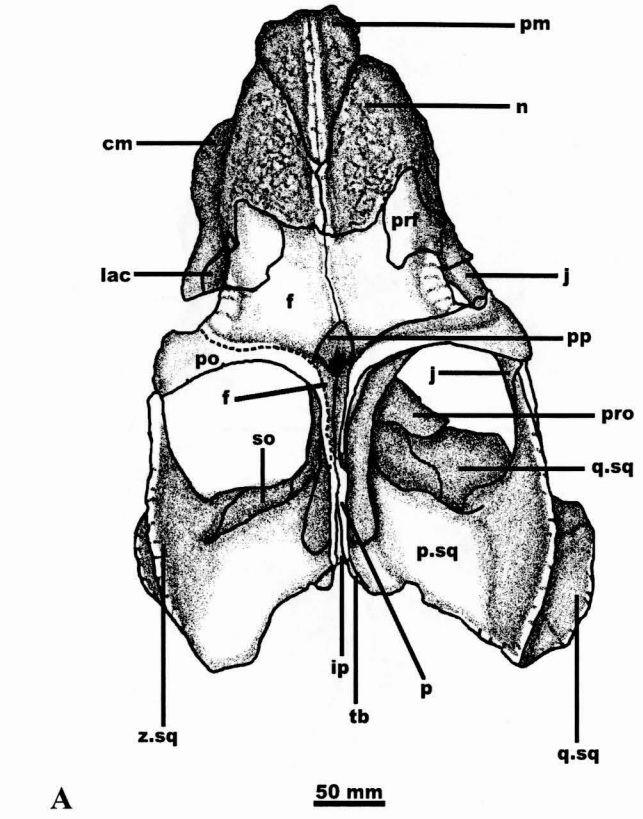


Figure 17. Photographs of the dorsal **A** and lateral **B** views of BP/1/2092.



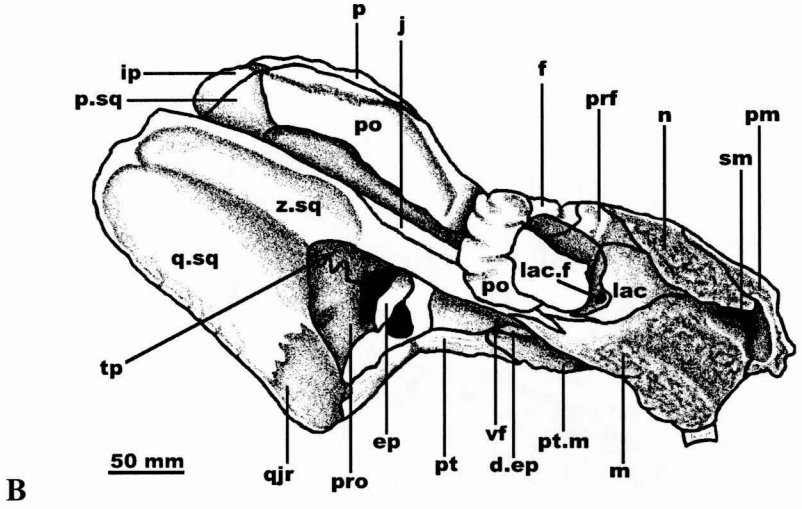


Figure 18. Dorsal **A** and lateral **B** views of SAM/PK/3017 (holotype of *K. erithrea* Haughton 1915), abbreviations as on p. ix.

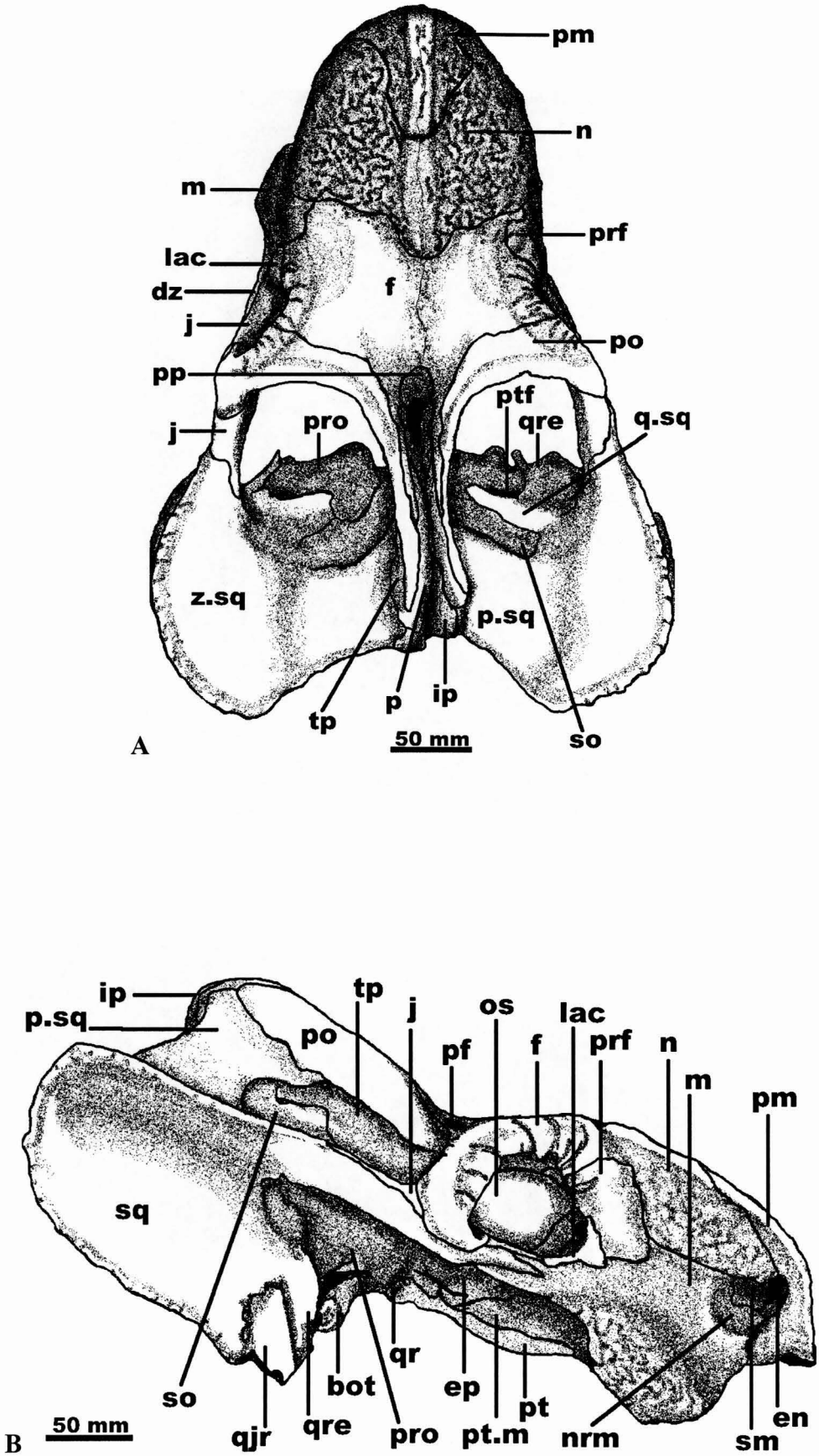


Figure 19. Dorsal **A** and lateral **B** views of BP/1/4523, abbreviations as on p. ix.

A



B

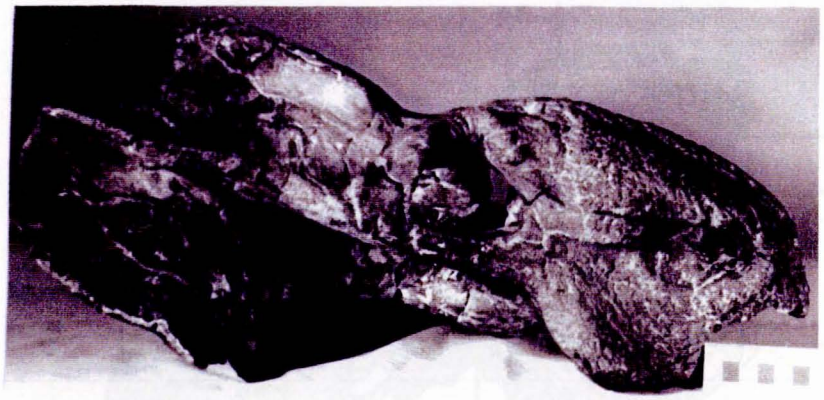
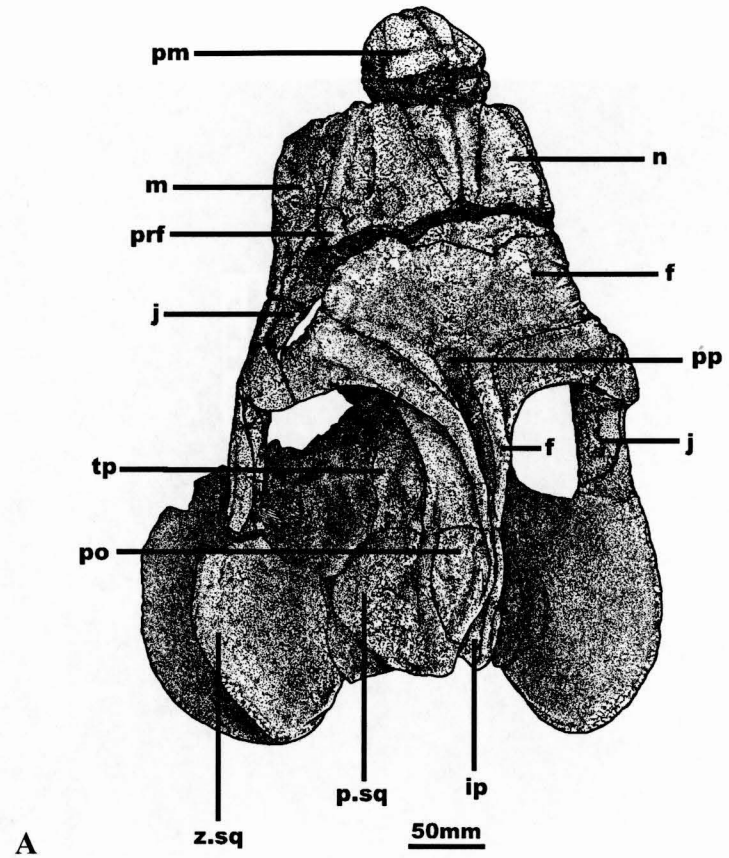


Figure 20. Photographs of the dorsal **A** and lateral **B** views of BP/1/4523.



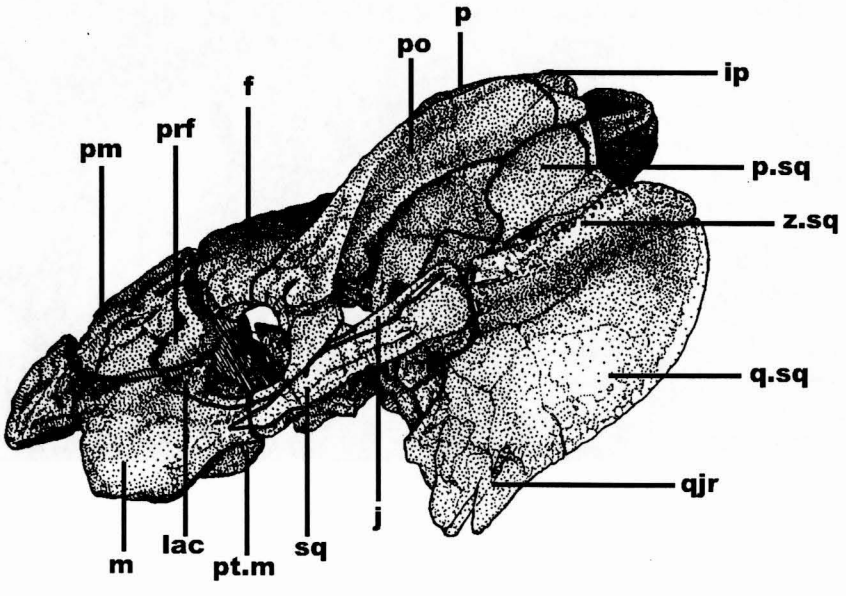
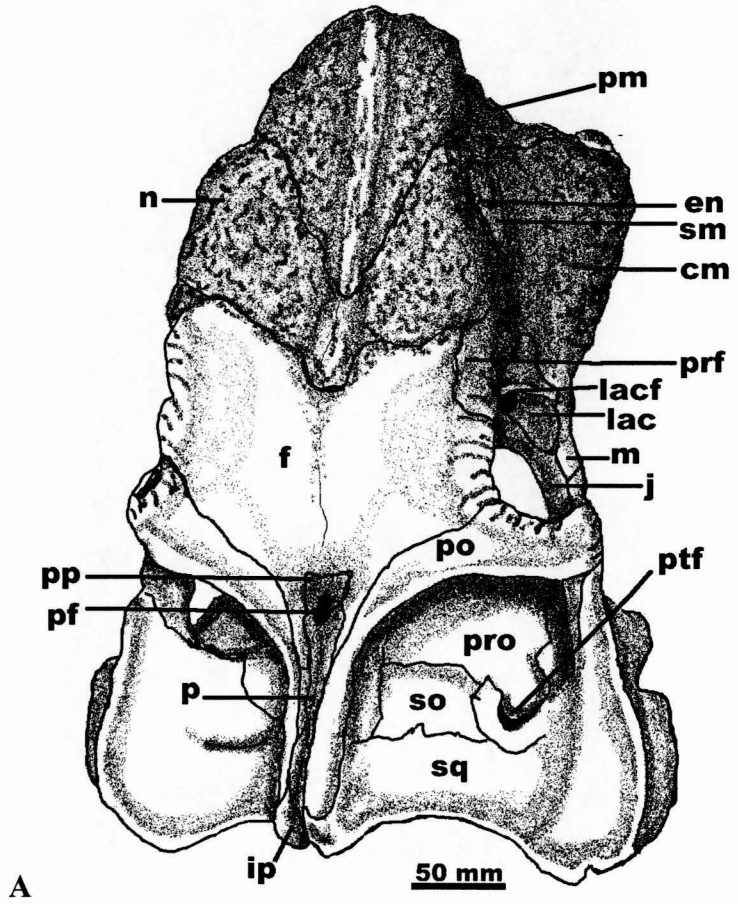


Figure 21. Dorsal **A** and lateral **B** views of EL/1 (holotype of *K. wilsoni* Broom 1937), abbreviations as on p. ix.



Figure 22. Photographs of the dorsal **A** and lateral **B** views of EL/1 (holotype of *K. wilsoni* Broom 1937).



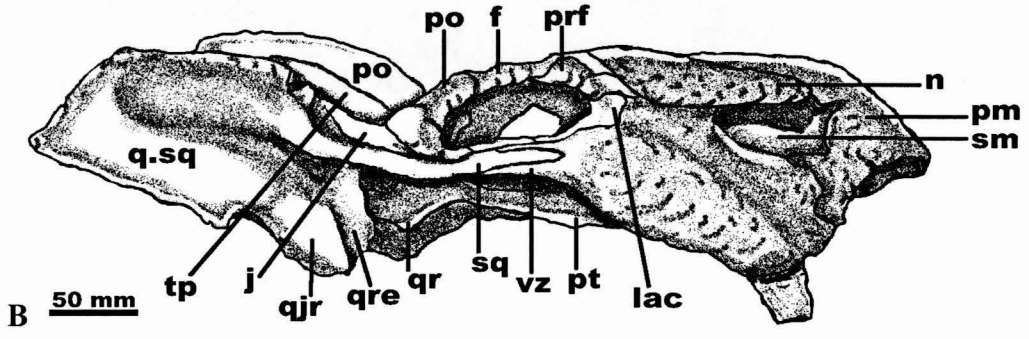


Figure 23. Dorsal **A** and lateral **B** views of BP/1/4524, abbreviations as on p. ix.

A



B

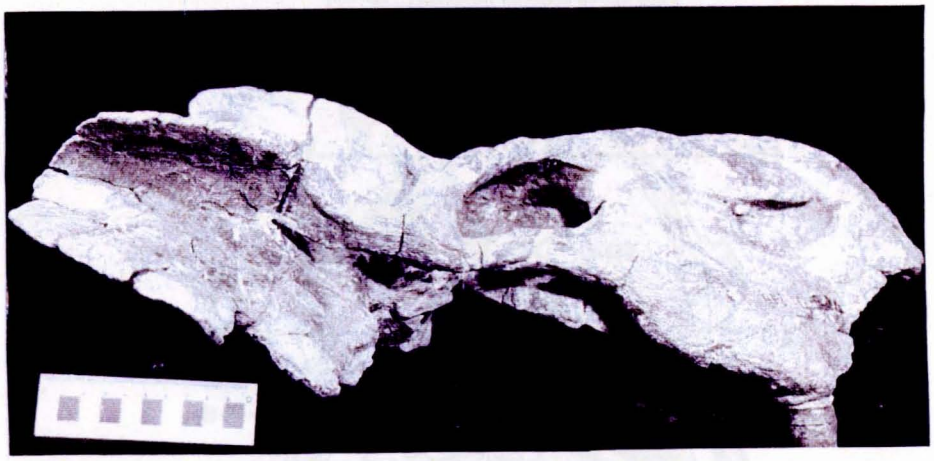


Figure 24. Photographs of the dorsal **A** and lateral **B** views of BP/1/4524.

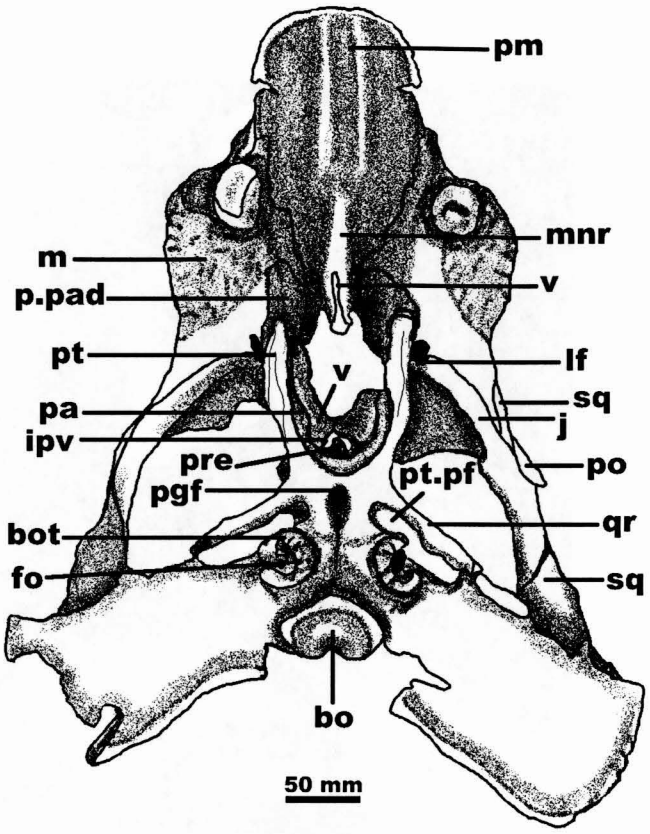


Figure 25. Ventral view of BP/1/5624, abbreviations as on p. ix.

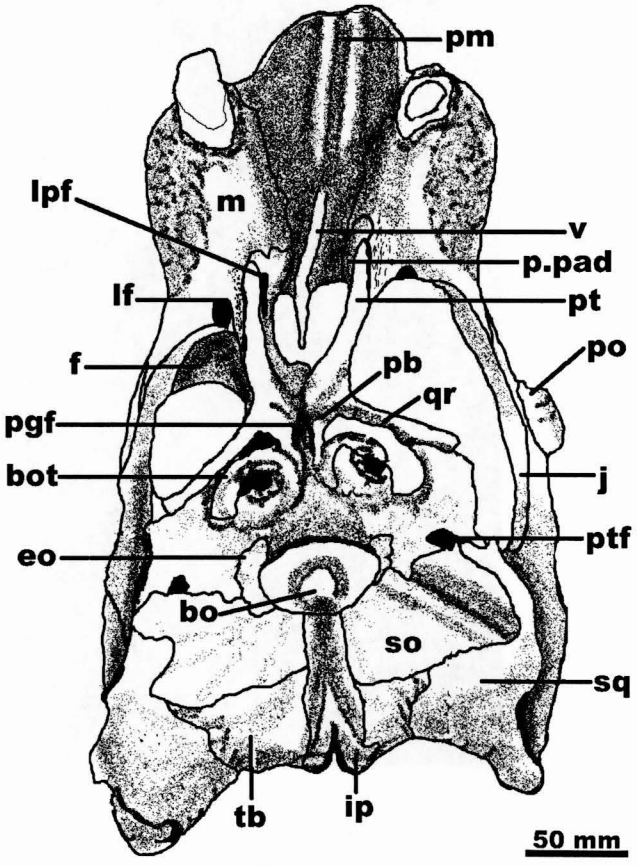
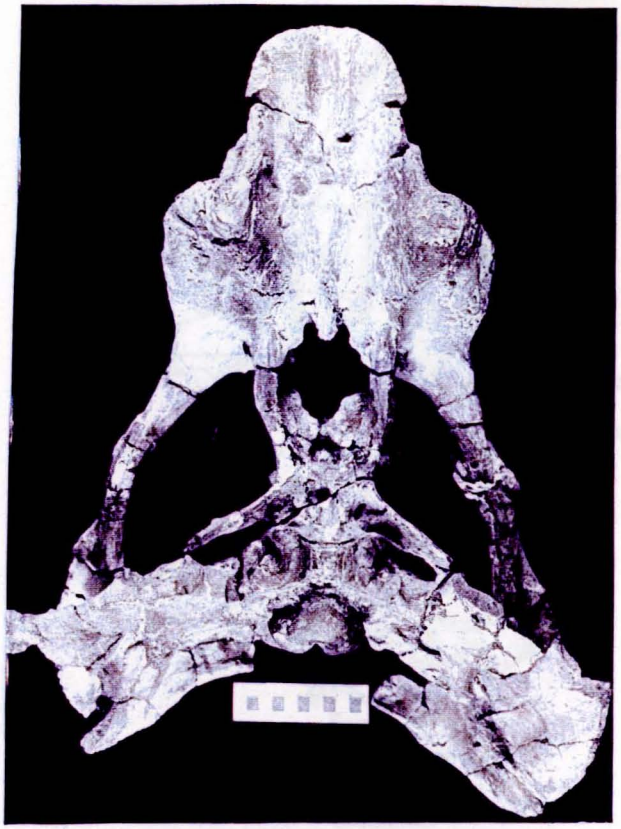


Figure 26. Ventral view of BP/1/1168, abbreviations as on p. ix.

A



B



Figure 27. Photographs of the ventral views of BP/1/5624 **A** and BP/1/1168 **B**.

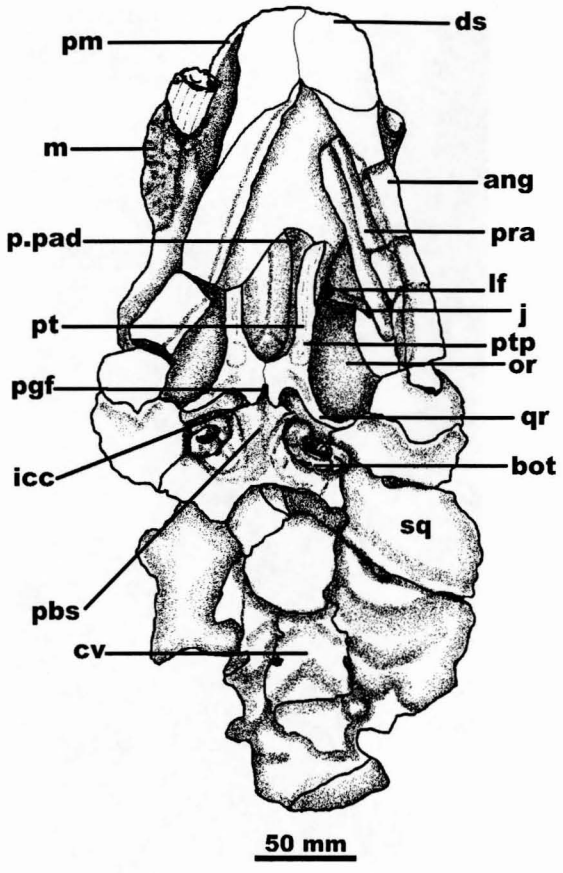


Figure 28. Ventral view of SAM/PK/10555, abbreviations as on p. ix.

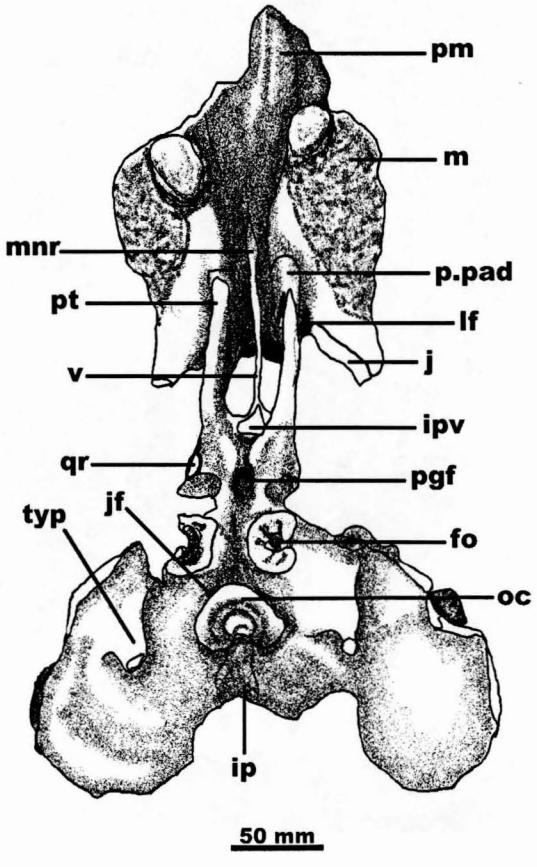


Figure 29. Ventral view of NMQR/1127, abbreviations as on p. ix

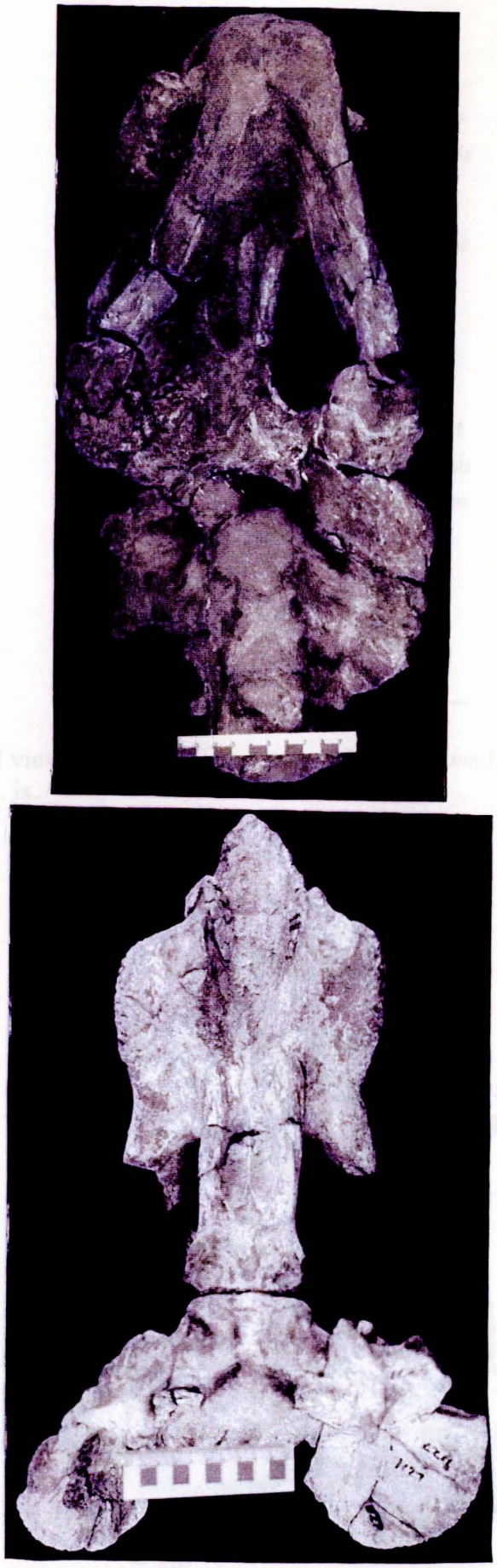


Figure 30. Photographs of the ventral views of SAM/PK/10555 **A** and NMQR/1127 **B**.

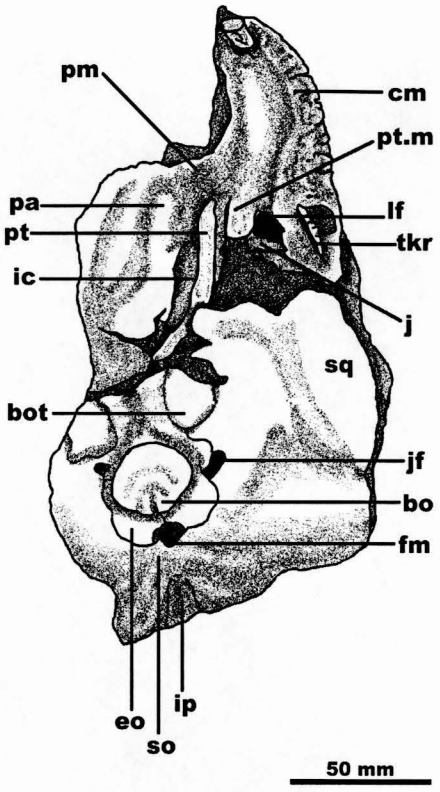


Figure 31. Ventral view of PE/1199P (holotype of *K. latifrons* Broom 1913), abbreviations as on p. ix.

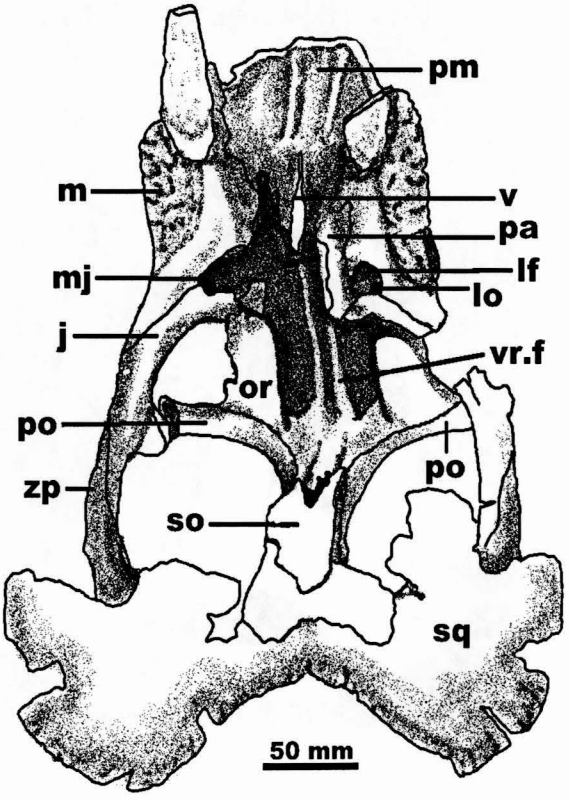


Figure 32. Ventral view of BP/1/4648, abbreviations as on p. ix.

A



B



Figure 33. Photographs of the ventral views of PE/1199P **A** and BP/1/4648 **B**.

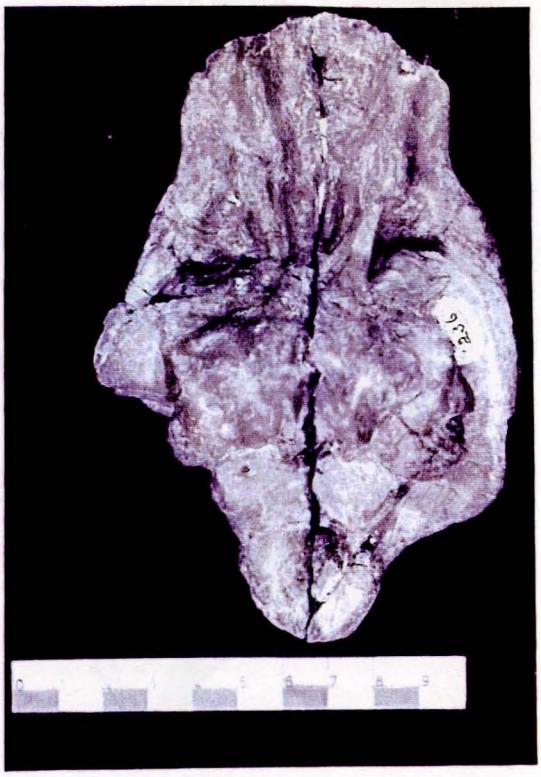


Figure 34. Ventral view of BP/1/989.

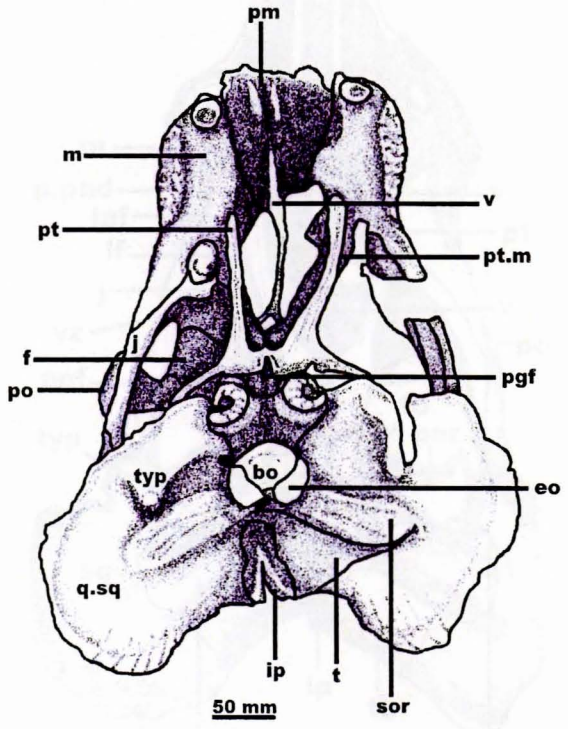


Figure 35. Ventral view of SAM/PK/3017 (holotype of *K. erithrea* Haughton 1915), abbreviations as on p. ix.

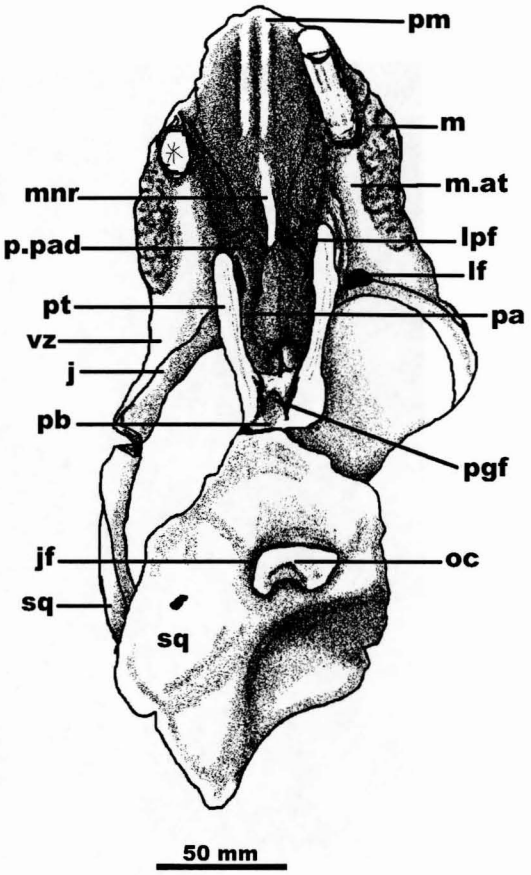


Figure 36. Ventral view of BP/1/2092, abbreviations as on p. ix.

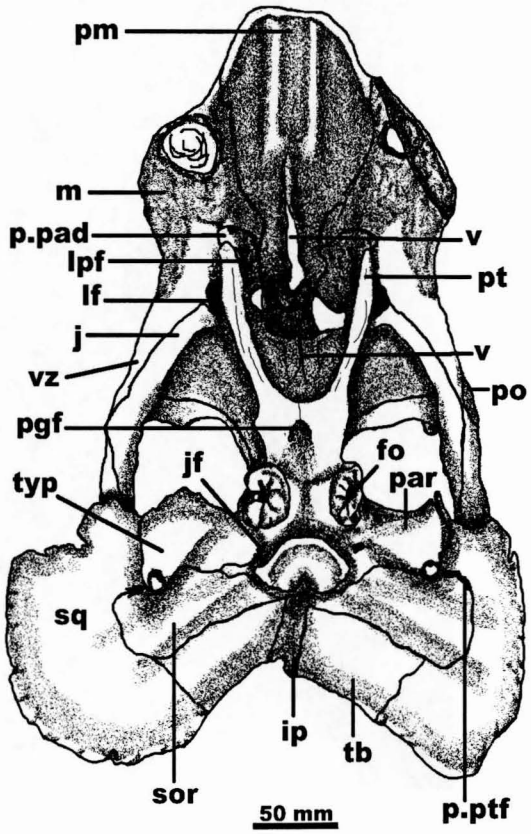


Figure 37. Ventral view of BP/1/4523, abbreviations as on p. ix.

A



B

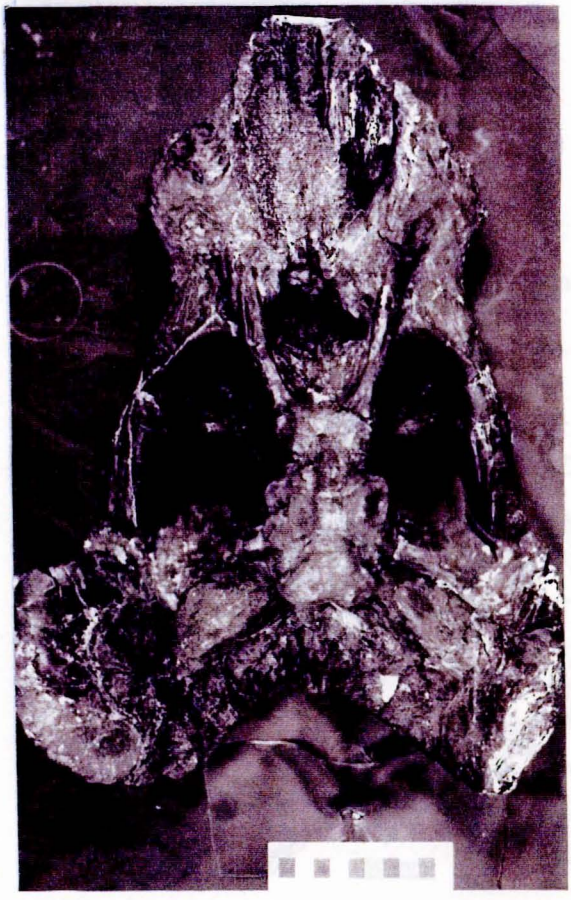


Figure 38. Photographs of the ventral views of BP/1/2092 **A** and BP/1/4523 **B**.

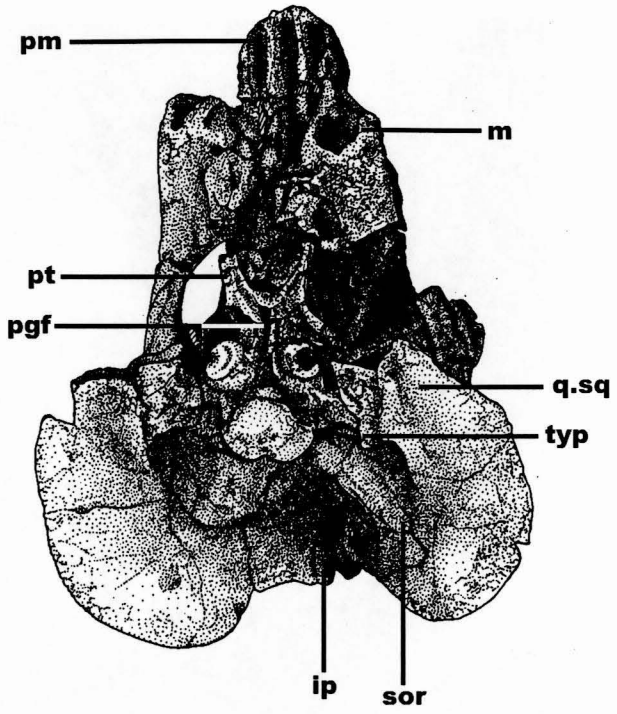


Figure 39. Ventral view of EL/1 (holotype of *K. wilsoni* Broom 1937), abbreviations as on p. ix.

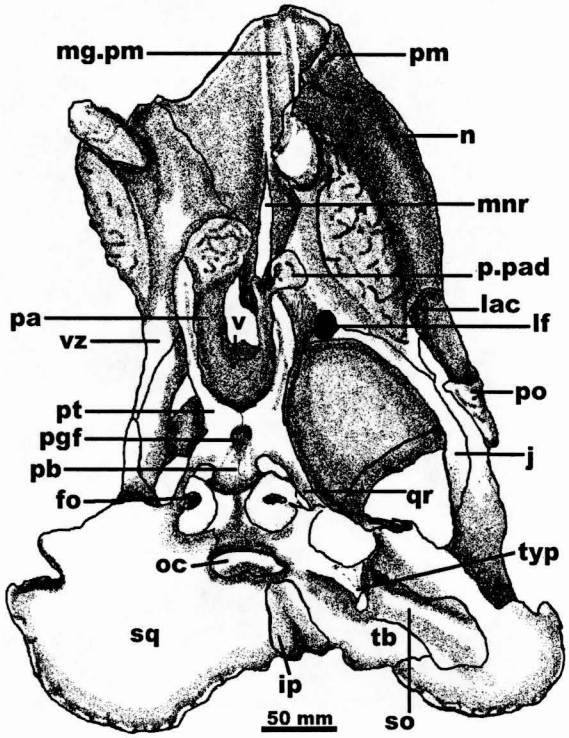
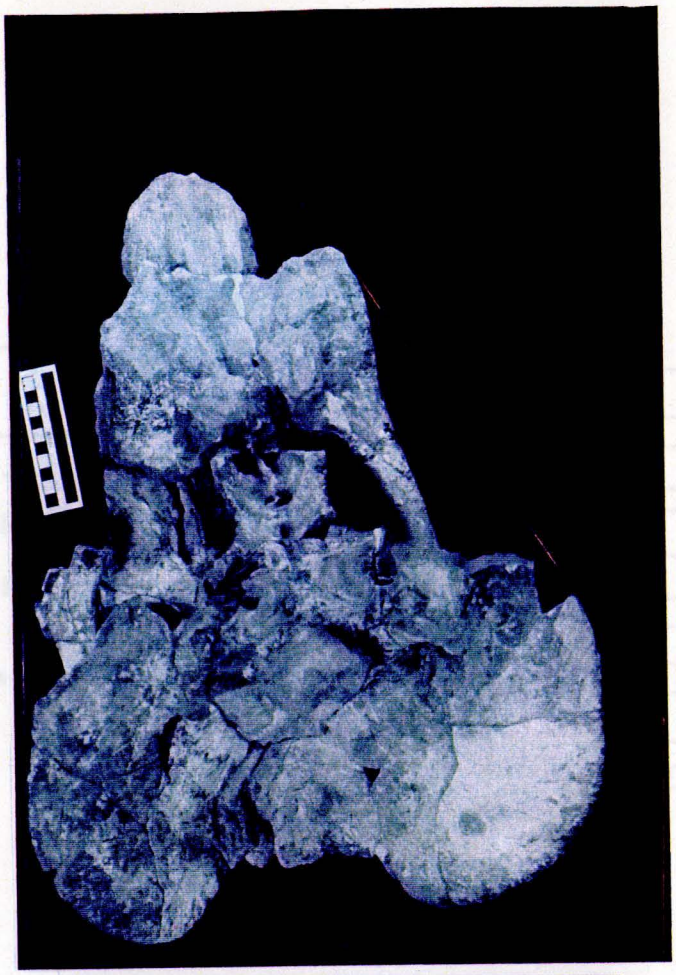


Figure 40. Ventral view of BP/1/4524, abbreviations as on p. ix.

A



B



Figure 41. Photographs of the ventral views of EL/1 **A** and BP/1/4524 **B**.

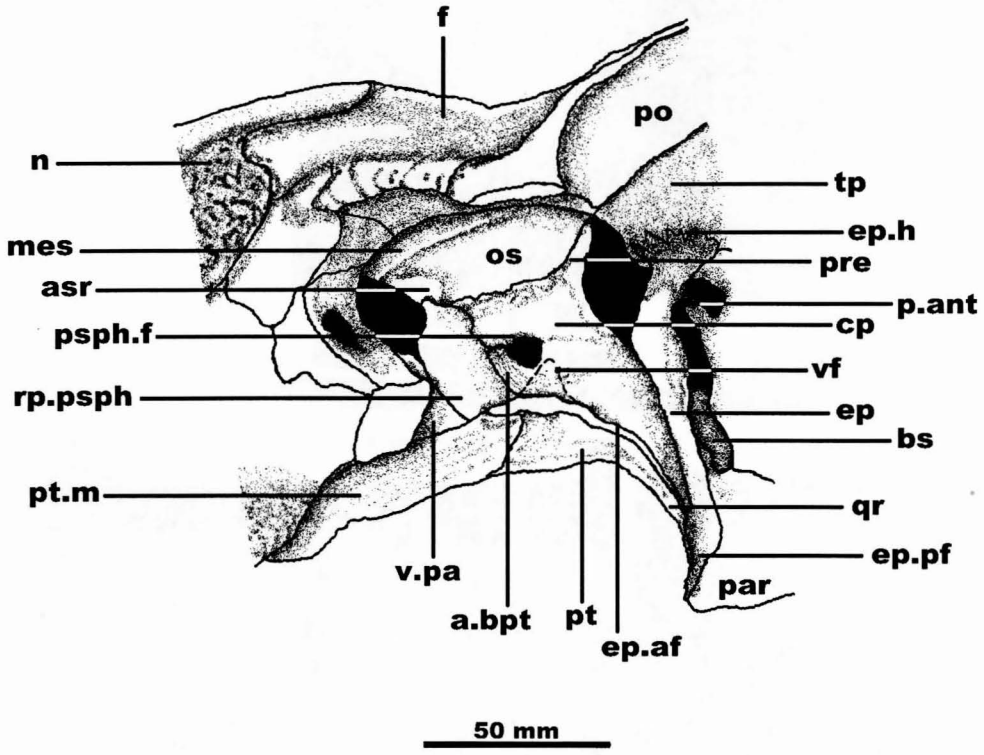


Figure 42. Sphenethmoid region of SAM/PK/3017, abbreviations as on p. ix.

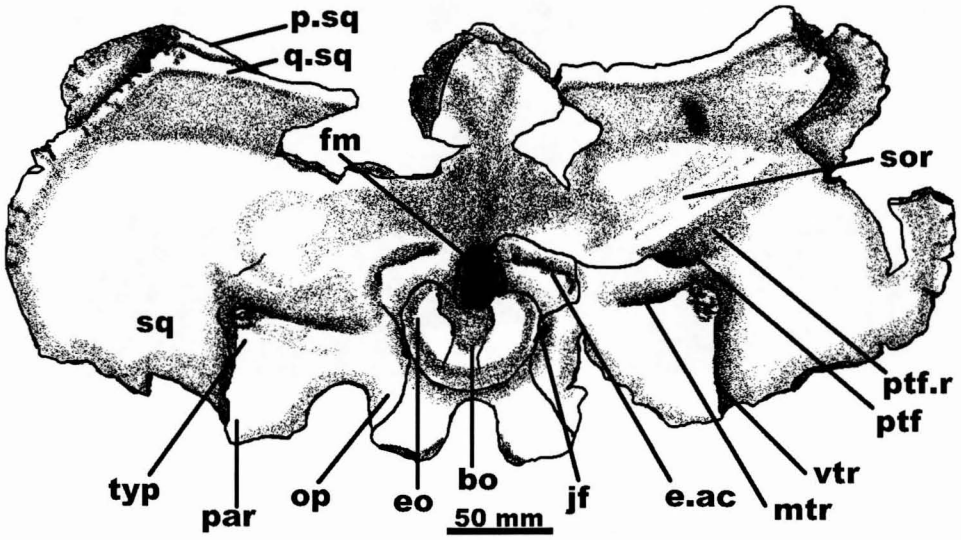


Figure 43. Occipital view of BP/1/5624, abbreviations as on p. ix.

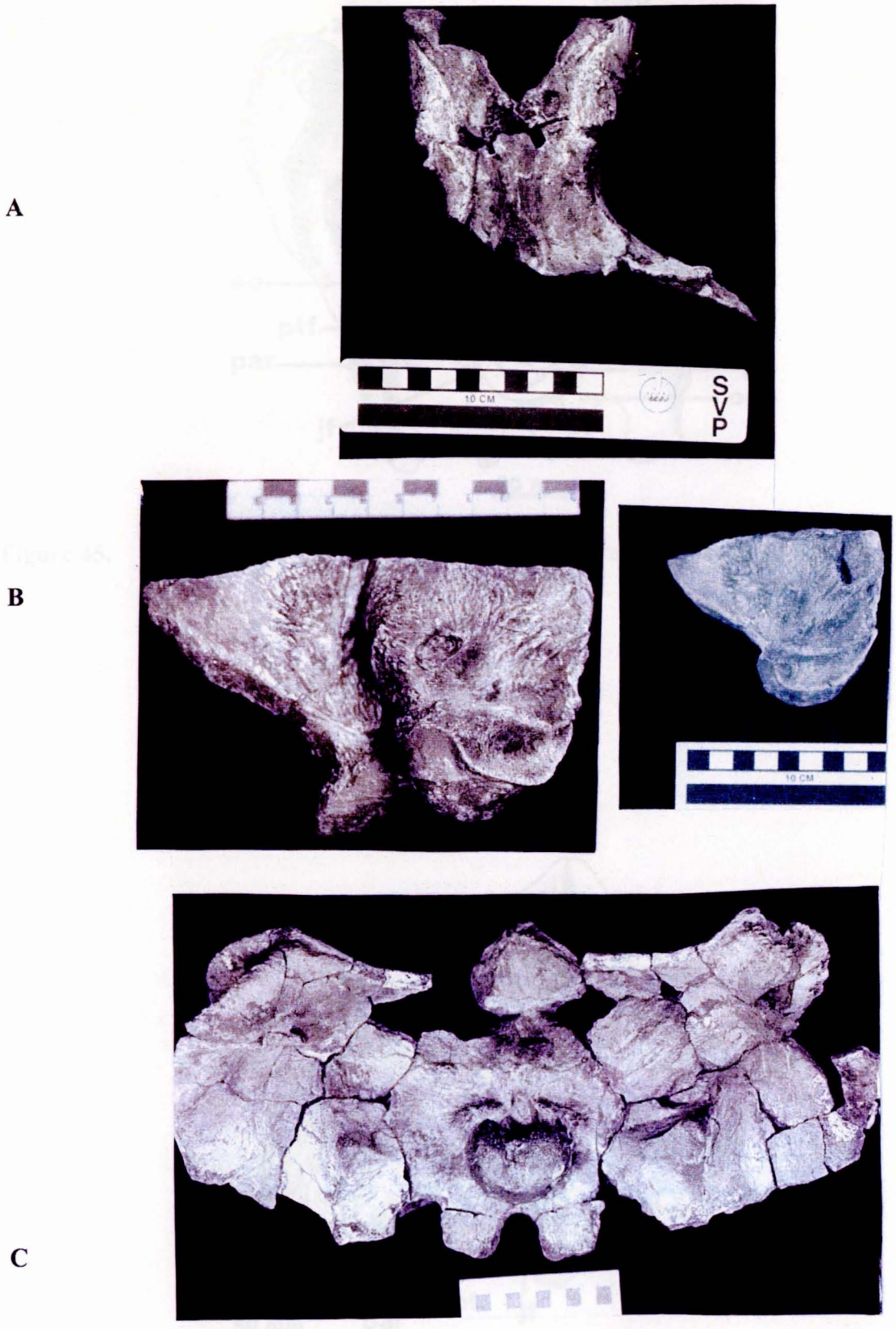


Figure 44. Photographs of the dorsal surface of the basisphenoid **A** of BP/1/5624 showing the dorsal trough and the exit of the internal carotid canals; and the distal end of the quadrate complex of BP/1/5624 showing the stapedial facet and ligament attachment area **B**; and the occiput **C** of BP/1/5624.

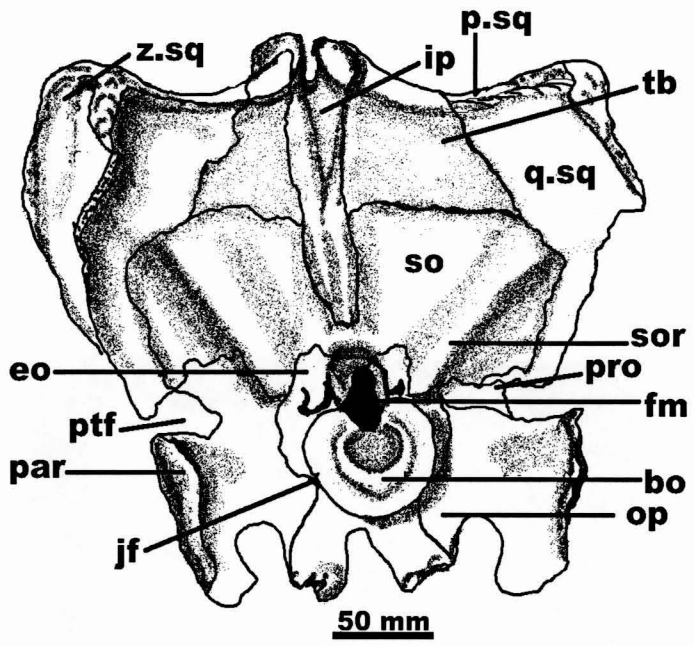


Figure 45. Occipital view of BP/1/1168, abbreviations as on p. ix.

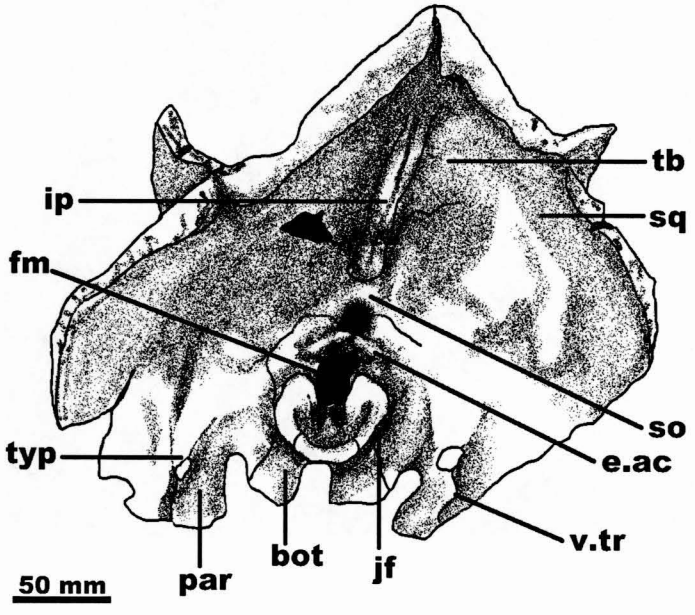


Figure 46. Occipital view of NMQR/1127, abbreviations as on p. ix.

A



B

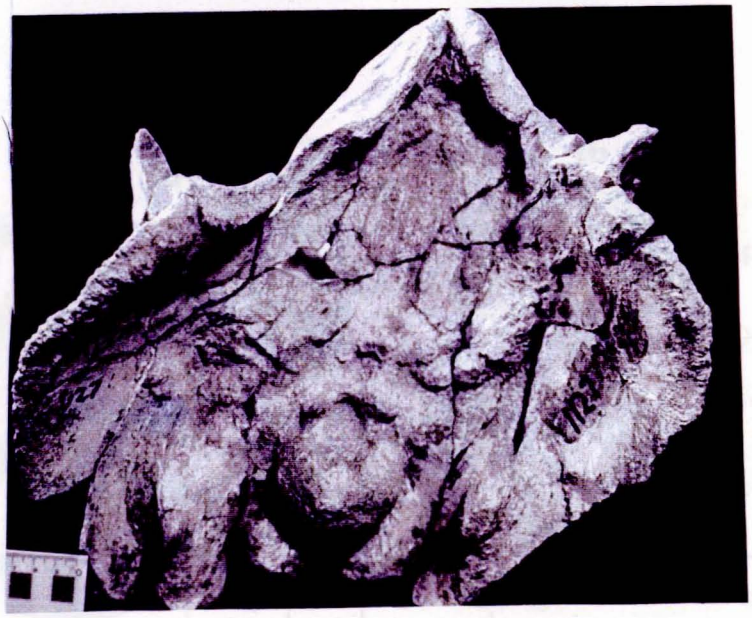


Figure 47. Photographs of the occipital views of BP/1/1168 **A** and NMQR/1127 **B**.

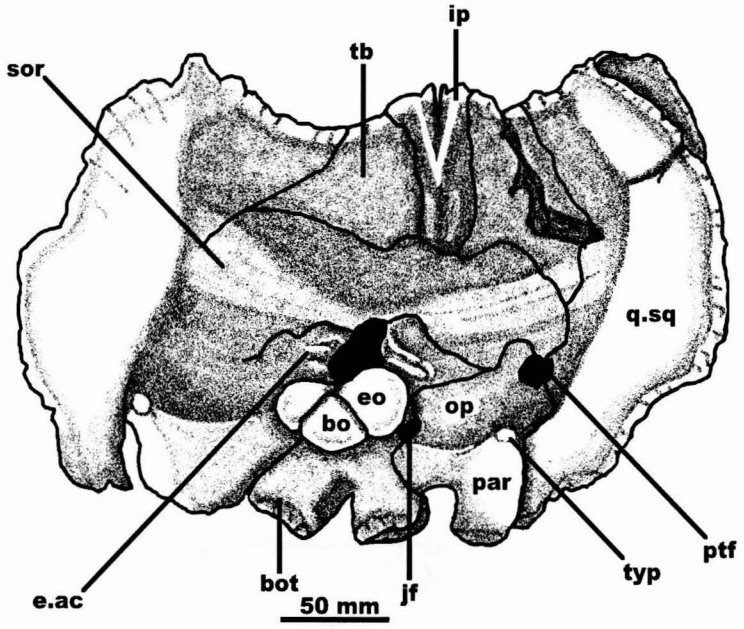


Figure 48. Occipital view of SAM/PK/3017 (holotype of *K. erithrea* Haughton 1915), abbreviations as on p. ix.

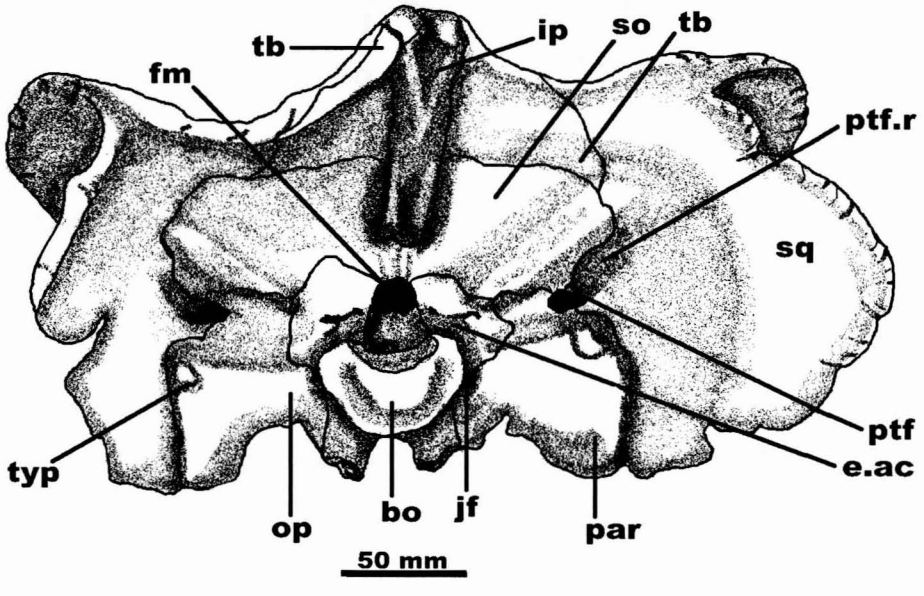


Figure 49. Occipital view of BP/1/4523, abbreviations as on p. ix.

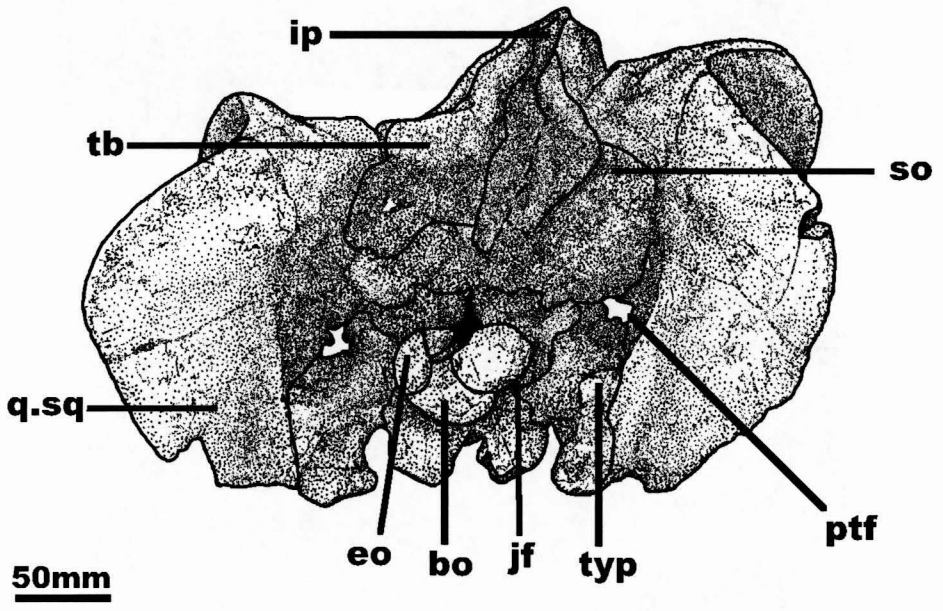
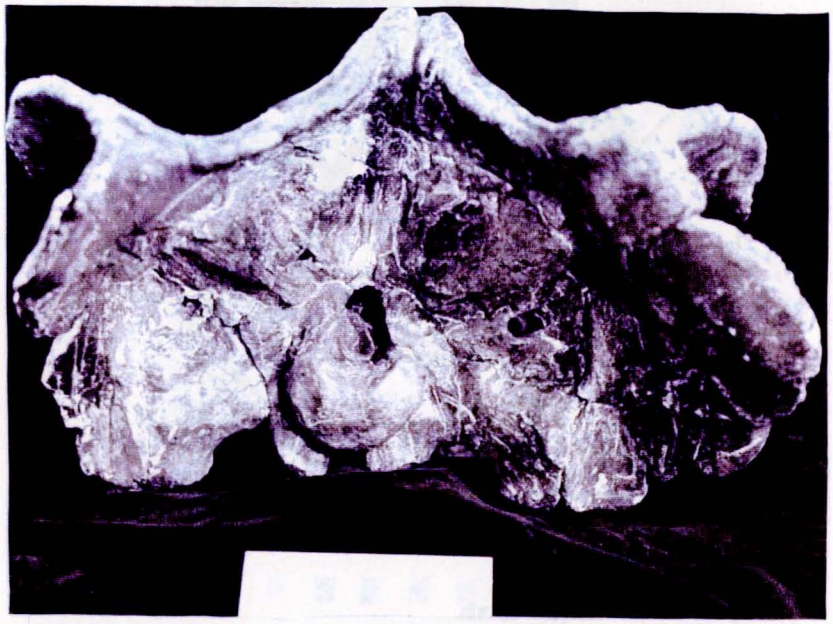


Figure 50. Occipital view of EL/1 (holotype of *K. wilsoni* Broom 1937), abbreviations as on p. ix.

A



B



Figure 51. Photographs of the occipital views of BP/1/4523 **A** and EL/1 **B.**

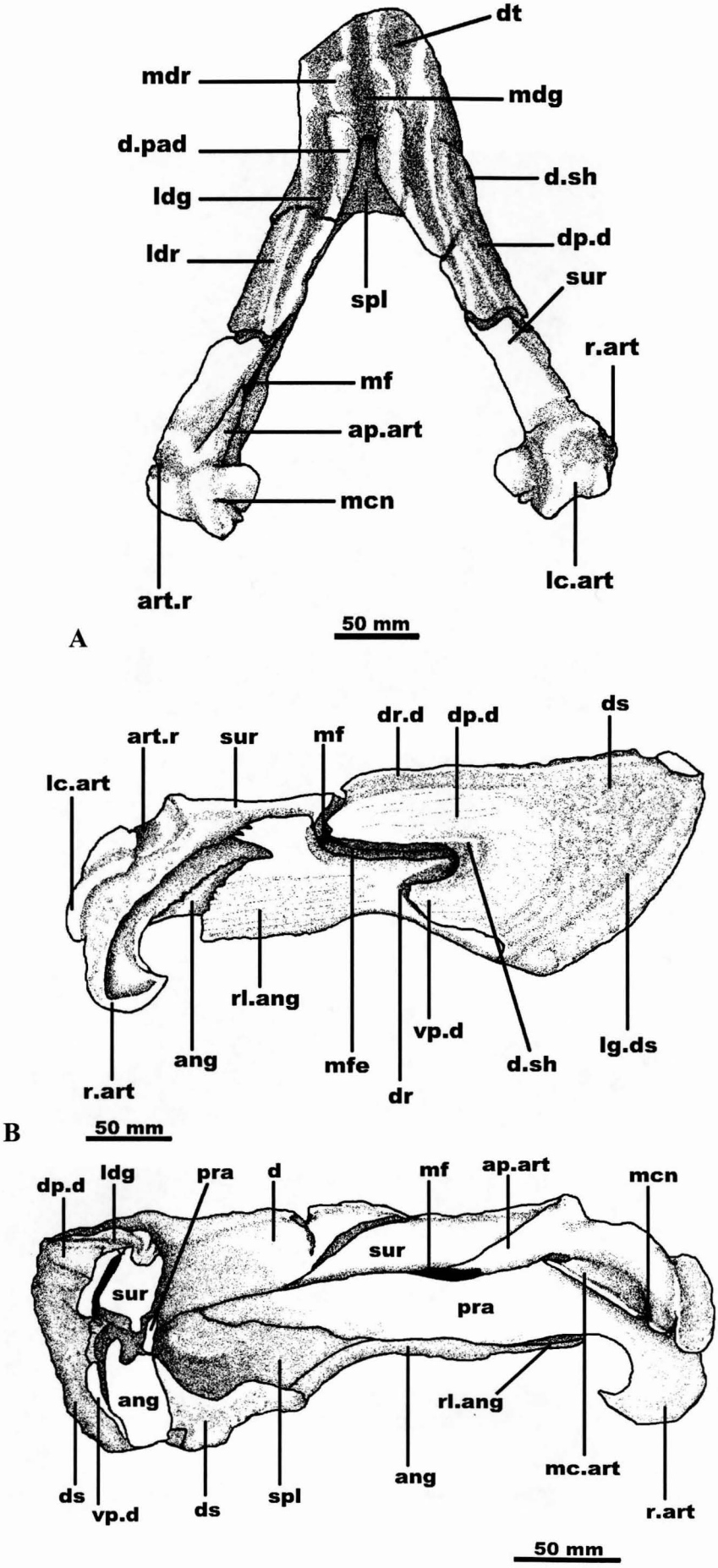


Figure 52. Dorsal **A**, lateral **B** and lingual **C** views of the lower jaw of BP/1/5624, abbreviations as on p. ix

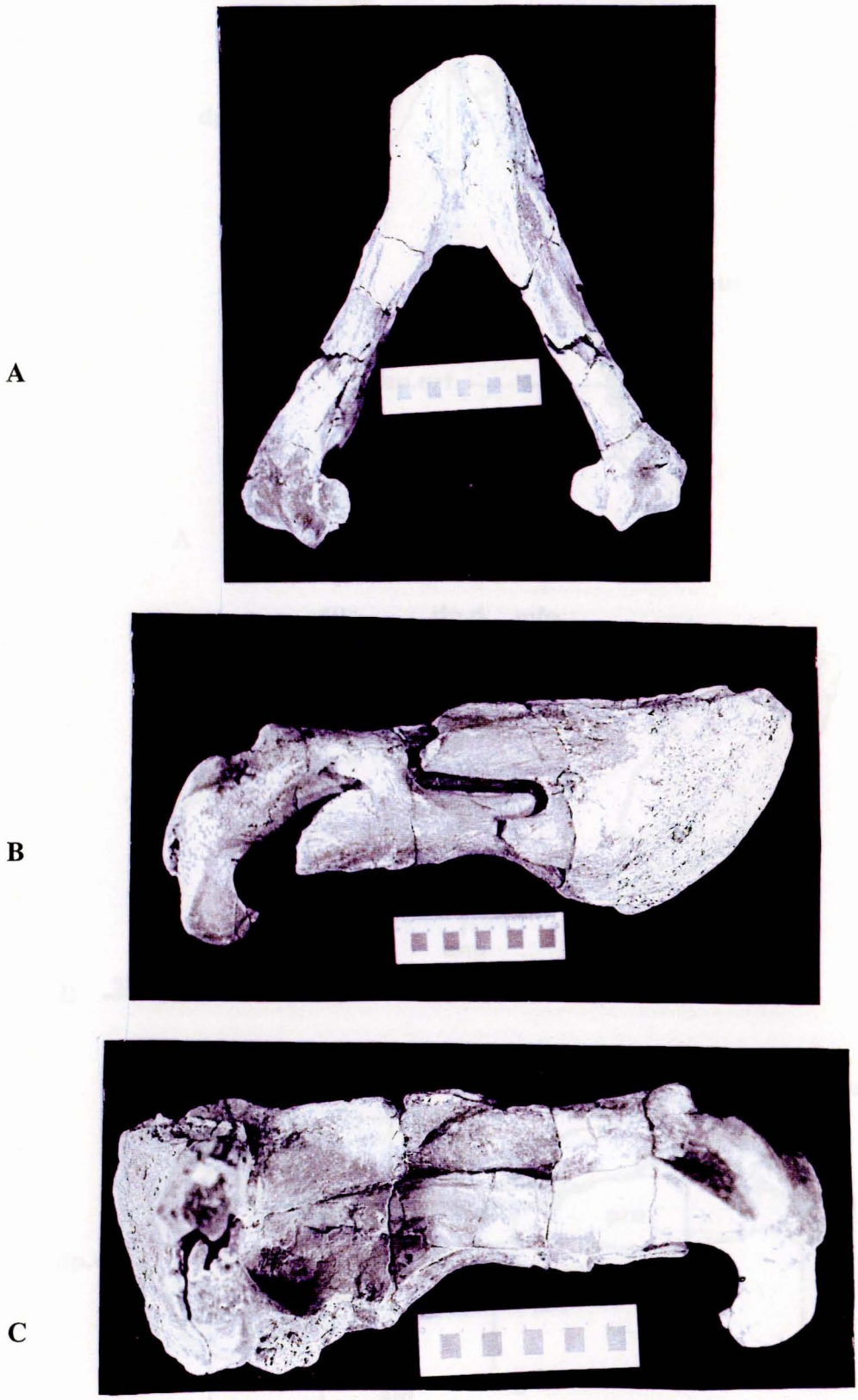


Figure 53. Photographs of the dorsal **A**, lateral **B** and lingual **C** views of the lower jaw of BP/1/5624.

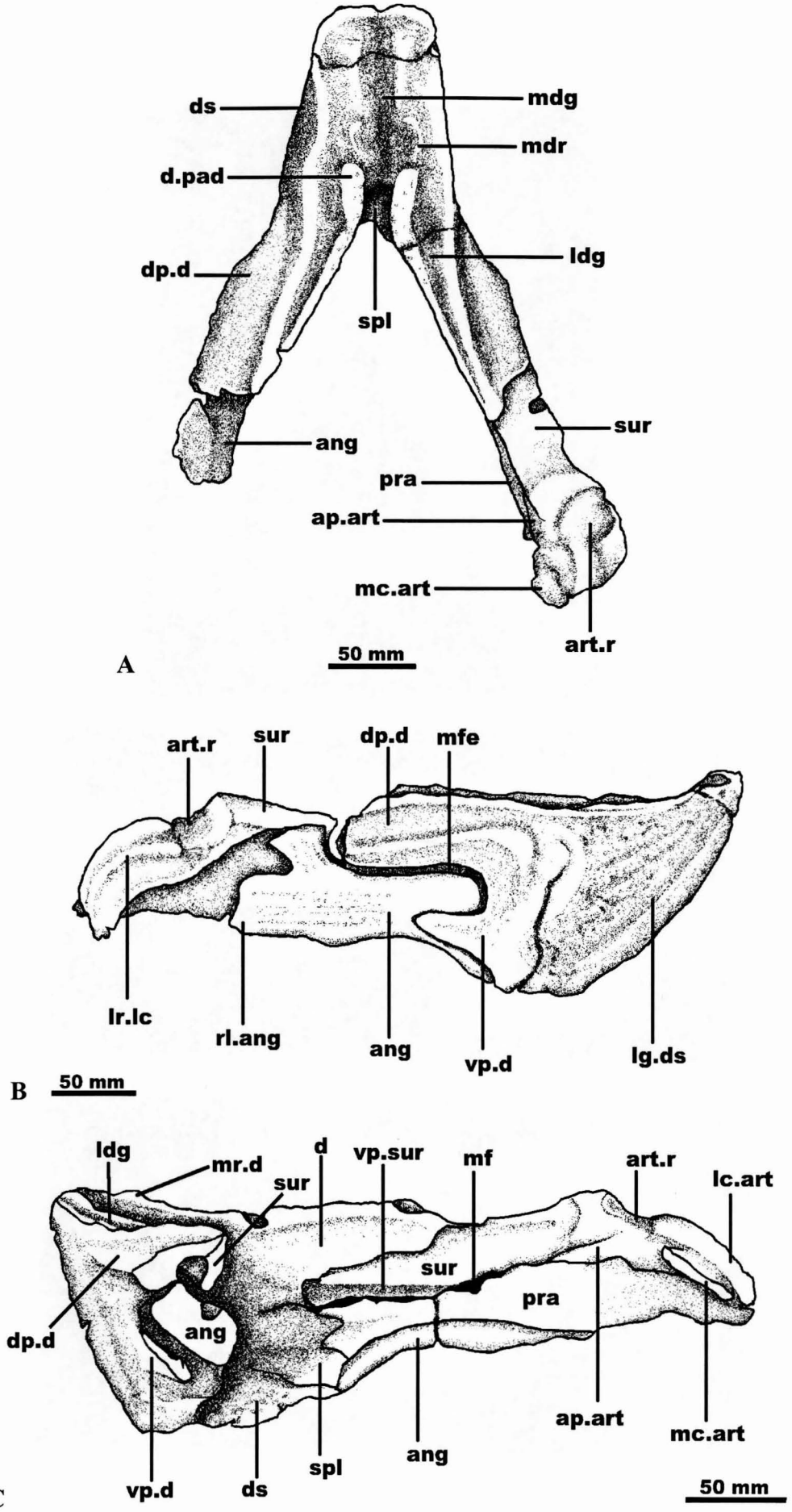


Figure 54. Dorsal **A**, lateral **B** and medial **C** views of the lower jaw of BP/1/4524, abbreviations as on p. ix.



Figure 55. Photographs of the dorsal **A**, lateral **B** and medial **C** views of the lower jaw of BP/1/4524.

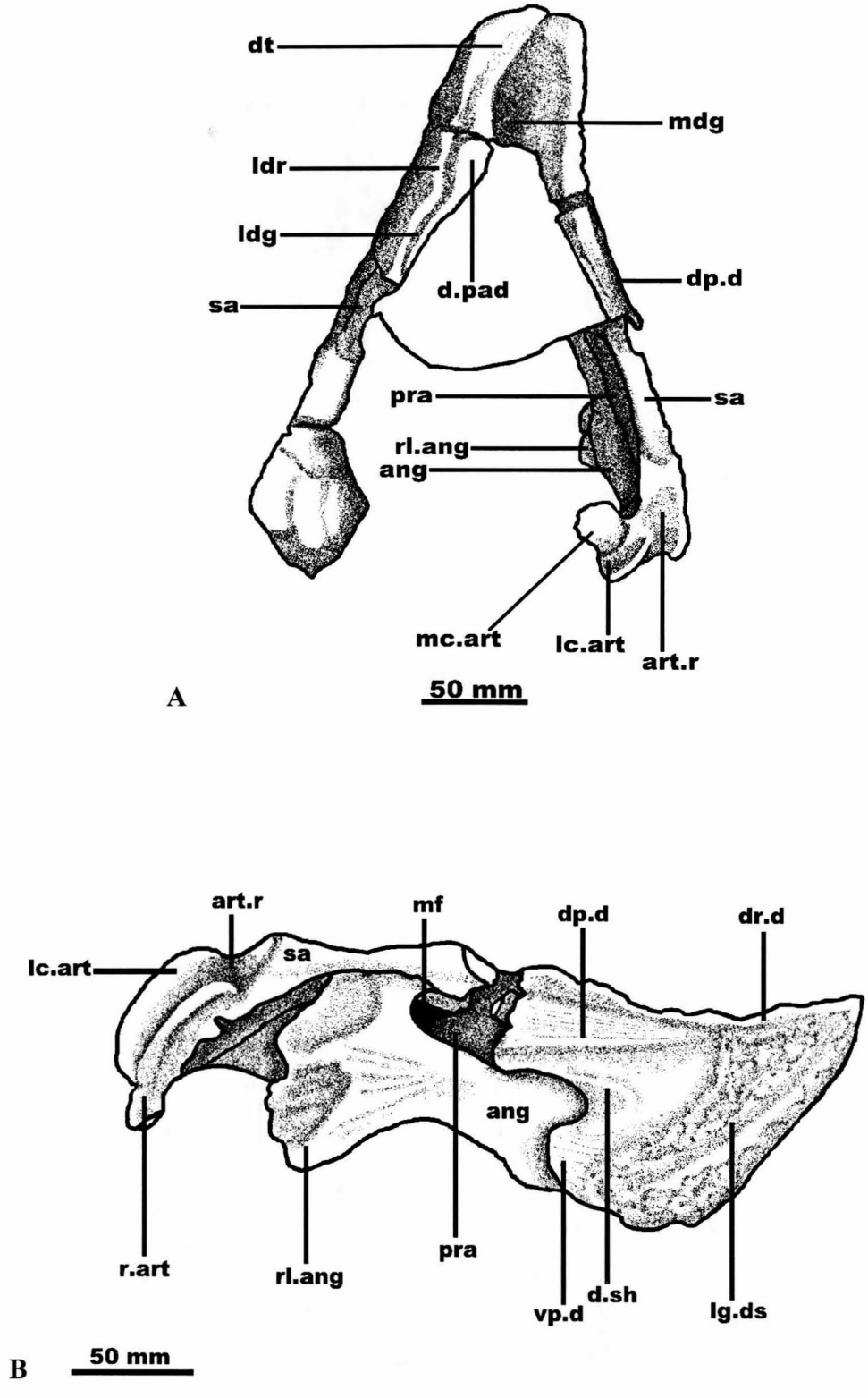


Figure 56. Dorsal **A** and lateral **B** views of the lower jaw of SAM/PK/3017 (holotype of *K. erithrea* Haughton 1915), abbreviations as p. ix.

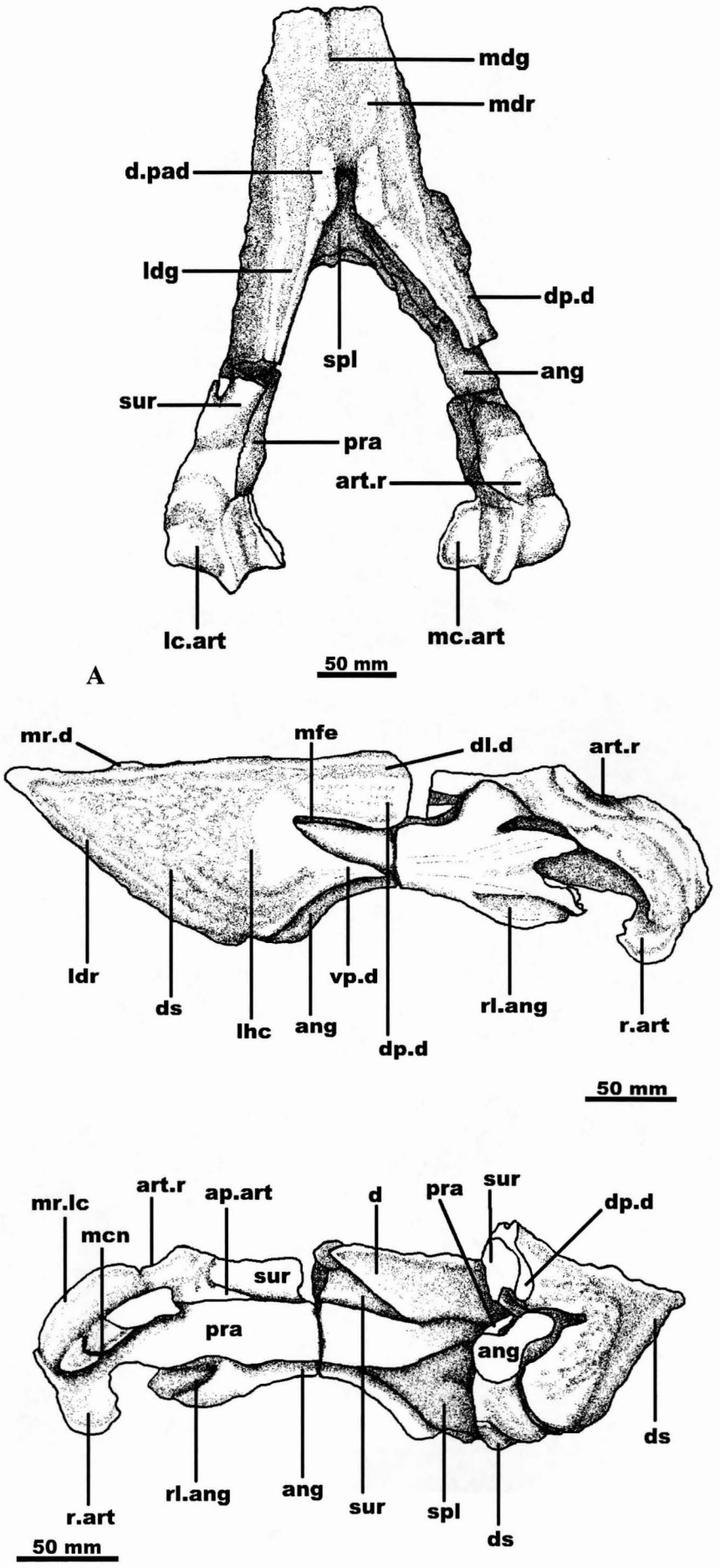


Figure 57. Dorsal **A**, lateral **B** and medial **C** views of the lower jaw of EL/1 (holotype of *K. wilsoni* Keyser & Cruickshank), abbreviations as on p. ix.

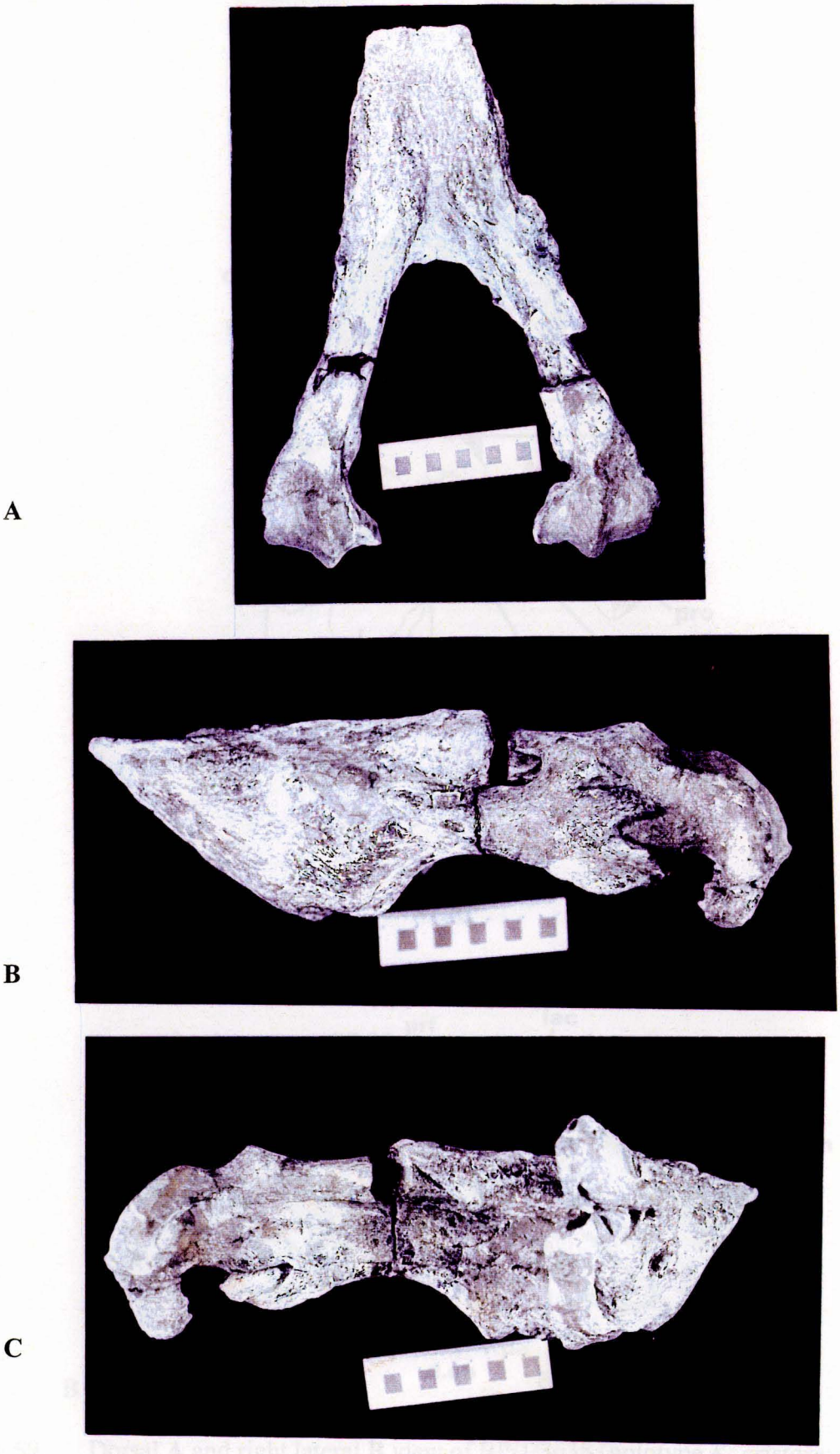
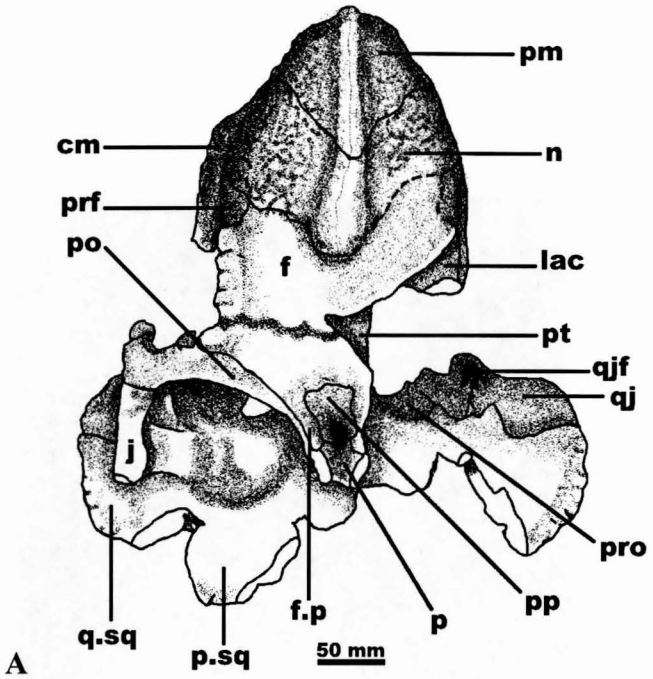


Figure 58. Photographs of the dorsal **A**, lateral **B** and medial **C** views of the lower jaw of EL/1.



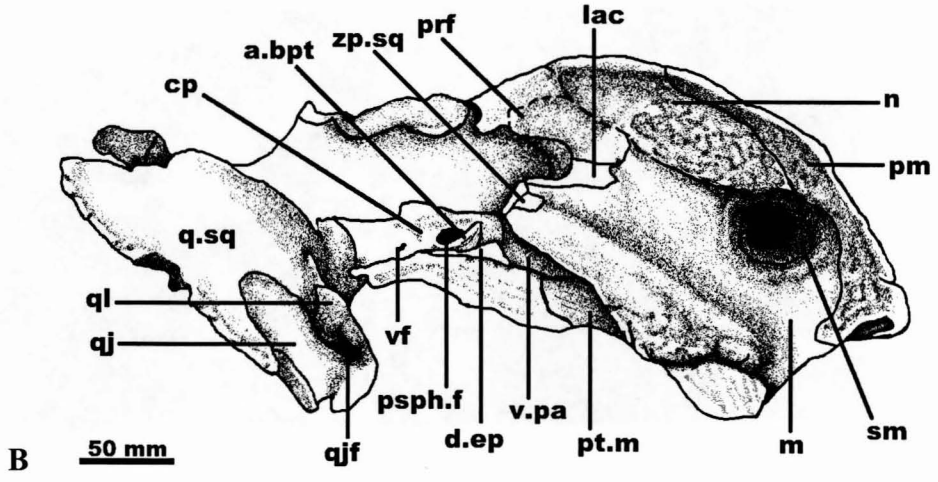
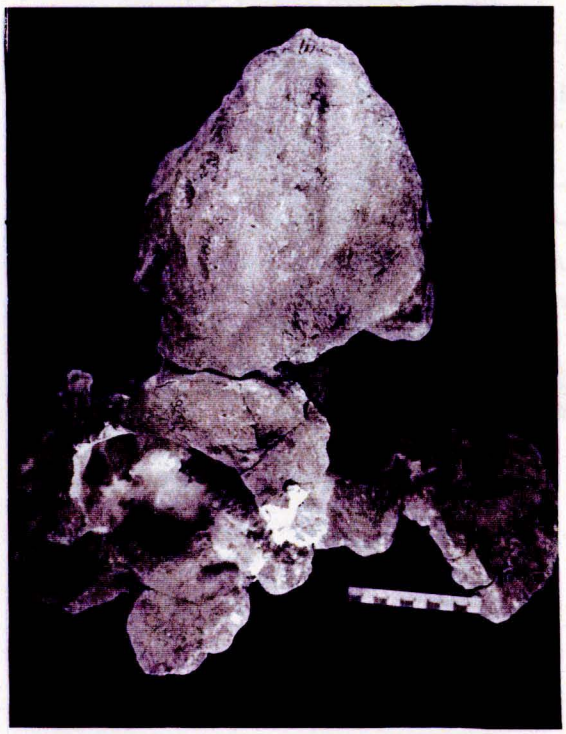


Figure 59. Dorsal **A** and right lateral **B** view of BP/1/3638 (holotype *K. cristarhynchus* Keyser & Cruickshank 1979), abbreviations as on p. ix.

A



B



Figure 60. Photographs of the dorsal **A** and right lateral **B** views of BP/1/3638.

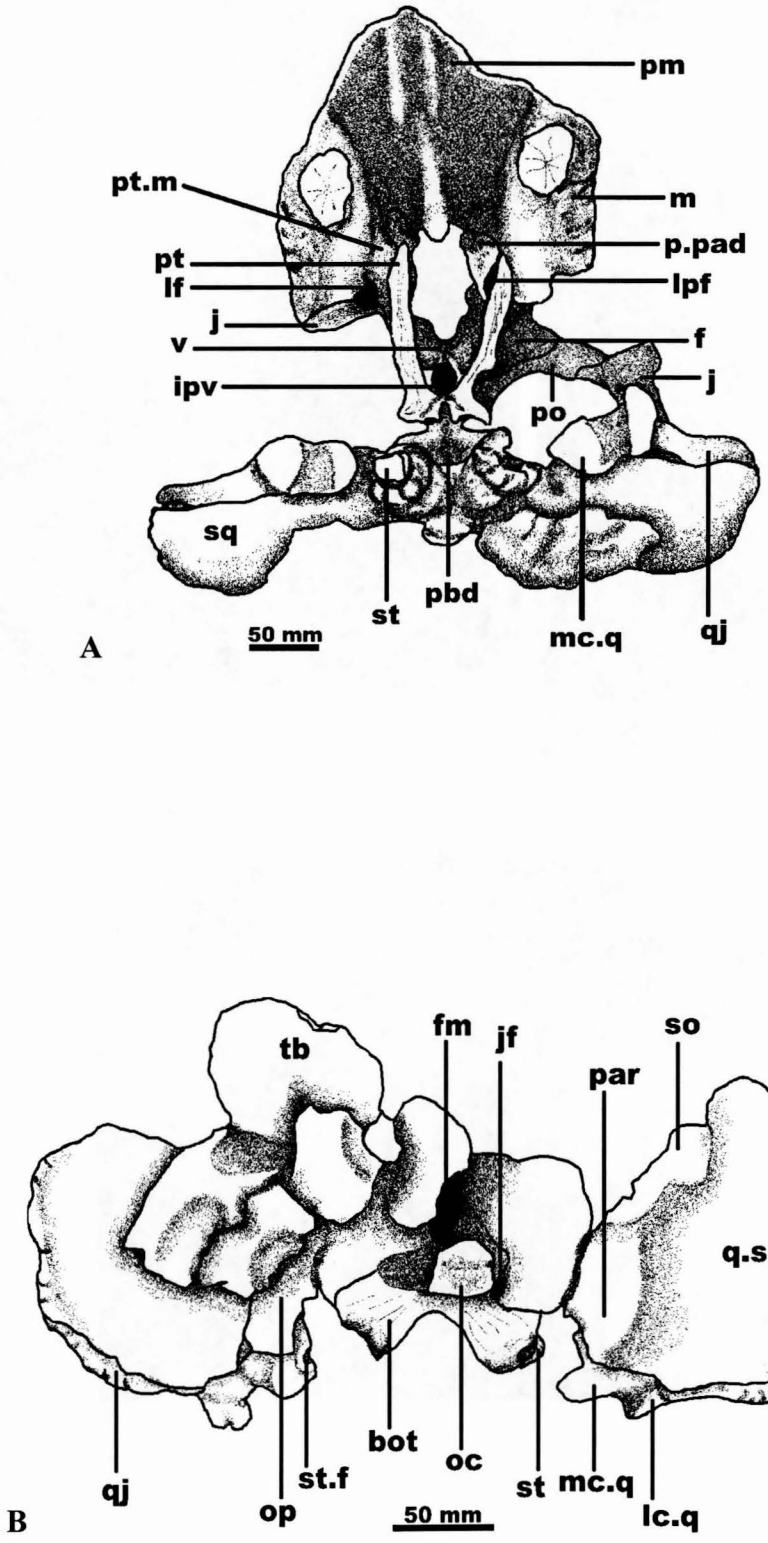


Figure 61. Ventral **A** and occipital **B** views of BP/1/3638 (holotype of *K. cristarhynchus* Keyser & Cruickshank 1979), abbreviations as on p. ix.

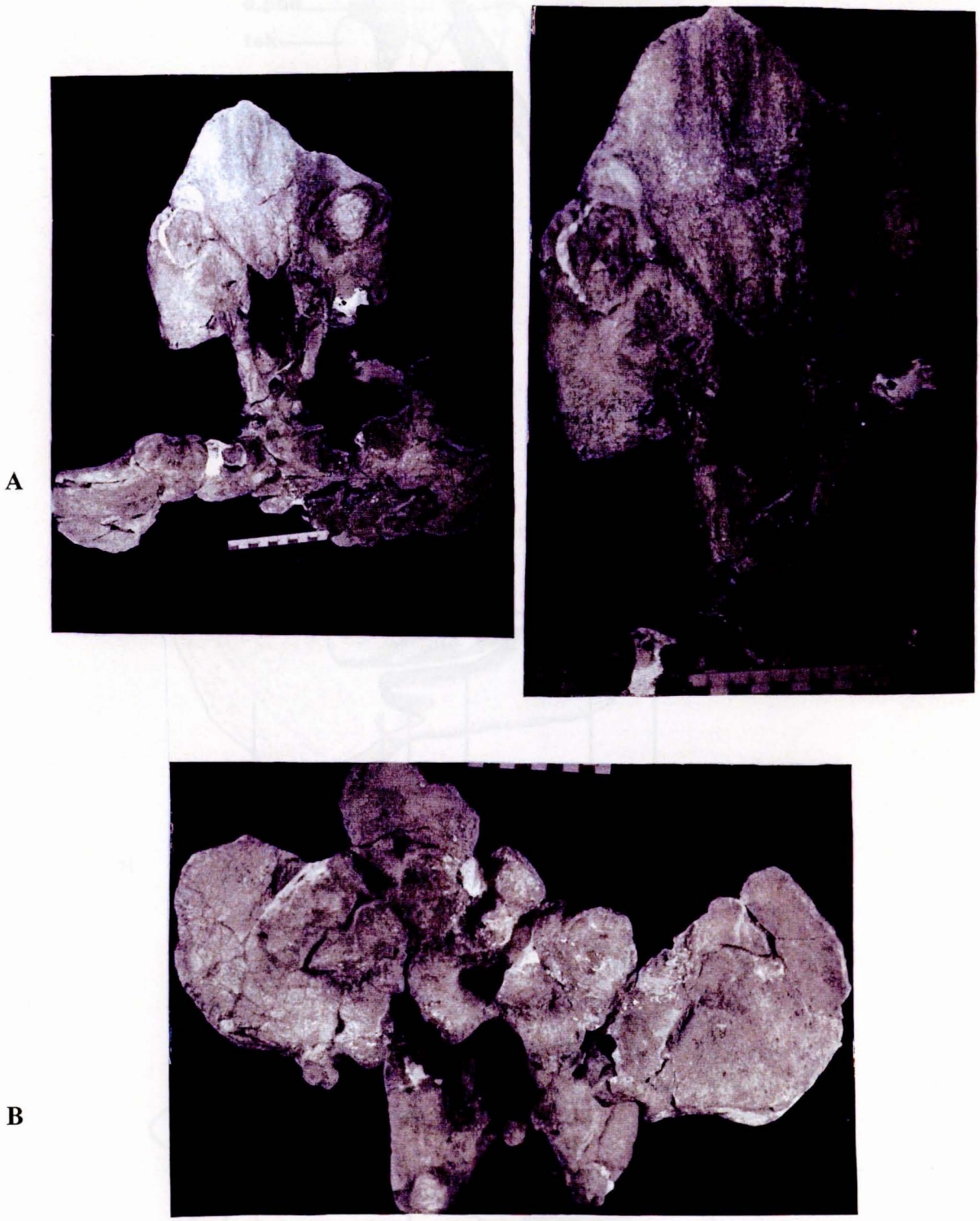


Figure 62. Photographs of the ventral **A** and occipital **B** views of BP/1/3638.

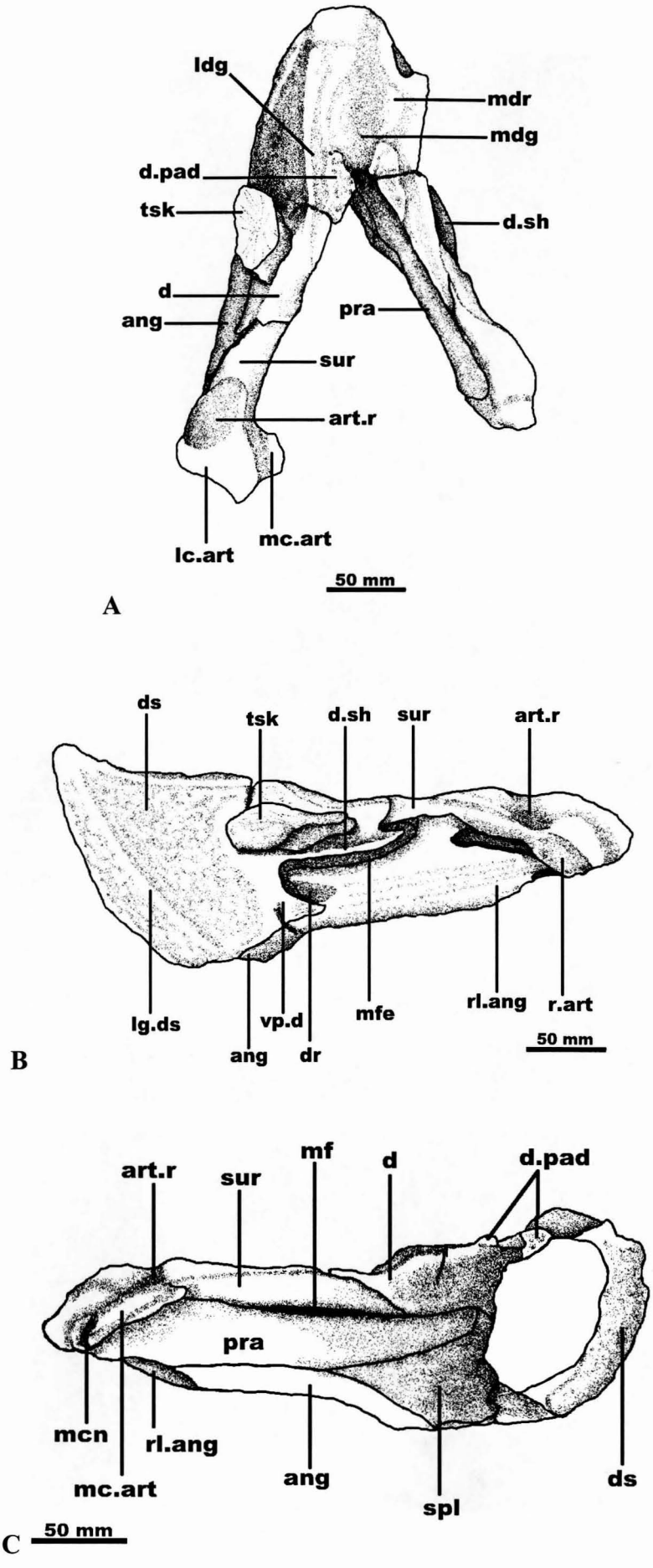


Figure 63. Dorsal **A**, lateral **B** and medial **C** views of the lower jaw of BP/1/3638 (holotype of *K. cristarhynchus* Keyser & Cruickshank 1979), abbreviations as on p. ix.

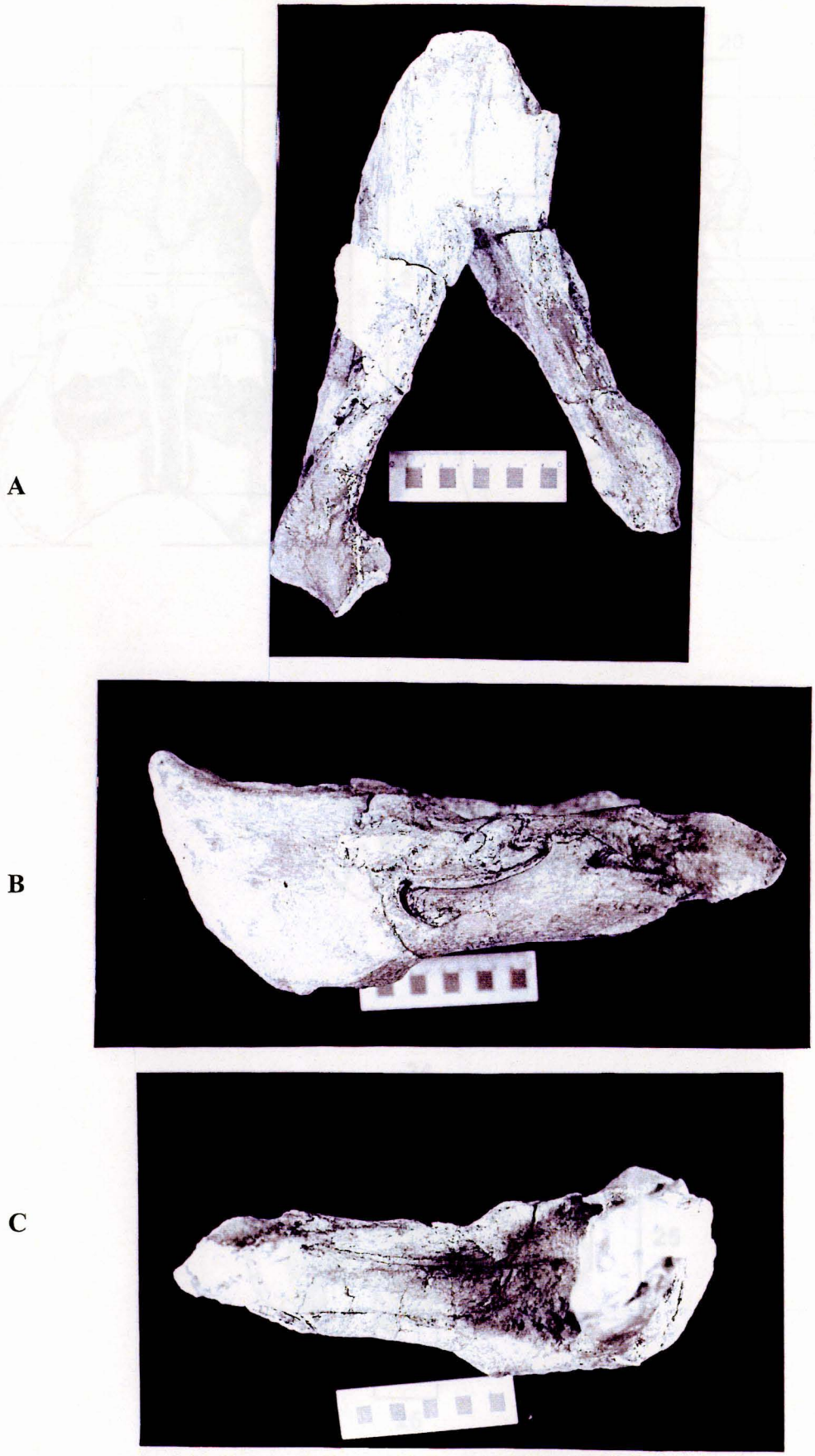


Figure 64. Photographs of the dorsal **A**, lateral **B** and medial **C** views of the lower jaw of BP/1/3638.

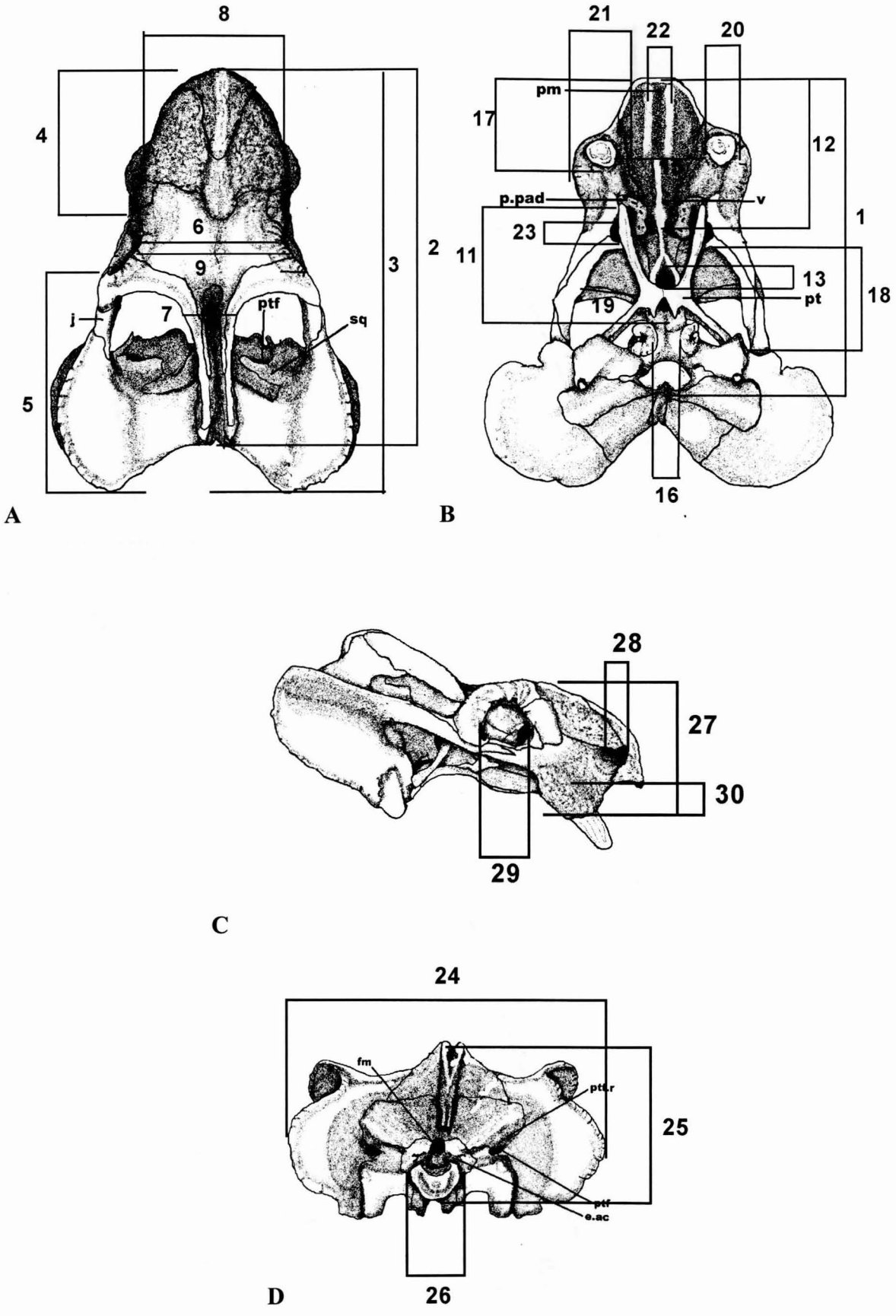


Figure 65. *Kannemeyeria* skull measurements. **A** - dorsal view, **B** - ventral view, **C** - lateral view, **D** - occipital view. Views not drawn to the same scale, and not all variables are shown.

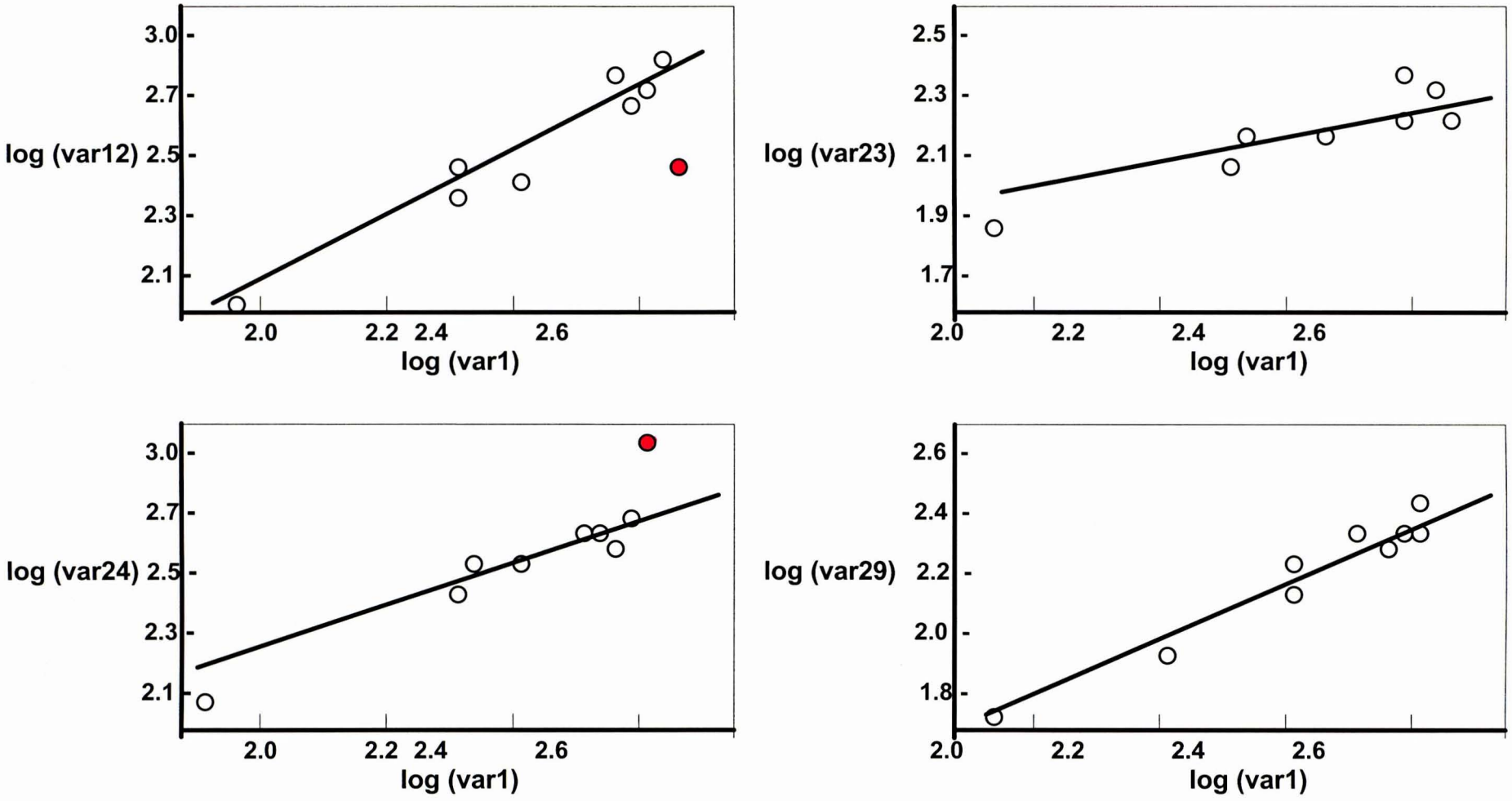
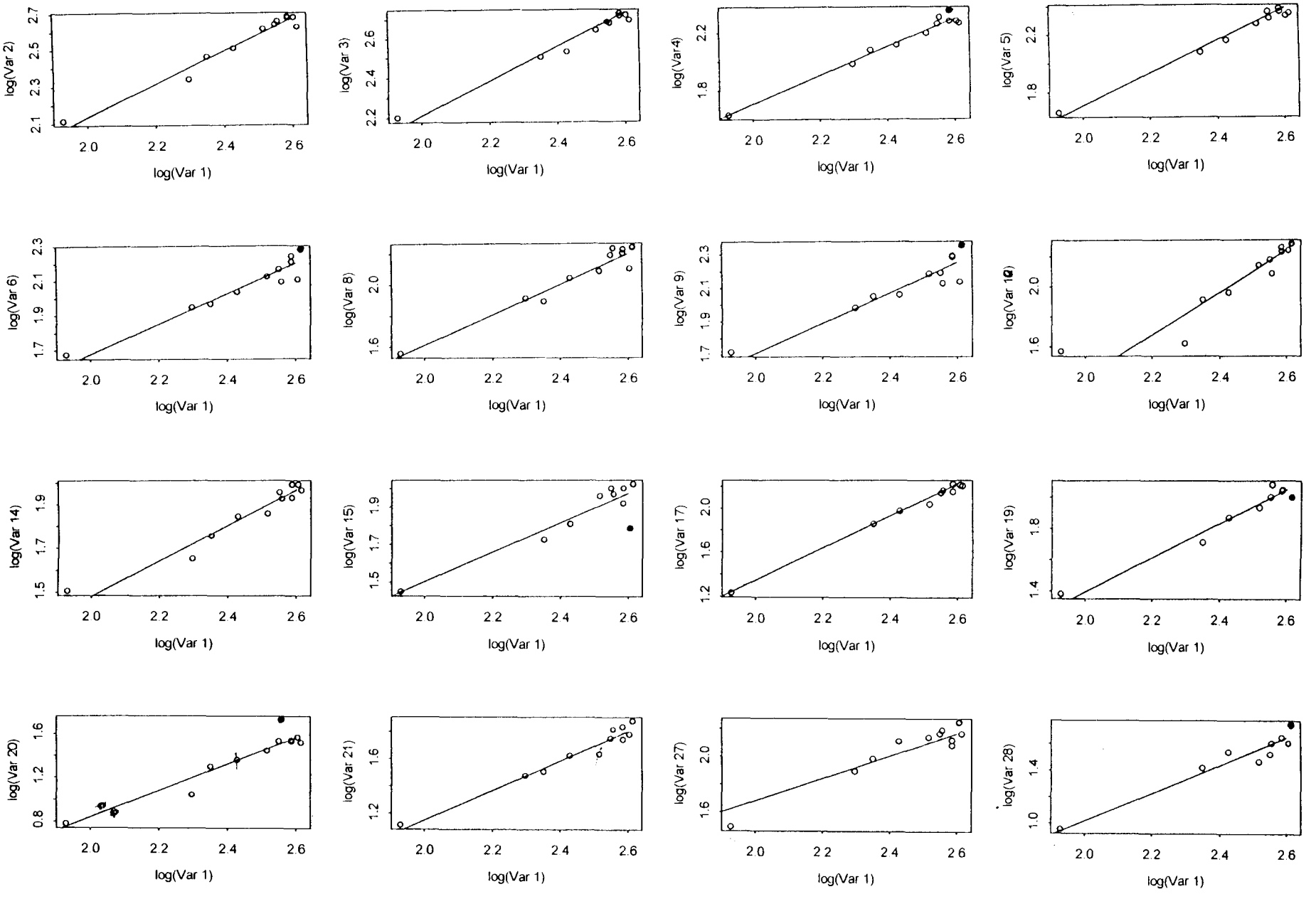


Figure 66. Selected bivariate plots of taxonomic significance, or demonstrating the effects of specific ontological growth patterns.

Figure 67. Further selected bivariate plots showing allometric-growth trends of the genus *Kannemeyeria*.



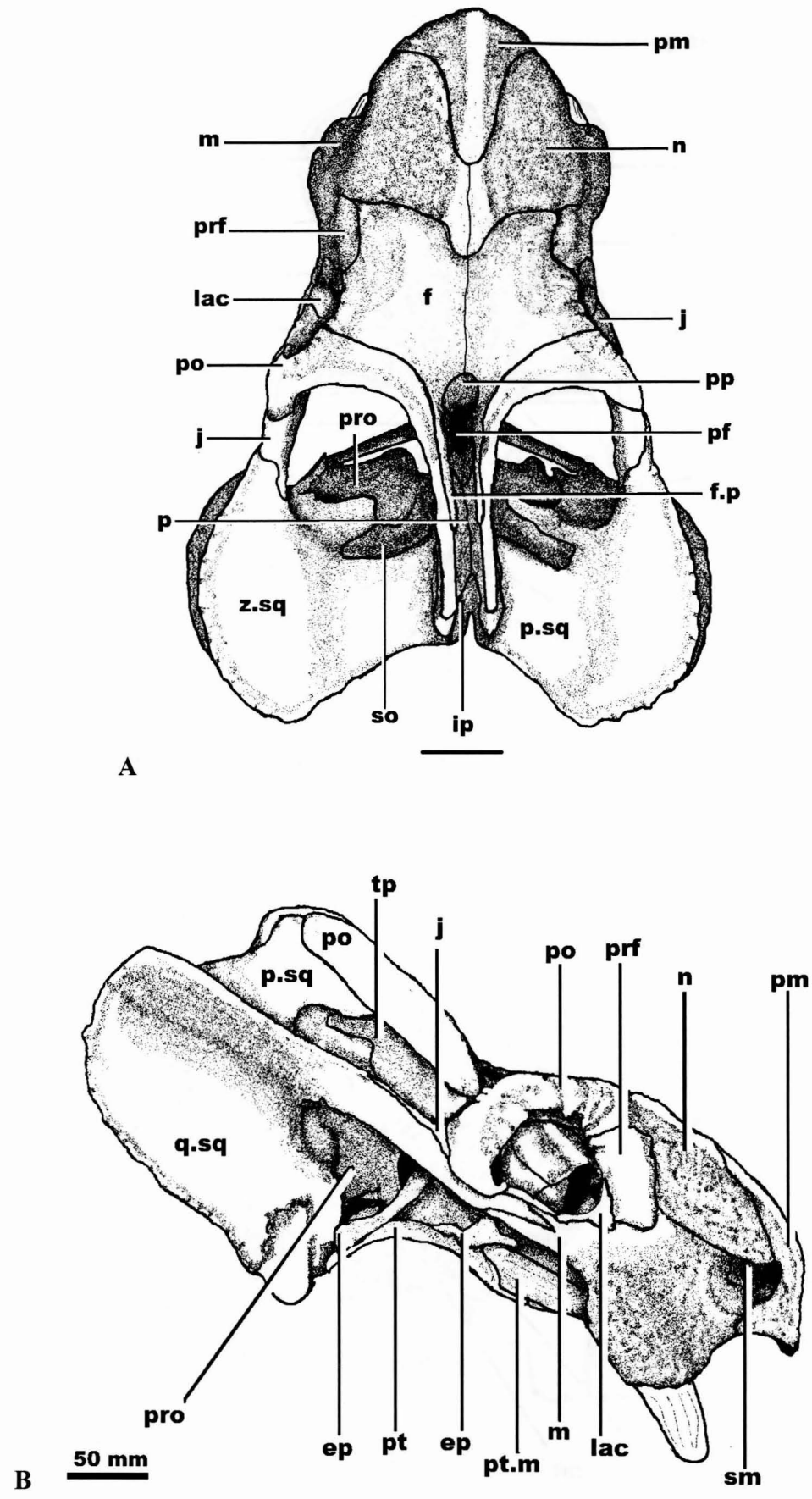


Figure 68. Cranial reconstructions of the skull of *Kannemeyeria simocephalus*. **A**-dorsal view, **B** - lateral view in revised orientation considered valid for this taxon (refer to Chapter 8). Abbreviations as on p. ix.

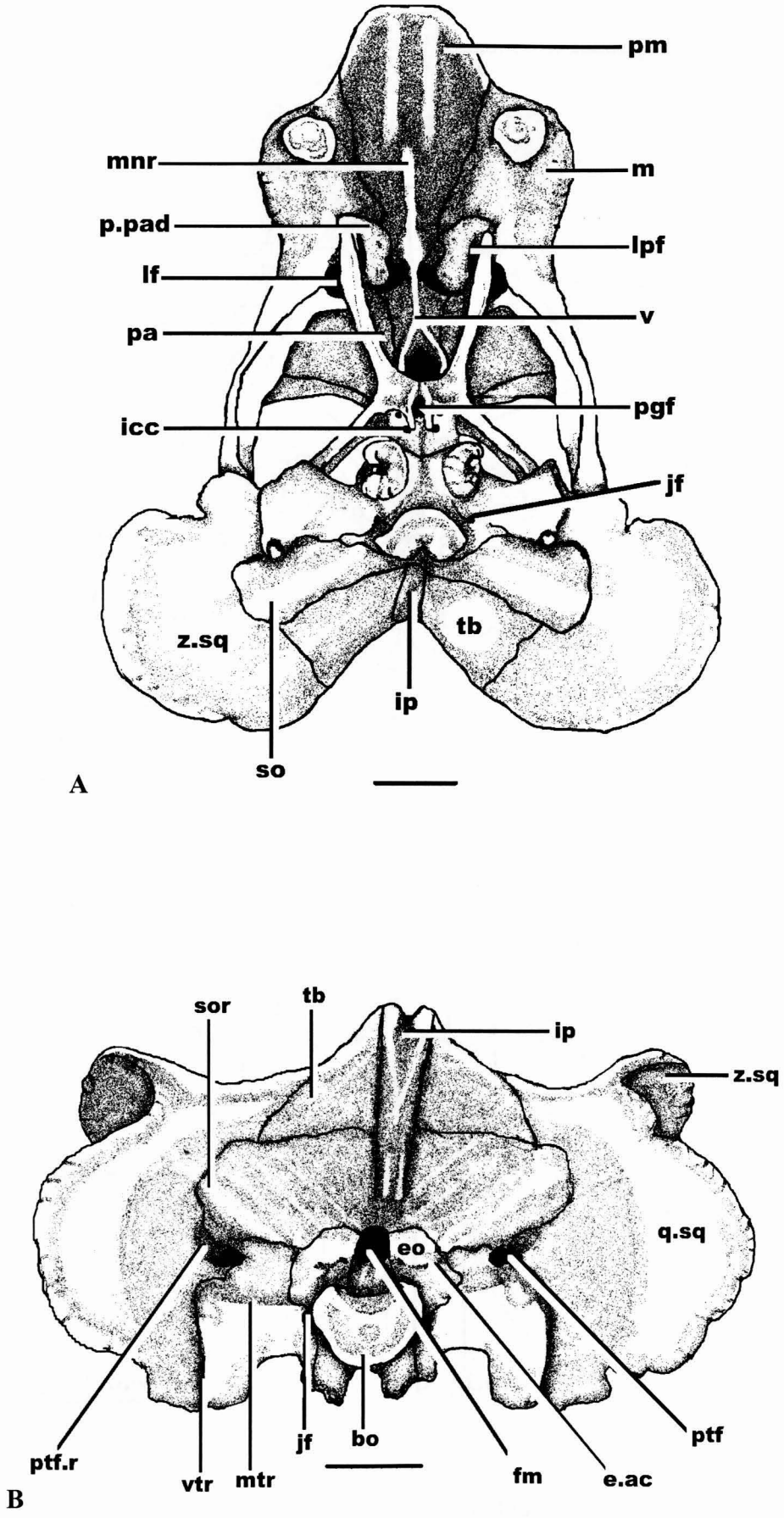


Figure 69. Cranial reconstructions of the skull of *Kannemeyeria simocephalus*. **A** - ventral view, **B** - occipital view, scale - 50mm. Abbreviations as on p. ix.

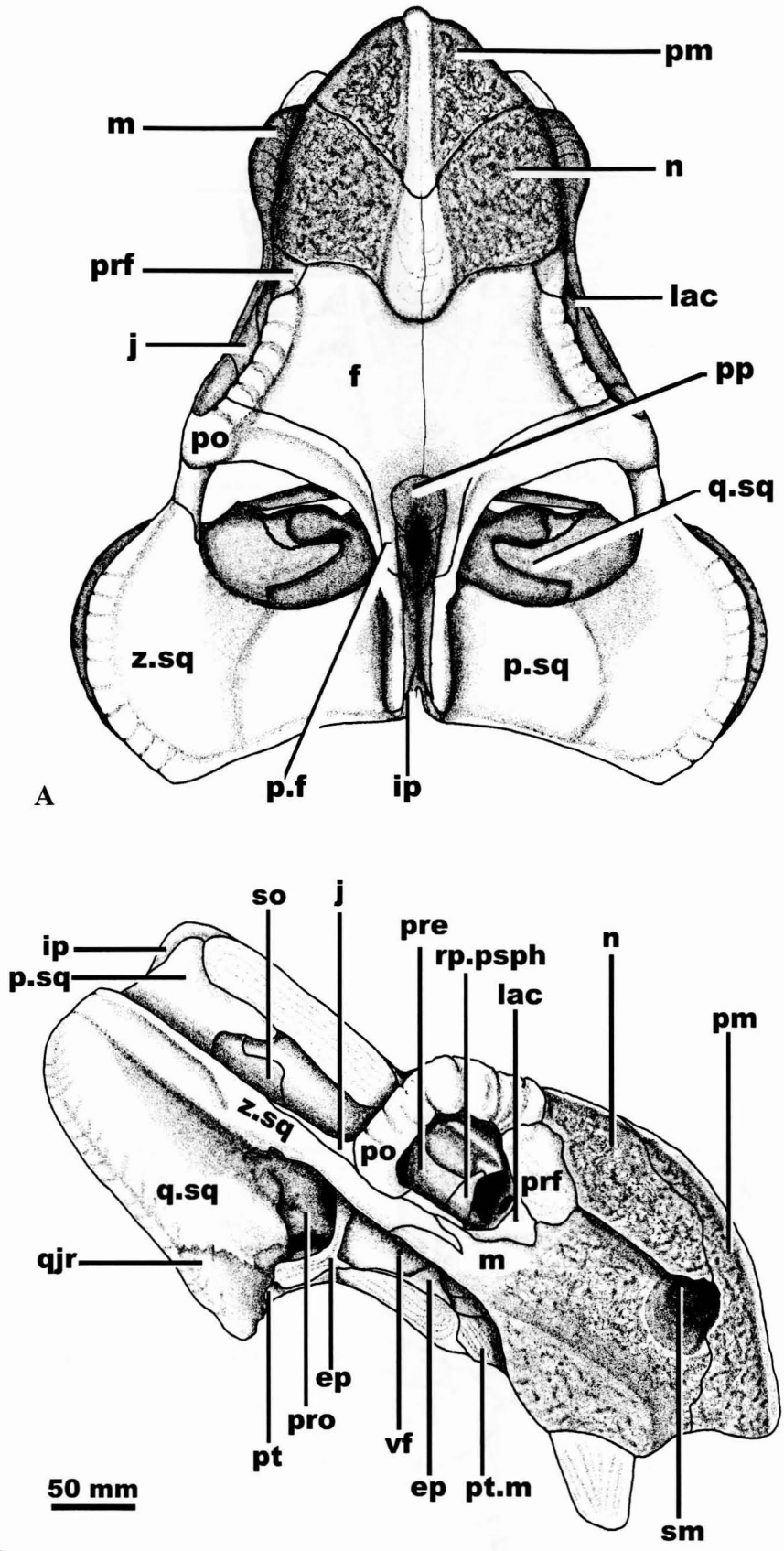


Figure 70. Cranial reconstruction of the dorsal - **A** and lateral - **B** views of the skull of *Kannemeyeria cristarhynchus*. Lateral view in revised orientation considered valid for this taxon (refer to Chapter 8). Abbreviations as on p. ix.

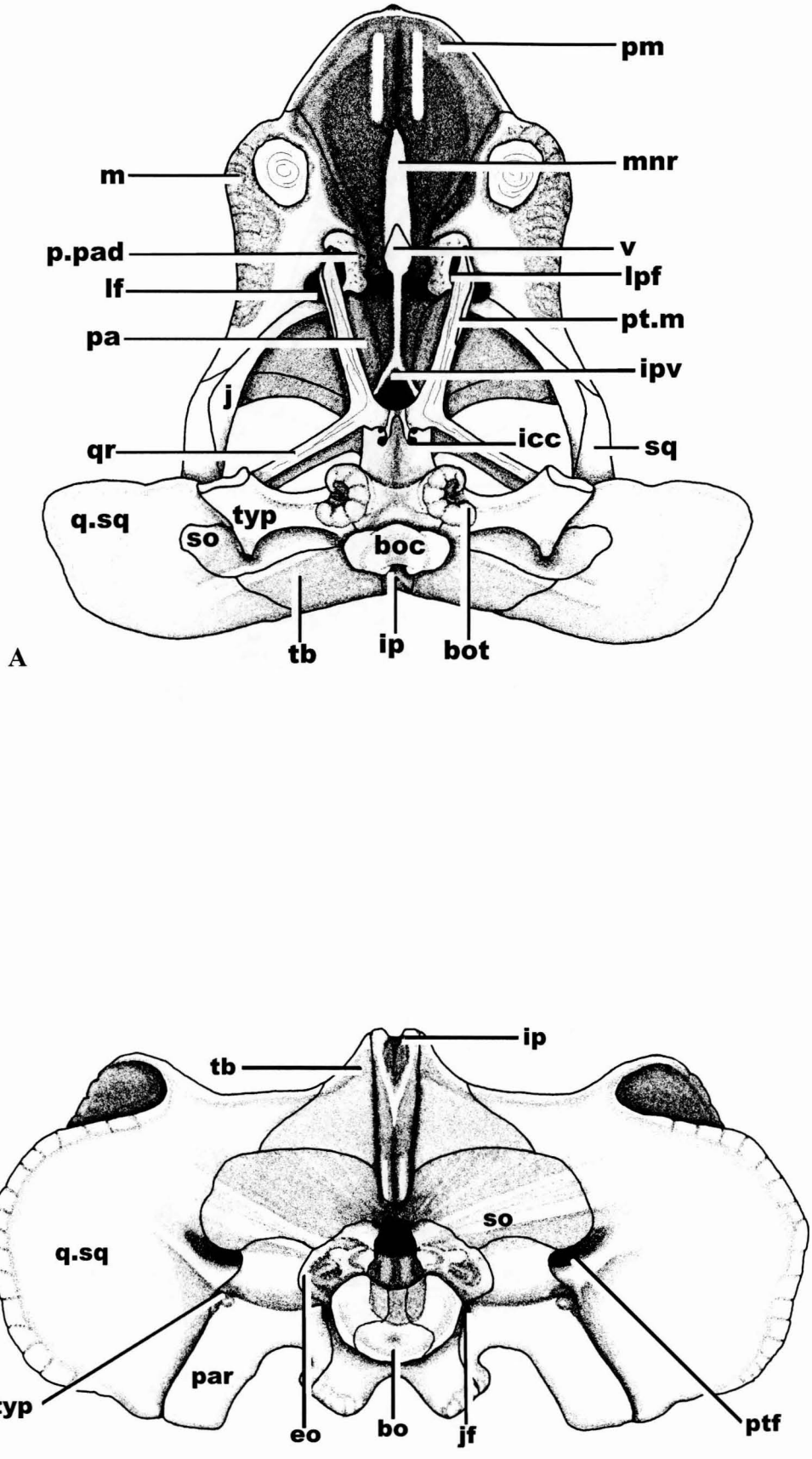


Figure 71. Cranial reconstructions of the skull of *Kannemeyeria cristarhynchus* **A** - ventral view, **B** - occipital view. Abbreviations as on p. ix.

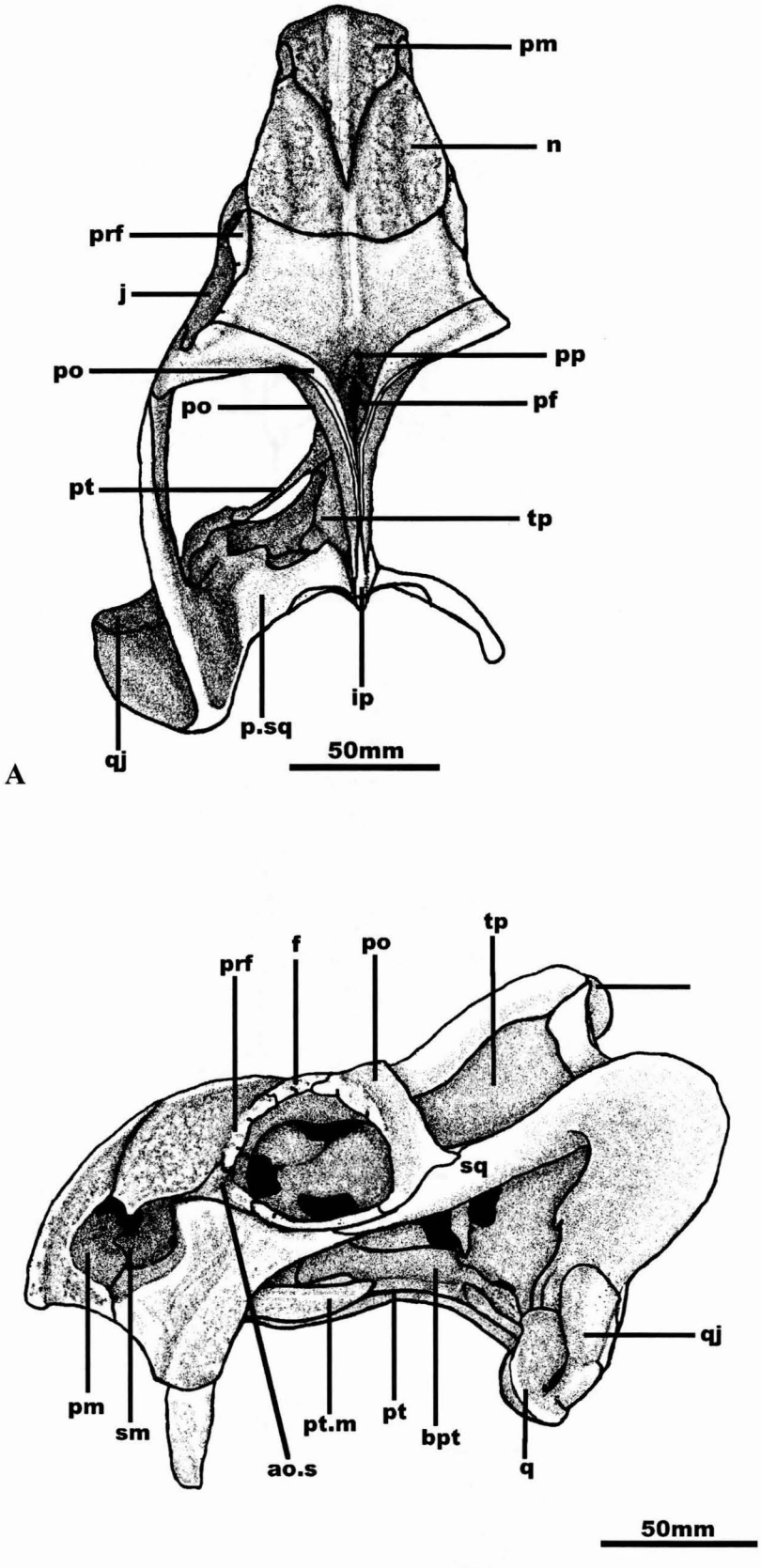


Figure 72. Dorsal **A** and lateral **B** views of PVL/3465 (holotype of *K. argentinensis* Boneparte 1966), abbreviations as on p. ix.

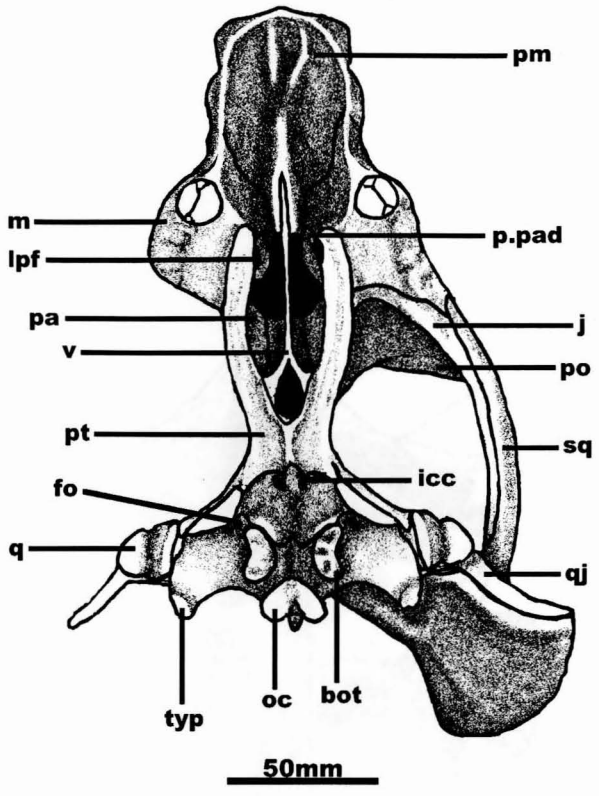


Figure 73. Ventral **A** and occipital **B** views of PVL/3465 (holotype of *K. argentinensis* Boneparte 1966), abbreviations as on p. ix.

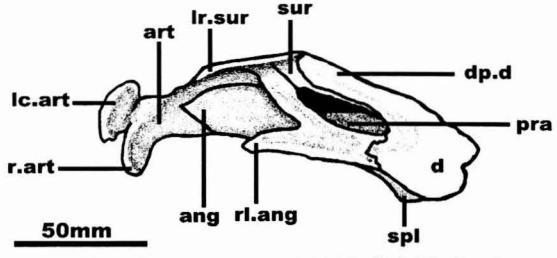


Figure 74. Lateral views of the lower jaw of PVL/3465 (holotype of *K. argentinensis* Boneparte 1966), abbreviations as on p. ix.

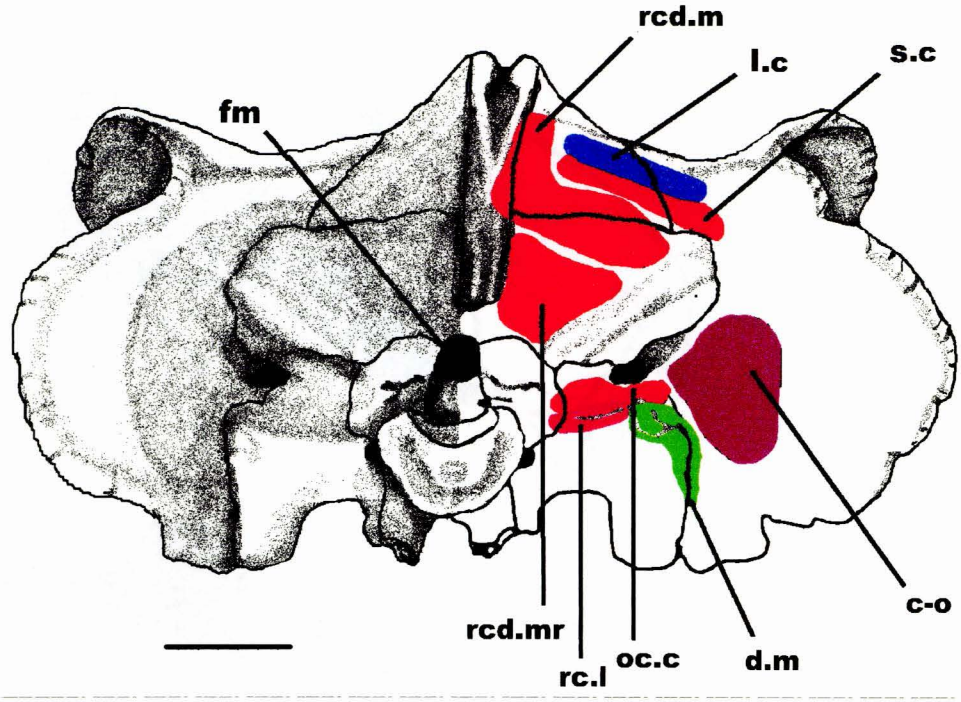


Figure 75. Occiput of *Kannemeyeria* demonstrating major muscle insertion sites, illustrated as functional units.

rcd.m - rectus capitis dorsalis major, rcd.mr - rectus capitis dorsalis minor, s.c - semispinalis capitis, l.c - longissimus capitis, oc.c - obliquus capitis cranialis, rc.l - rectus capitis lateralis, d.m - depressor mandibulae, c-o - cleido-occipitalis.

Scale - 50mm.

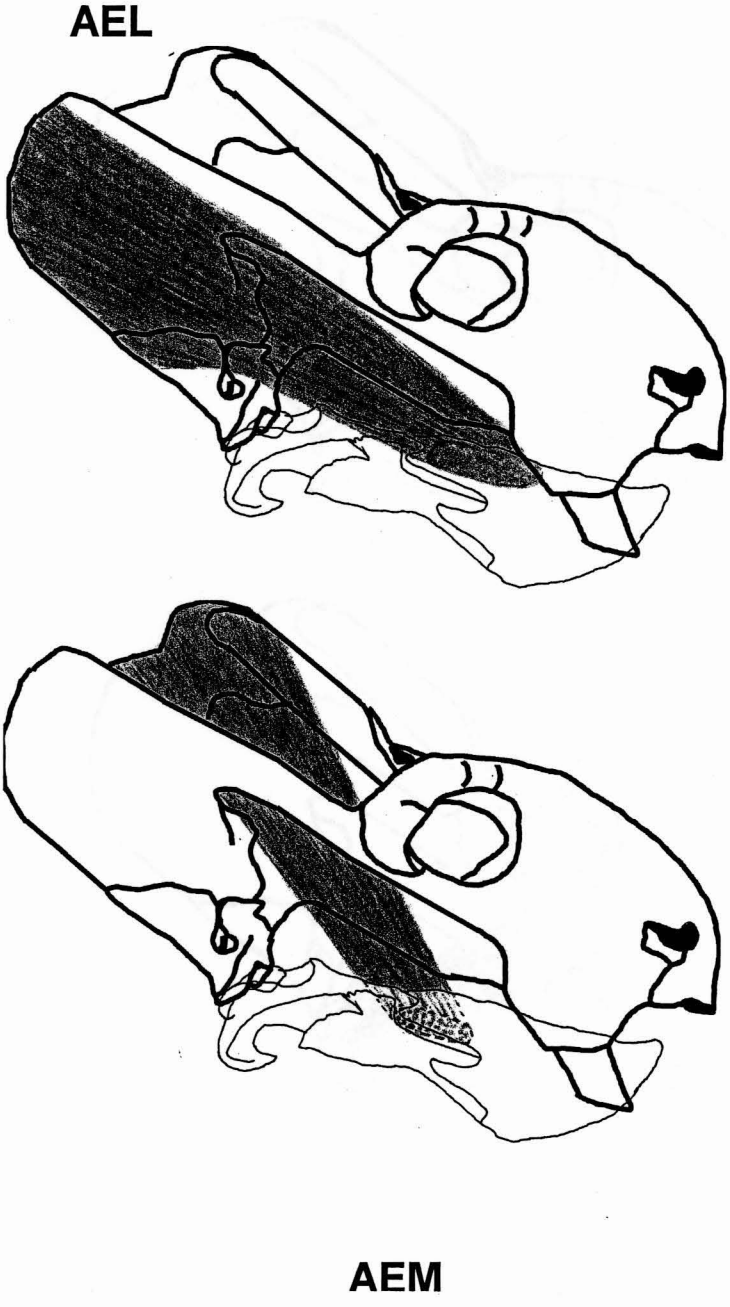


Figure 76. Diagrammatic representation of the *Kannemeyeria* external adductor musculature. AEL - lateral external adductor, AEM - medial external adductor.

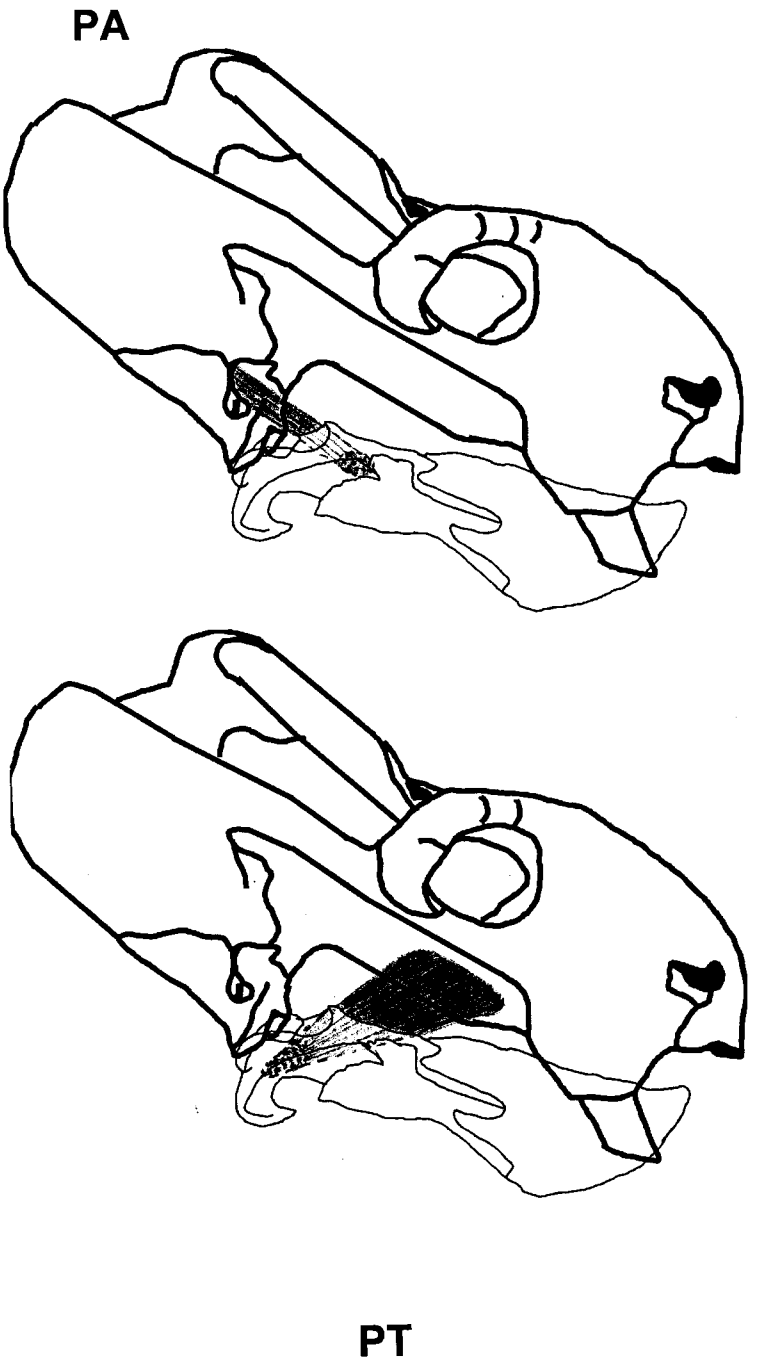


Figure 77. Diagrammatic representation of the posterior adductor (PA), and the internal adductor musculature. PT - pterygoideus muscle.

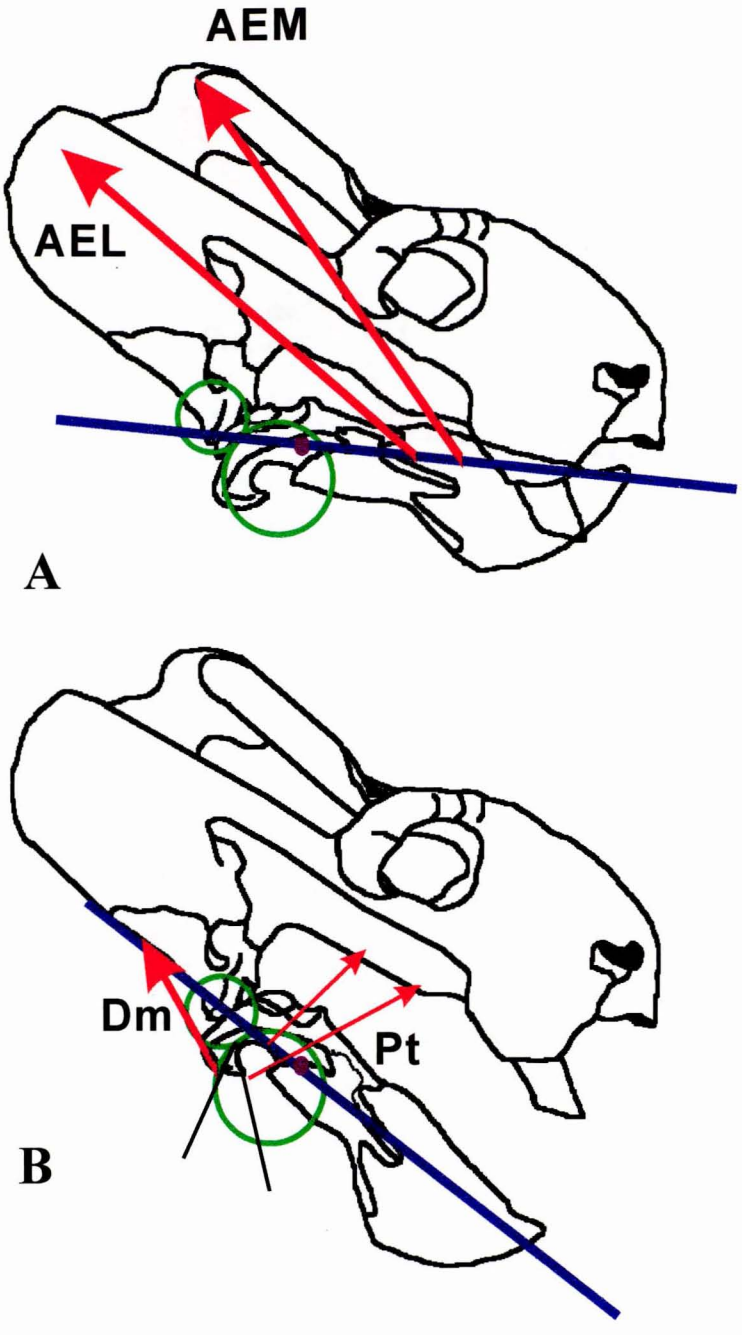


Figure 78. Phase One of the *Kannemeyeria* masticatory cycle.
A - elevation: primarily performed by the contraction of the external adductor muscles (**AEL** and **AEM**) to achieve the beak-bite between the anterior ends of the dentary and the alveolar border of the snout. **B - depression:** achieved by gravity and the contraction of the m. depressor mandibulae (**Dm**). Partial muscular control of the action is provided by a minor contribution from the pterygoideus musculature (**Pt**). **Red arrows** - traction lines indicating the muscle forces involved in the production of jaw movement during Phase One. Traction lines show maximal force at, or near, the main lever arm of the lower jaw (**blue line**). **Green circles** - arc described by the articulating surfaces of the lateral quadrate and articular condyles, and are apt to change their position determined by the position of the lower jaw during the cycle. **Purple dot** - actual pivot point of the entire lower jaw, which remains static regardless of the position the jaw assumes.

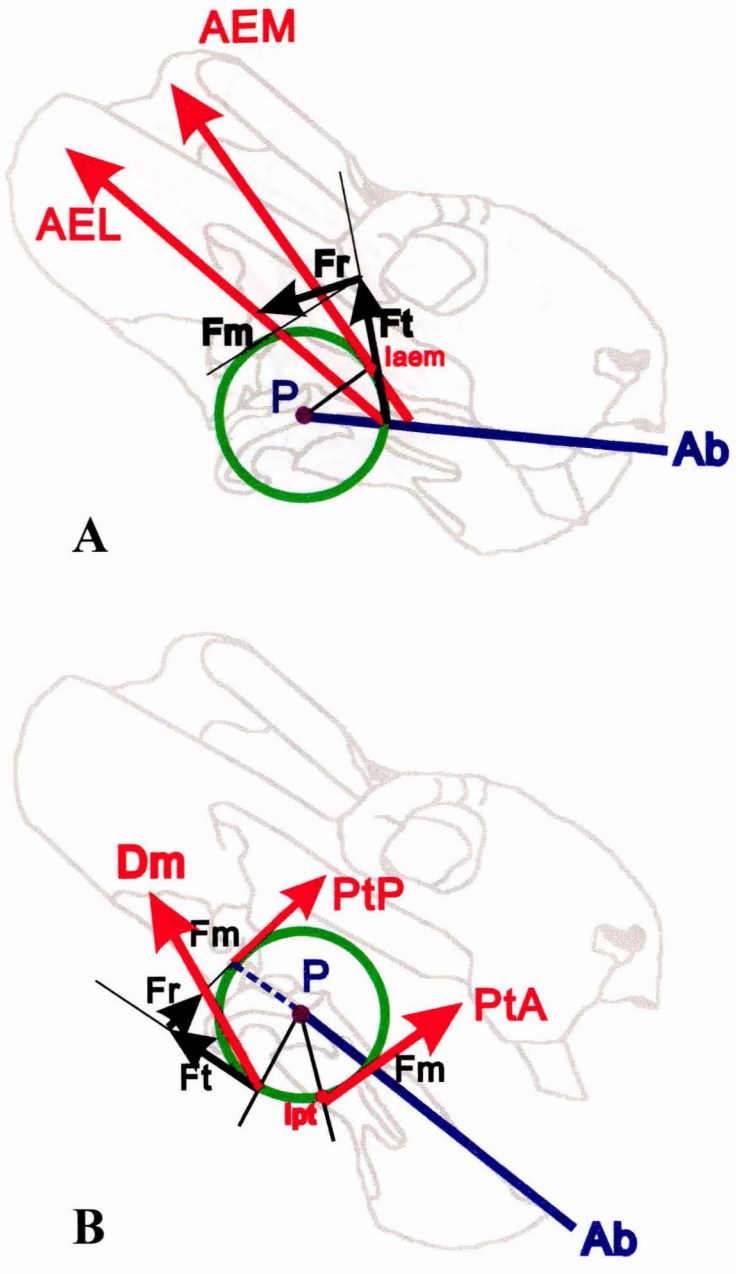


Figure 79. Force diagrams depicting the movements of the lower jaw during Phase One of the *Kannemeyeria* masticatory cycle.

A - elevation, **B** - depression. **Green circle** - radius of bell-crank curve, determined by the point of action of the traction line of the depressor mandibulae (**Dm**, see text). The arc of action of the bell-crank circle matches the arc of action of the anterior end of the alveolar border of the lower jaw (**Ab**). **P** - pivot point of the lower jaw, around which the bell-crank circle operates. All traction lines (**red arrows**) are redrawn according to the pivot point and the bell-crank circle. They lie either tangential to this circle or pass through the circle and their force needs to be described via the Pythagorean Theorem (see text). In actuality all muscle force is translated at the joint articulation but to a lesser or greater degree as shown by the force diagram. **PtP** - posterior pterygoideus fibres, **PtA** - anterior pterygoideus fibres, **Iaem** - interception point of the medial external adductor muscle, **Ipt** - interception point of the anterior pterygoideus muscle fibres.

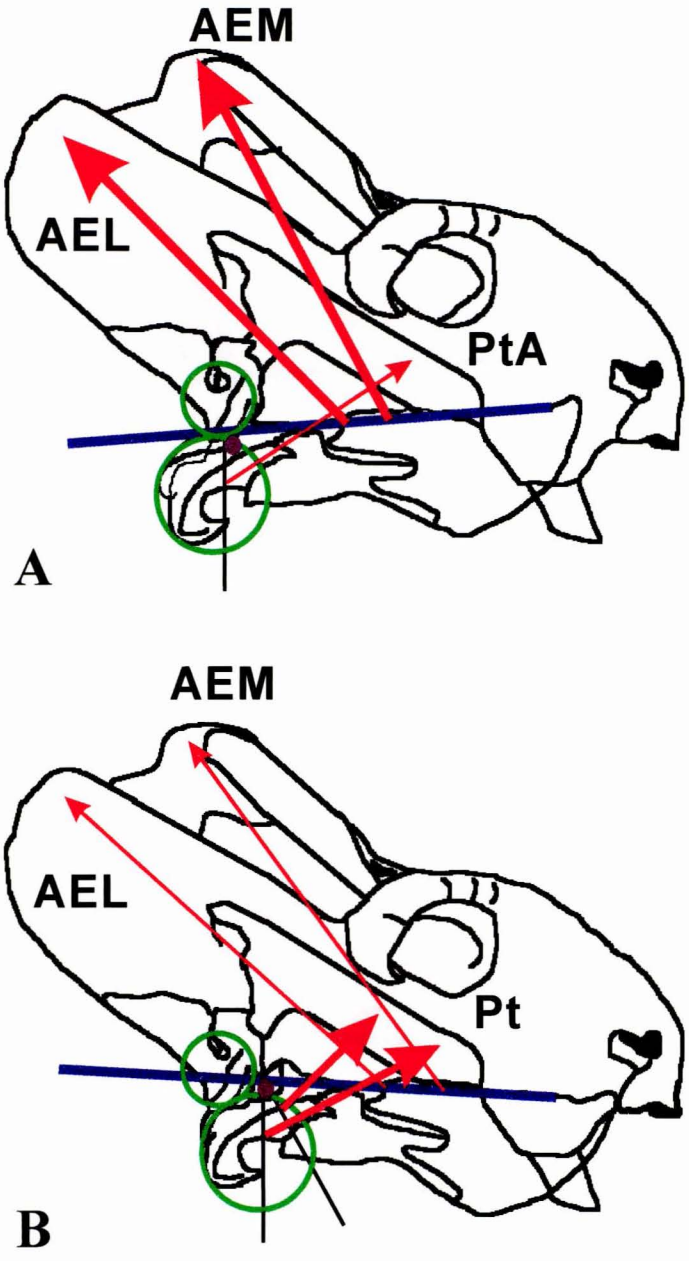


Figure 80. Phase Two of the *Kannemeyeria* masticatory cycle.
A - postero-dorsal crushing and grinding action, resulting from the vertical force applied by the external adductor musculature (**AEM** and **AEL**), mediated by a small antero-medial component from the pterygoideus musculature (**PtA**). **B - antero-dorsal** crushing and grinding action, resulting from the vertical force applied by the pterygoideus musculature (**Pt**), functionally subdivided into anterior and posterior fibre units. Mediated by a small posterior contribution from the external adductor muscles. The pivot point (**purple dot**) closely corresponds to the point of contact of the quadrate condyle with the articular recess.
Red arrows - traction lines of the muscle forces involved in the movement of the lower jaw relative to the upper jaw when the mouth is effectively closed.

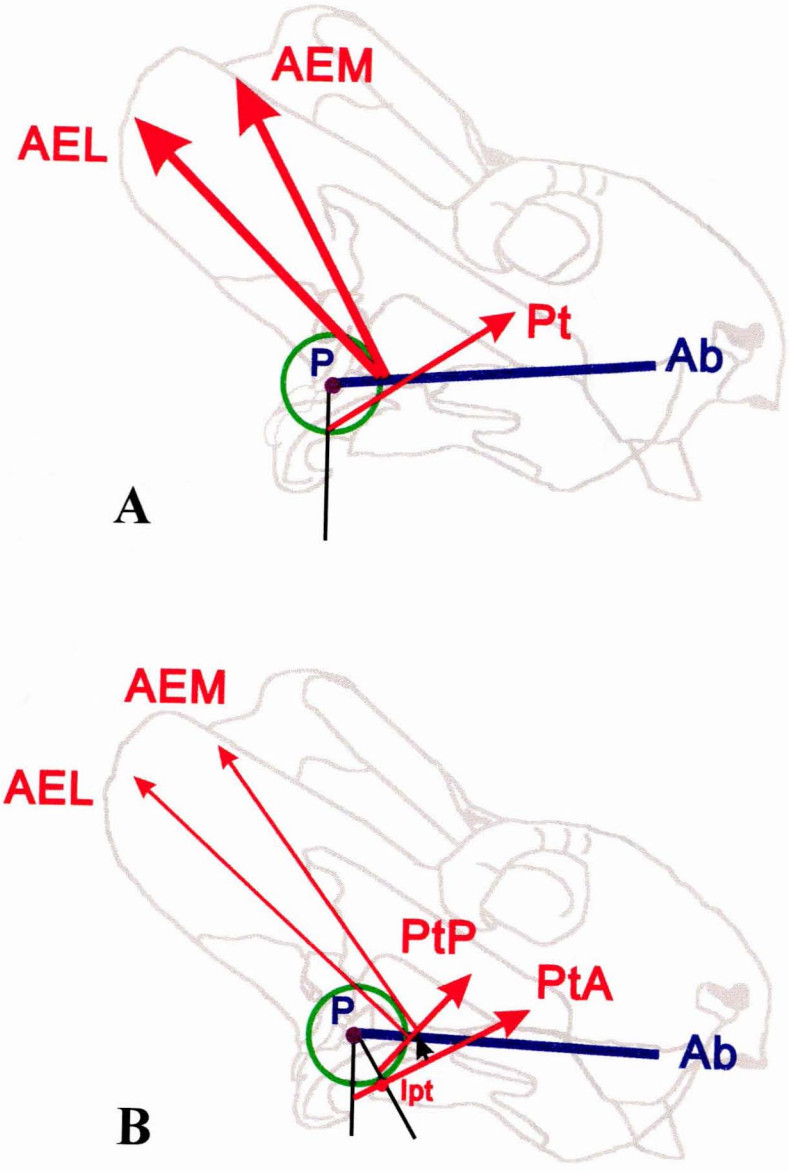


Figure 81. Force diagrams depicting the movements of the lower jaw during Phase Two of the *Kannemeyeria* masticatory cycle.
A - postero-dorsal stroke, the traction lines of the external adductor muscles (**red arrows**) both lie nearly tangential to the circle around the pivot point (**P**) which reflects the smaller arc of action of the lower jaw of Phase 2. This radius is determined by the anterior fibres of the pterygoideus musculature (**PtA**). The upward and backward force of **AEM** and **AEL** pulls the lever arm of the lower jaw (**P - Ab**) firmly against the palatal pads of the upper jaw. **B - antero-dorsal stroke**, most of the force is exerted by the anterior and posterior (**PtP**) fibres of the pterygoideus musculature. The anterior fibres are nearly tangential to the bell-crank curve, whilst the traction line of the posterior fibres runs through the circle and is described by the Pythagorean Theorem, which matches the path of the traction line of the anterior fibres. The insertion point (**Ipt**) marks the point of action of the anterior fibres.

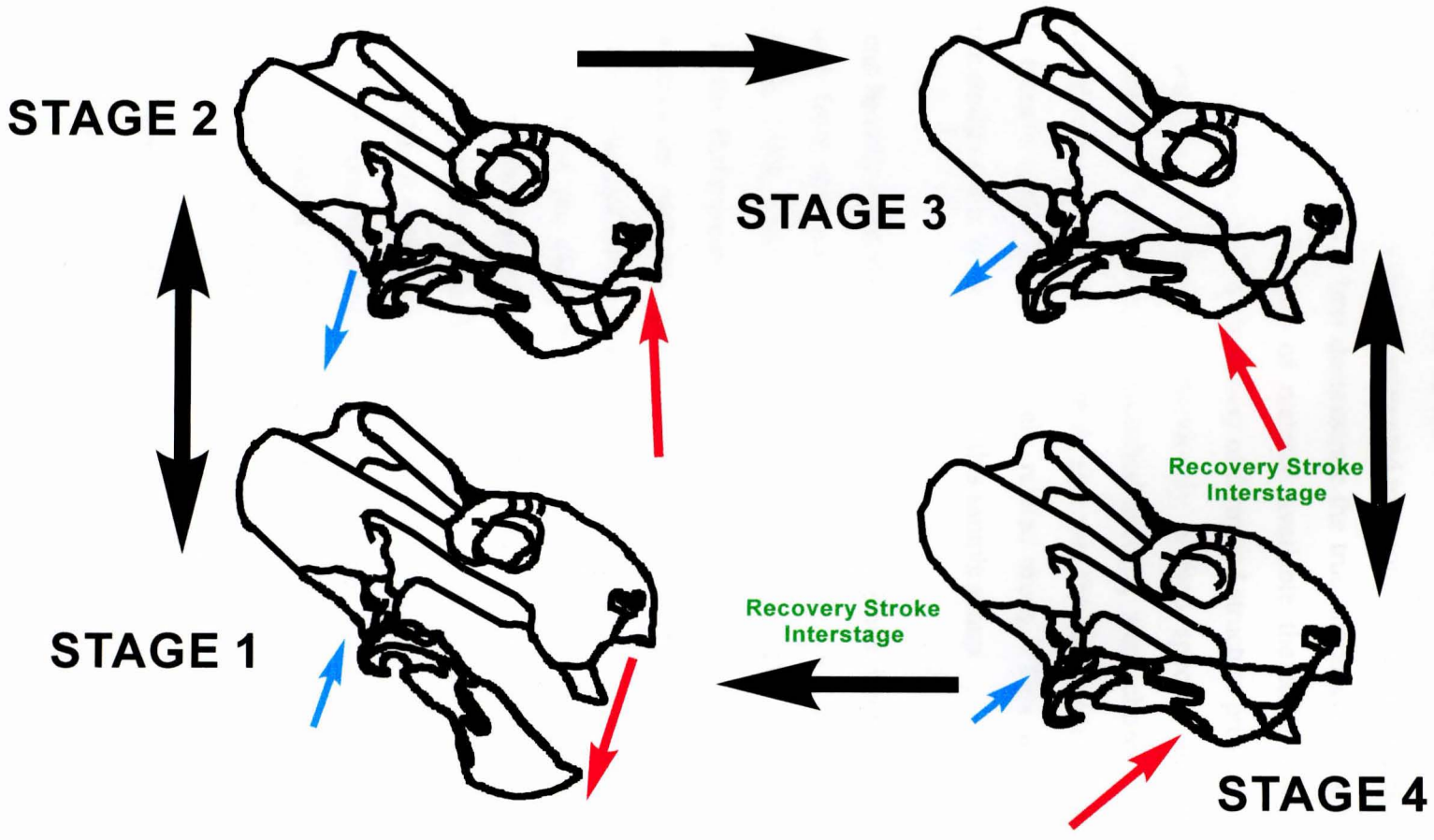


Figure 82. Masticatory cycle of *Kannemeyeria*.
Blue arrow - direction of movement of jaw joint, **red arrow -** direction of maximum applied force and thus direction of movement of the entire lower jaw, **black arrows -** progression of masticatory cycle from depression (**Stage 1**) to elevation (**Stage 2**) to orthal jaw action (**Stages 3** & **4**), and finally back to depression.

APPENDIX A

A.1 Materials and Methods

A vast number of specimens, in various institutions, can be reliably attributed to the genus *Kannemeyeria*, but this study has attempted to produce an accurate rendering of the genus based on those specimens which best demonstrate the true characteristics of the genus. This means that from the large collection of material available the least distorted and best preserved specimens, which still reflect the variety of form and structure present in the genus, were chosen for examination. Holotypes of previously erected species, including those which were subsequently synonymised with established species, were chosen for study. A final factor influenced the composition of the sample size was the attempt to obtain as many specimens as possible from a single area, or closely related areas. This is of particular importance if allometric studies are to be performed on this sample group.

Specimens broadly identifiable as belonging to the genus *Kannemeyeria* were determined and recognised from the genotype of *Kannemeyeria simocephalus* (HMV/8178), described by Weithofer in 1888, from Dwarsvlei farm Aliwal North District, South Africa, and currently housed in the Hofmuseum, Vienna. Although this holotype specimen was not available for study, a museum cast and photographs of the specimen was used for comparison and examination. The cast (BP/11/129) revealed that this specimen was very incomplete lacking the entire left half of the skull, and much of the palate and braincase. Consequently, most observations of the elements of the palatal surface, nasal cavity and braincase of skulls diagnosed as *Kannemeyeria* have previously relied on descriptions of other dicynodonts (Pearson, 1924a). A meaningful description of the morphology of this genus must, therefore, be founded on the examination of well preserved referred material. As part of the recognition of a specimen as a member of the genus *Kannemeyeria* it is critical to investigate the nature and extent of the distortion suffered, these description are included in this section.

Mechanical means of preparation of the specimen refers to the use of air-scribe tools tipped with a tungsten needle point, whereas occasional acid preparation is described in detail for those specimens where it was used.

A.2 List of Reference Specimens

Specimen No.	Taxon	Description
BP/1/296	*Lystrosaurus*	Small, complete & well preserved skull & lower jaw.
BP/1/300	*Aulacephalodon*	*A. baini* Large well preserved and undistorted skull.
BP/1/315	*Pristerodon*	Small, complete skull.
BP/1/555	*Dicynodon*	Holotype of *D. daptocephaloides* Toerien 1955. Medium sized well preserved & complete skull.
BP/1/766	*Aulacephalodon*	Large well preserved & complete lower jaw.
BP/1/878	*Lystrosaurus*	Holotype of *L. primitivus* Small, complete skull & lower jaw.
BP/1/2188	*Dicynodon*	= *Daptocephalus*. Large skull, bilaterally compressed, but complete.
BP/1/2642	*Pristerodon*	Small, well preserved & complete skull & lower jaw. Used by Crompton & Hotton (1967) to establish their model on dicynodont jaw cycle.
BP/1/3532	*Shansiodon*	A small to medium sized skull & lower jaw, identified as a *Shansiodon* sp. by Hancox, 1998.
BP/1/4233	*Dicynodon*	Large, well preserved & complete skull.
BP/1/4545	*Kannemeyeria*	Right caniniform process & tusk.
BP/1/4675	*Kannemeyeria*	Large, right caniniform & tusk.
BP/1/4798	*Lystrosaurus*	Small, well preserved & complete skull & lower jaw.
BP/1/5287	*Dicynodon*	= *Daptocephalus*. Large, complete skull with partial lower jaw.
MACN/18.055	*Ischigualastia*	Holotype of *I. jenseni* Cox 1965. Large, nearly complete skull, partial lower jaw (uncatologued).
PVL/3831	*Vinceria*	Holotype of *V. andina* Boneparte 1967. Small, complete skull & lower jaw. Rio Mendoza Formation, Argentina.
PVL/3832	*Vinceria*	Small, sub-adult complete skull.
R/313	*Kannemeyeria*	*K. cristarhynchus* large, well preserved & complete skull.
RC/9	*Dinanomodon*	Holotype of *D. rubidgei* Broom 1938. Large, near complete skull.

APPENDIX B

B.1 Log-Transformed Data for Allometric Analysis

	Specimen										
Variable	BP/1/989	PE/1199P	BP/1/2092	BP/1/4648	SAM/10555	BP/1/4523	BP/1/3638	EL/1	BP/1/4524	QR/1127	BP/1/5624
var1	1.92941893	2.29666519	2.350248	2.42813479	2.51587384	2.560228353	2.5663025	2.58546073	2.5865873	2.60530505	2.61489722
var2	2.1172713	2.34242268	2.462398	2.51054501	2.6180481	2.643452676	2.6580114	2.68574174	2.67760695	2.68124124	2.62838893
var3	2.19865709		2.50515	2.53147892	2.64147411	2.686741739	2.67669361	2.72835378	2.71600334	2.7201593	2.6946052
var4	1.63346846	1.98227123	2.079181	2.11394335	2.19589965	2.260071388	2.31175386	2.2787536	2.35410844	2.2787536	2.26717173
var5	1.66275783		2.079181	2.15836249	2.2764618	2.361727836	2.31597035	2.38381537	2.36361198	2.33445375	2.35218252
var6	1.67209786	1.94939001	1.968483	2.0374265	2.1271048	2.167317335	2.09342169	2.20951501	2.24303805	2.10720997	2.2787536
var7	1.50514998	1.63346846	1.556303	1.67209786	1.71600334	1.77815125	1.80617997	1.90308999	1.8920946	1.78632984	1.83250891
var8	1.5563025	1.91381385	1.892095	2.04139269	2.08635983	2.184691431	2.23044892	2.19865709	2.22271647	2.10037055	2.23552845
var9	1.71600334	1.98227123	2.049218	2.06069784	2.18752072	2.190331698	2.13033377	2.28555731	2.29225607	2.13672057	2.35218252
var10			2.271842	2.11394335	2.40483372	2.431363764	2.38916608	2.52113808	2.37106786	2.26481782	2.46982202
var11	1.47712125	1.53147892	1.832509	1.84509804	2.09691001	2.096910013	2.19589965	2.1271048	2.13033377	2.1271048	2.15228834
var12	1.56820172	1.62324929	1.913814	1.95904139	2.13987909	2.178976947	2.08635983	2.25527251	2.23044892	2.2380461	2.2787536
var13	0.90308999		1.041393		1.30103	1.342422681	1.25527251	1.34242268	1.32221929	1.38021124	1.38021124
var14	1.50514998	1.65321251	1.755875	1.84509804	1.8573325	1.954242509	1.92427929	1.92941893	1.99122608	1.99122608	1.96378783
var15	1.44715803		1.724276	1.80617997	1.95904139	2	1.96848295	1.91907809	2	1.78632984	2.0211893
var16	1.17609126	1.20411998	1.431364		1.36172784	1.342422681	1.69019608	1.49136169	1.44715803	1.34242268	1.44715803
var17	1.23044892		1.857332	1.97312785	2.03342376	2.136720567	2.16436286	2.21748394	2.1430148	2.2121876	2.20411998
var18			2.041393	1.93951925	2.1271048	2.190331698	1.89762709	2.13987909	2.24551267	2.08990511	2.10037055
var19	1.38021124		1.70757	1.86923172	1.93449845	2	2.08278537	2.04139269	2.05307844		2
var20	0.77815125	1.04139269	1.30103	1.36172784	1.44715803	1.531478917	1.72427587	1.54406804	1.53147892	1.56820172	1.51851394
var21	1.11394335	1.47712125	1.50515	1.62324929	1.63346846	1.748188027	1.81291336	1.83250891	1.74036269	1.77815125	1.87506126
var22	0.84509804	0.95424251	1.079181	1.04139269	1.34242268	1.361727836	1.43136376	1.38021124	1.36172784	1.07918125	1.34242268
var23	1	1.14612804	1.230449	1.30103	1.25527251	1.342422681	1.39794001	1.32221929	1.36172784	1.25527251	1.30103
var24				2.42160393		2.509202622	2.64836001	2.55870857	2.60314437	2.46538285	2.5797836
var25		2.08990511		2.1271048	2.32014629	2.346352974		2.37106786	2.33041377	2.45939249	2.32633586
var26		1.63346846				1.785329835		1.83250891	1.75587486	1.76342799	1.80617997
var27	1.49136169	1.8920946	1.982271	2.11058971	2.13672057	2.164352856	2.18752072	2.11394335	2.07918125	2.24303805	2.161368
var28	0.95424251		1.414973	1.53147892	1.462398	1.51851394	1.60205999		1.64345268	1.60205999	1.74036269
var29	1.5797836	1.69897	1.792392	1.77815125	1.85125835	1.851258349	1.95904139	1.90848502	1.93951925	1.81291336	1.87506126
var30	0.60205999	1.41497335	1.518514	1.59106461	1.64345268	1.602059991	1.77815125	1.70757018	1.71600334	1.69897	1.71600334

mean.X1	2.251116732
mean.X2	2.540801566
mean.X3	2.598062574

B.2 Statistical Results of Allometric Analysis: Bartlett's 'Best-Fit' Procedure

Variable	N	B	a	Sxx	Sxy	Syy	s(B)	t	d.f.	reject	95% Conf. Int(B) LCL.B	95% Conf. Int(B) UCL.B	95% Conf. Int(a) LCL.a	95% Conf. Int(a) UCL.a
var1	11													
var2	11	0.893768	0.3624167	0.1483034	0.114085	0.095331	0.035121	-1.252883	8	FALSE	0.80409	0.983426518	0.339151	0.365682006
var3	10	0.873388	0.4645424	0.1483034	0.099005	0.072672	0.04296	-0.862176	7	FALSE	0.798075	0.948701652	0.452857	0.476227899
var4	11	0.98713	-0.265093	0.1483034	0.145124	0.156312	0.042293	-0.310252	8	FALSE	0.917288	1.056972251	-0.27542	-0.254760327
var5	10	1.129135	-0.544624	0.1483034	0.142859	0.149084	0.047131	-1.710429	7	FALSE	0.964835	1.293435219	-0.57012	-0.519131018
var6	11	0.872701	-0.065986	0.1483034	0.106681	0.096889	0.054356	1.0797861	8	FALSE	0.992321	0.753080301	-0.08368	-0.04828951
var7	11	0.753723	-0.116778	0.1483034	0.040468	0.030249	0.081774	1.0235508	8	FALSE	0.583136	0.924310657	-0.14201	-0.091542037
var8	11	0.975418	-0.335687	0.1483034	0.135441	0.150822	0.058843	-1.106656	8	FALSE	0.842701	1.10813631	-0.35532	-0.316053508
var9	11	0.906861	-0.101771	0.1483034	0.106177	0.105381	0.068926	1.3293281	8	FALSE	0.72825	1.085470735	-0.12819	-0.075347953
var10	10	0.616289	0.845996	0.1483034	0.01175	0.07252	0.127819	-0.806923	7	FALSE	0.40608	0.826498454	0.81338	0.878611861
var11	11	1.333511	-1.310686	0.1483034	0.102845	0.120425	0.117184	-1.188105	8	FALSE	1.049754	1.617268296	-1.35266	-1.26870708
var12	11	1.396626	-1.387598	0.1483034	0.105954	0.124318	0.121263	0.5670248	8	FALSE	1.25649	1.536763126	-1.40833	-1.366866184
var13	10	1.106872	-1.466763	0.1483034	0.111526	0.088937	0.05824	1.0890196	7	FALSE	0.977607	1.236137441	-1.44671	-1.486819134
var14	11	0.804393	-0.123923	0.1483034	0.091776	0.071423	0.049668	0.4241469	8	FALSE	0.761458	0.847328548	-0.13027	-0.117570914
var15	10	0.784545	-0.063992	0.1483034	0.100683	0.10819	0.07699	-1.70712	7	FALSE	0.516676	1.052413909	-0.10555	-0.022429815
var16	10	0.465491	0.2500246	0.1483034	0.043299	0.123443	0.128323	-1.063784	7	FALSE	0.187276	0.743705761	0.206857	0.29319214
var17	10	1.461991	-1.573844	0.1483034	0.214405	0.340133	0.066585	-0.858944	7	FALSE	1.347002	1.576980396	-1.59169	-1.556002877
var18	10	0.442319	0.9992761	0.1483034	0.007573	0.081737	0.12192	0.936916	7	FALSE	0.209013	0.675625627	0.963077	1.035475606
var19	9	1.09283	-0.78777	0.1483034	0.131412	0.136747	0.068634	-0.9578	6	FALSE	0.962755	1.222903691	-0.80904	-0.766495844
var20	11	1.210535	-1.578193	0.1483034	0.167128	0.255946	0.092629	-2.010597	8	TRUE	0.830961	1.590109487	-1.63435	-1.522039728
var21	11	1.085631	-1.017516	0.1483034	0.145479	0.172177	0.062342	0.3977491	8	FALSE	1.035093	1.136168329	-1.02499	-1.010039067
var22	11	0.896126	-0.999415	0.1483034	0.062924	0.097318	0.113818	-2.358525	8	TRUE	0.349016	1.443235298	-1.08035	-0.918476273
var23	11	0.405425	0.269023	0.1483034	0.082788	0.066536	0.064525	-1.695764	8	FALSE	0.228095	0.582756112	0.242789	0.295256932
var24	7	0.375133	1.61945	0.1483034	0.005348	0.014399	0.088398	-1.109894	4	FALSE	0.17517	0.575096171	1.582367	1.656533161
var25	8	0.758901	0.4322637	0.1483034	0.0241	0.042311	0.135015	0.0615572	5	FALSE	0.741962	0.775839805	0.429325	0.435202118
var26	6	0.449723	0.6581513	0.1483034	0.019253	0.015381	0.09671	0.0756437	3	FALSE	0.434813	0.464632498	0.655165	0.66113788
var27	11	0.807917	0.0666583	0.1483034	0.176532	0.230733	0.072706	-1.587728	8	FALSE	0.572646	1.04318714	0.031853	0.101463775
var28	9	1.042603	-1.064314	0.1483034	0.163613	0.206305	0.066265	1.9499281	6	TRUE	0.779257	1.30594907	-1.10738	-1.021242996
var29	11	0.494805	0.6070575	0.1483034	0.06162	0.045049	0.060472	-1.206924	8	FALSE	0.370663	0.618946883	0.588692	0.625422849
var30	11	1.233575	-1.485572	0.1483034	0.302948	0.648614	0.125932	-0.545504	8	FALSE	1.093568	1.373584162	-1.50628	-1.464859386

B.3 Cranial Measurements. Variables (Var) 1 to 30 are explained in the text (Volume 1 Chapter 7). All measurements are in millimetres, and represent the average of three independent readings.

	Specimen										
Variable	BP/1/989	BP/1/2092	BP/1/3638	BP/1/4523	BP/1/4524	BP/1/4648	BP/1/5624	PE/1199P	QR/1127	EL/1	SAM/PK/10555
var1	85	224	360	355	386	268	412	198	403	385	328
var2	131	290	455	440	476	324	425	220	480	485	415
var3	158	320	475	485	520	340	495		525	535	438
var4	43	120	205	182	226	130	185	96	190	190	157
var5	46	120	207	230	231	144	225		216	242	189
var6	47	93	124	147	175	109	190	89	128	162	134
var7	32	36	64	60	78	47	68	43	61	80	52
var8	36	78	170	153	167	110	172	82	126	158	122
var9	52	112	135	155	196	115	225	96	137	193	154
var10		187	245	270	235	130	295		184	332	254
var11	30	68	157	125	135	70	142	34	134	134	125
var12	37	82	122	151	170	91	190	42	173	180	138
var13	8	11	18	22	21		24		24	22	20
var14	32	57	84	90	98	70	92	45	98	85	72
var15	28	53	93	100	100	64	105		61	83	91
var16	15	27	49	22	28		28	16	22	31	23
var17	17	72	146	137	139	94	160		163	165	108
var18		110	79	155	176	87	126		123	138	134
var19	24	51	121	100	113	74	100			110	86
var20	6	20	53	34	34	23	33	11	37	35	28
var21	13	32	65	56	55	42	75	30	60	68	43
var22	7	12	27	23	23	11	22	9	12	24	22
var23	10	17	25	22	23	20	20	14	18	21	18
var24			445	323	401	264	380		292	362	
var25				222	214	134	212	123	288	235	209
var26				61	57		64	43	58	68	
var27	31	96	154	146	120	129	145	78	175	130	137
var28	9	26	40	33	44	34	55		40		29
var29	38	62	91	71	87	60	75	50	65	81	71
var30	4	33	60	40	52	39	52	26	50	51	44